Department of Precision and Microsystems Engineering

Temperature control system for Organ-on-a-Chip applications

Shiemaa A.M. Elhassan

Report no : 2023.001
Coach : Ir. Gürhan Özkayar
Professor : Dr. Murali Krishna Ghatkesar
Specialisation : Micro- and Nano- Engineering
Type of report : Master's Thesis
Date : 11-01-2023

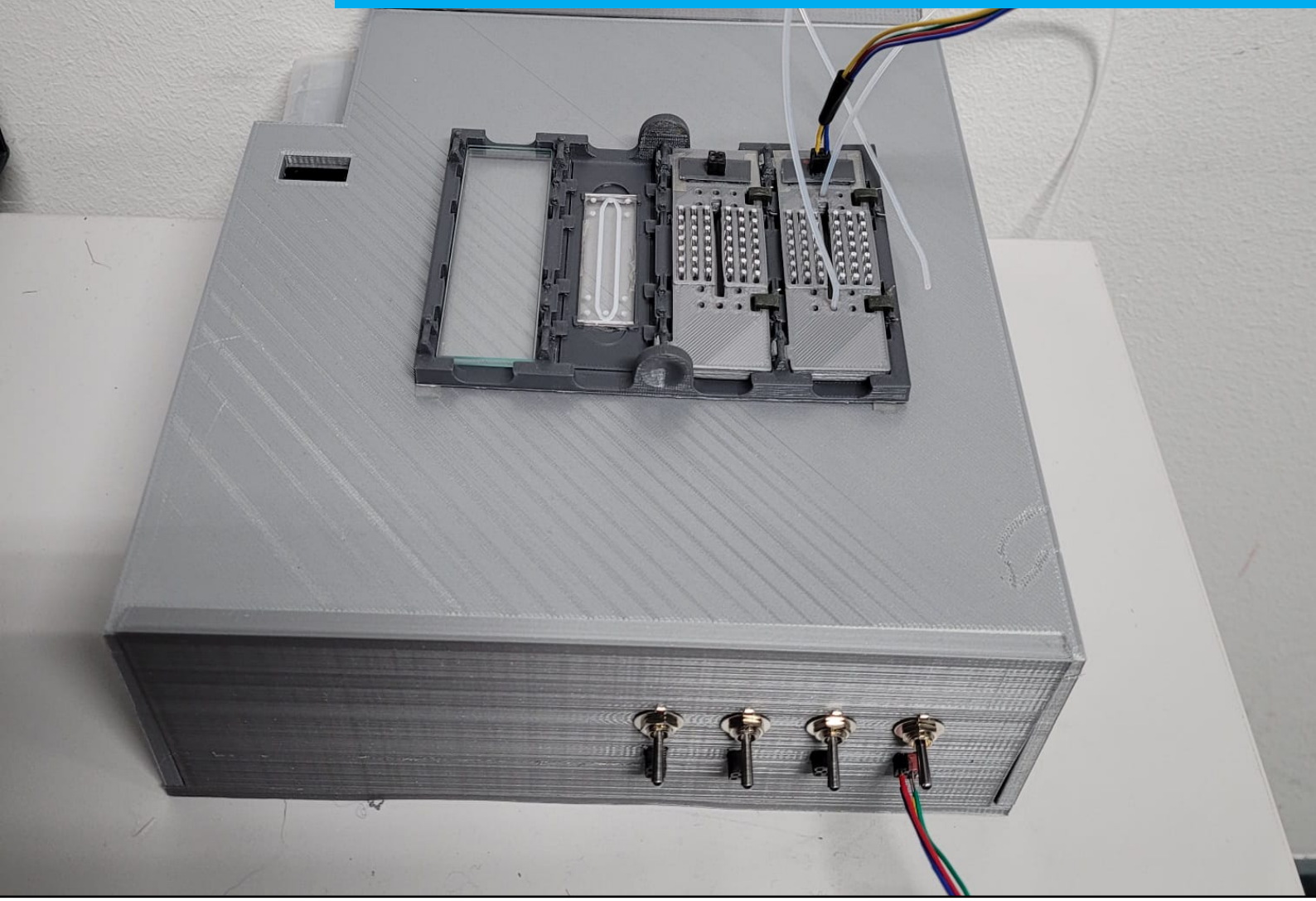

TU Delft Delft University of Technology

Challenge the future

Temperature control system for Organ-on-a-Chip applications

Master's Thesis

by

Shiemaa A.M. Elhassan

in partial fulfilment of the requirement of the degree of
Master of Science
in Mechanical Engineering
at the Delft University of Technology

Student number:	4609999	
Supervisor:	Dr. Murali Krishna Ghatkesar,	TU Delft
Daily Supervisor:	Ir. Gürhan Özkayar,	TU Delft
Chair:	Dr. Murali Krishna Ghatkesar,	TU Delft
External:	Dr. Harold Raat,	Erasmus MC
	Prof.Dr.Ir. Joost Lötters,	TU Delft
	Dr. Sabina Caneva,	TU Delft

Date of submission: 11-01-2023

Contents

List of Figures

List of Tables

1 Introduction

In the past few years, much research has been performed on Organ-on-a-Chip (OoC). An OoC is a microfluidic chip that contains human cells, and the chip mimics the microenvironment of these cells. A schematic drawing of an OoC can be seen in Figure 1.

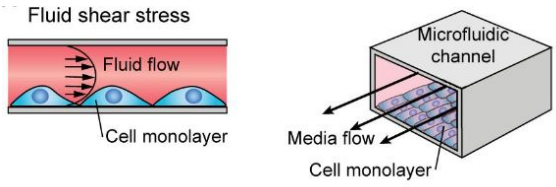

Figure 1: Schematic drawing of OoC [1]

To use these chips, a platform is required to control the parameters that resemble the cells' natural environment. One of the main purposes of using these platforms in OoC experiments is to obtain a controlled fluid flow in the system. One of these platforms is designed by Zhu et al. [2]. It can create the flow rates needed to operate several OoCs, such as Tissue-on-a-chip, Gut-on-a-chip, and Lung-on-a-chip. However, this platform does not have any temperature control. Temperature control is required to ensure that the cells and fluid/air are at 37°C since most cells in the human body function at 37°C [3]. The research question will therefore be: How to build a portable local temperature control system for Organ-on-a-Chip applications? The system should be portable so that experiments can continue when moving from one lab to an other lab.

Another device that the platform does not have at the moment is an Oxygenator. This is a device that reduces the concentration of oxygen in the medium that flows through the chip [4]. These parts will be considered in the literature survey but are not considered in the actual design since this part is still in development progress.

Chapter 2 contains the literature review. It starts with a short explanation of the OoC and why they are being developed. Then the importance of temperature control on the OoC platform is discussed in more detail. Afterwards, the requirements for the temperature control system are defined. Then the principles of all the components of the temperature control system are explained. An explanation of the design approach is given, and the decision for the components of the temperature control system is made. Some design concepts, as well as the overall design of the platform, are also given in this chapter.

Chapter 3 contains a paper with all the results and conclusion of this project.

Chapter 4 shows an overview of the target and achieved specifications, and recommendations.

Chapter 5 contains my reflection on the project and the acknowledgement.

2 Literature review

2.1 Litareature

In this chapter, the OoC and the reason why they are being developed will be explained. In addition, the requirements and all the components needed for this design project will be described in this chapter.

2.1.1 Organ-on-a-Chip and Organ-on-a-Chip platform

2.1.1.1 Introduction to Organ-on-a-Chip

What is an OoC?
An Organ-on-a-Chip (OoC) is a microfluidic chip that contains human cells inside of it [5]. Depending on the type of cells used, the OoC can have one, two, three or four channels inside of it, where medium or air can flow to recreate the natural environment of the cells. An example of how an OoC works will be given. In Figure G1a a schematic OoC is represented. Where the cells are placed at the bottom of the channel and a medium flows trough the channel to mimic for instance a blood flow. There are several more types of OoC such as Liver-on-a-chip [5], Heart-on-a-chip, Gut-on-a-chip etc. [5], as can be seen in Figure G1b.

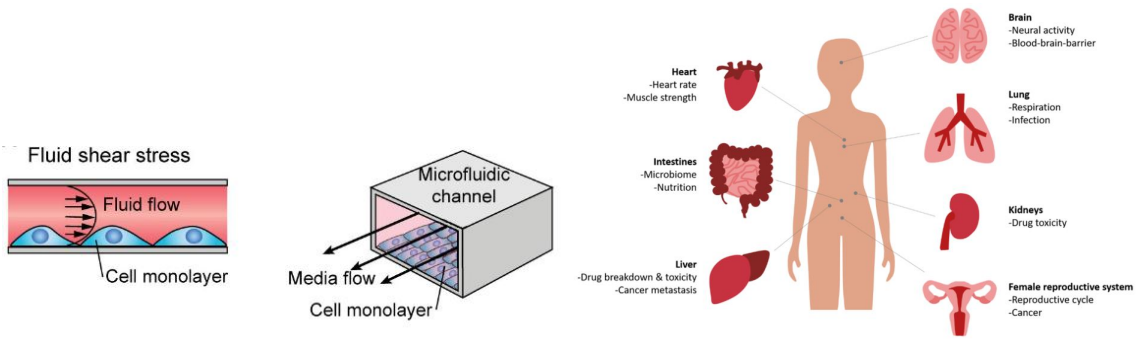

(a) (b)

Figure 2: (a) Schematic of a OoC [1] (b) An overview of organs that can be used in OoC and the diseases that can be modelled [5]

Why OoCs are developed?
At the moment, for a drug to be able to be brought onto the market, it has to pass through several stages before it is FDA approved [5]. Not only is this time consuming, but only a handful of drugs pass all the stages. In Figure 3a the several stages that a drug needs to pass are shown before one is approved by the FDA. The time from the moment that the drug is tested to being FDA approved is 14 years [5]. To reduce this time, OoCs can be used [5]. Since human cells are used in OoCs and the environment of the cells is being recreated, tests done with OoC are more representative than animal models and 2D cell cultures [5]. This makes it more ethical (no animal models are needed to be used) and can reduce the experiment time and make the data more reliable. Another advantage is that it is also possible to use OoC to develop personalized drugs. This makes the chances of a drug working for a particular patient larger. Another significant advantage of using OoCs is that it is possible to do more research on how the human body is breaking down drugs and how potentially harmful chemicals might be produced by the human body [5]. An overview of the advantages can be seen in Figure 3b.

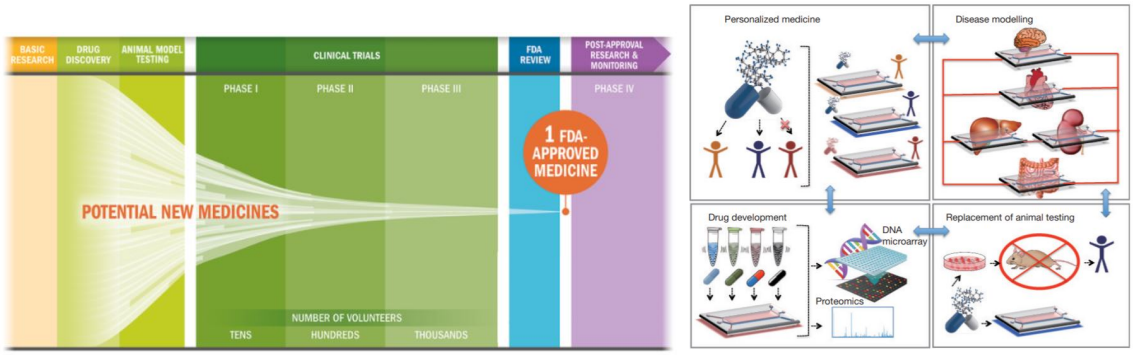

(a) (b)

Figure 3: (a) Stages that a drug have to pass before it can be brought on the market [5] (b) An overview of the advantages of the usages of OoC [6]

2.1.1.2 The importance of temperature control

In the human body, maintaining the same temperature is essential. The regular temperature of a human body is 37 °C. A slight decrease in the temperature will not harm the cell too much, but it will mainly slow down the metabolism of the cells and/or their growth [7]. However, an increase in temperature is more harmful to the cells [7]. Cells will only survive for a few hours if the temperature is 39 °C and die rapidly at a temperature of 40 °C [7]. Not only does changes in temperature influence the lifetime of a cell and their growth, but it has been reported that the thermal environment of the cell influences the physiology of the cells [7]. This shows that small fluctuations in temperature can significantly impact the cells and thus how important it is that cells should be kept at their optimal temperature. This all shows that temperature control for cells and thus also for OoCs is important since cells will be placed inside of the OoCs. The research question will therefore be: How to build a portable local temperature control system for Organ-on-a-Chip applications? The system should be portable so that tests can continue when moving the system from one place to another.

2.1.1.3 Requirements

One of the main requirements is that the cells in the chip are heated to a temperature of 37 ± 0.5 °C since most of the cells in the human body work at this temperature range. It is important that, when the cells are overheated, the temperature is changed as fast as possible to the ideal temperature. The maximum response time of the temperature sensor and controller is chosen to be 2 to 3 minutes. Another requirement is that the heating control system can work on a battery. This will keep the platform portable. The temperature control system must not interfere with the cells inside the chip since this might interfere with the obtained experimental results. The fluid/air should be heated to a temperature of 37 °C before entering the chip and maintaining this temperature when it reaches the cells. This is important since this could cool down or heat up the cells. Another important point is that there should be no bubble generation in the system. Bubbles can harm the cells due to shear stresses at the surface. To validate the experiments and be able to do multiple experiments simultaneously, the holder should be able to hold at least two chips. The holder should be transparent at least on one side so that a microscope can be used to view the cells. The holder should also clamp the chip so that no fluid leakage will occur.
The OoC platform should be able to work for a certain duration of time. The power

consumption of the components of the OoC platform is 23.72W, which is also a boundary condition. With only the components of the OoC, this would make the battery last for approximately 2 hours. To estimate how much power will be needed to heat the OoC, a simulation was made in COMSOL v5.6. The results of surface temperature change can be seen in Figure 4. These simulations heated the OoC to 37°C in one hour. Figure 4a shows the initial temperature of the chip. Figure 4b illustrates the result when the chip is heated for 1 hour at 35W when the fluid that enters the chip is 20°C. Figure 4c illustrates the result when the chip is heated for 1 hour at 10W when the fluid that enters the chip has a temperature of 37°C. This shows that when the fluid that enters the chip is preheated, less power is needed. If this 10W is added to the total power consumption, the battery will last for 1.4 hours. Take note that this simulation took into account that the fluid that flows into the chip has a temperature of 37°C. The heating outside the chip was not taken into account. This means that more than 10W might be needed, which means that the battery will last less than 1.4 hours. Also, it took one hour to reach the desired temperature. If it is preferred to reach this temperature faster, more power will be needed. This means that the duration of an experiment can not be longer than 1.4 hours. For the requirement, a duration of 30 minutes is chosen, then 70W can be used by the temperature control system. All these assumptions are done with the following formula [8]:

$$\frac{QV}{P * 1000} = t \tag{1}$$

Where Q is the electrical charge in mAh, V is the Voltage in V, P is the power in Watts, and t is the time in hours. Where 24V was taken for the voltage and 2000mAh was taken for the electrical charge.
An overview of the requirements can be found in Table 8. In Table 2 the boundary conditions are given.

It is preferred if four chips can be heated at the same time so that several experiments can be done simultaneously. It is also preferred that the holder is transparent at both sides to measure the oxygen levels while a microscope is used. It is preferred that the holder can be used for a variety of OoCs.

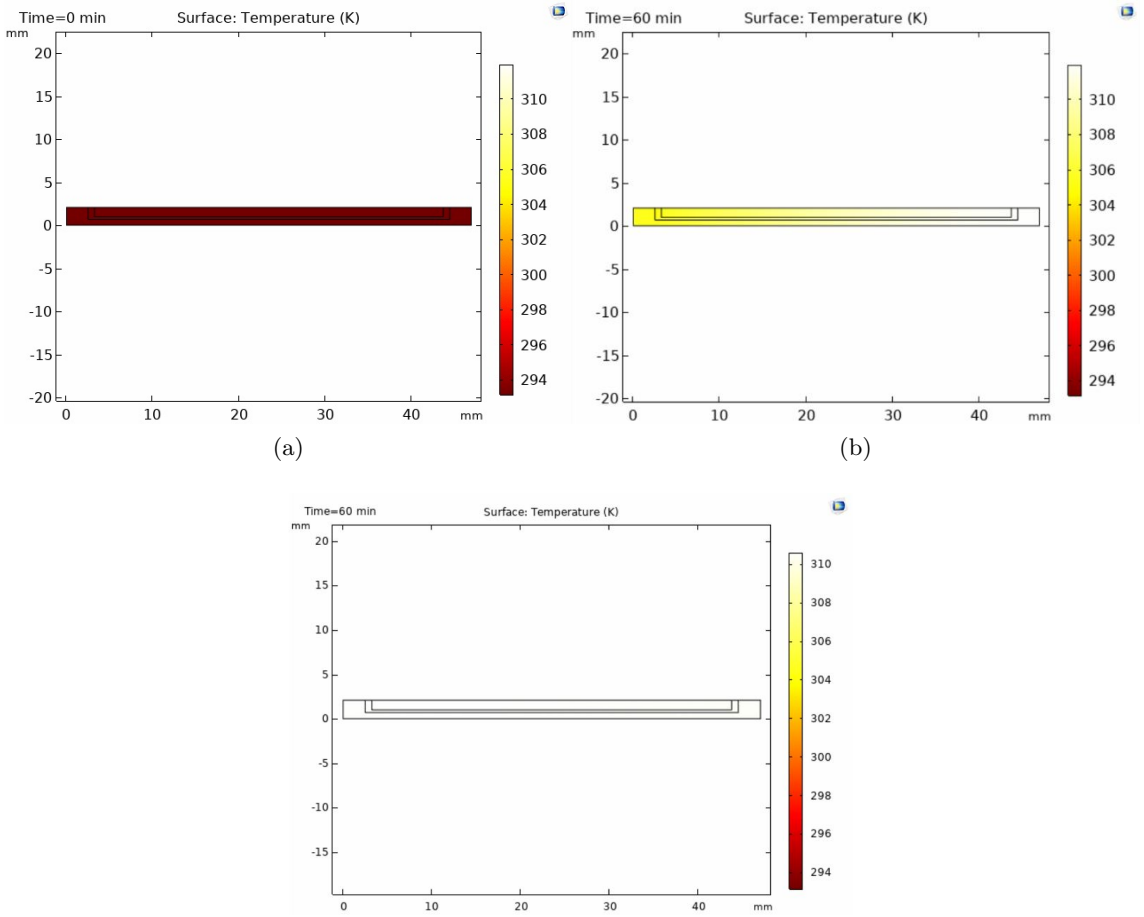

Figure 4: (a) Initial state of the chip at t=0s (b) Simulation of heating the OoC from the bottom at 35W for one hour without heated medium, at t=3600s (c) Simulation of heating the OoC from the bottom at 10W for one hour with heated medium, at t=3600s

Table 1: Required specifications

Components	Variety	Specifications
Heater	Temperature at the cells	37 ± 0.5 °C
	Temperature of the medium (before entering chip and at the chip)	37 ± 0.5 °C
	Precision	0.1 °C
Temperature sensor	Resolution	0.1 °C
	Interference with cells	No
	Response time	2-3 min
Battery	Duration heating	0.5 hour(s)
	Max power consumption	24.28 W
Controller	Response time	2-3 min
Holder	Number of chips	2
	Chip dimensions	45x15x2.1mm (Micronit)
	Transparent	One side
	Clamping	No leakage
Other	Bubble generation	No

Table 2: Boundary conditions

Voltage Battery	24V
Battery capacity	2000mAh
Power consumption other components	23.72W

2.1.2 Heaters

As explained earlier, the liquid and the cells must be heated to a temperature of 37°C. In the following sub-chapters, several types of heaters will be explained.

2.1.2.1 Peltier

One way of heating an OoC is using a Peltier element. The principle of a Peltier element is that two dissimilar materials are connected [9]. Since the two metals are dissimilar, the average energy of the electrons involved in the transfer of electric current is different [9]. When a current flows through the materials, the electrons will move from one material to the other. Depending on the direction, the electrons will extract heat from the environment, which causes cooling or transfer their energy to the environment, which causes heating [9]. This causes one side of the Peltier element to cool down while the other side will heat up. A schematic drawing can be seen in Figure 5.

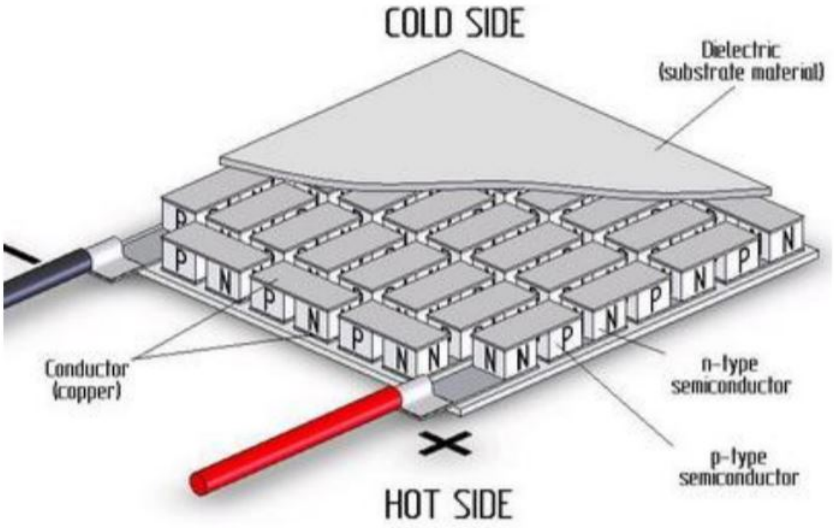

Figure 5: Schematic drawing of a Peltier element [10]

Xianbo Qui et al. [11] designed a large volume, portable, real-time polymerase chain reaction (PCR) reactor. They used a double-sided heater system consisting of a Peltier element (Master TE) and a waveguide connected to another Peltier element (Slave TE) [11]. These two heaters are used to heat the chip from the top and bottom. A schematic drawing of the setup can be seen in Figure 6. They achieved an accuracy of ± 0.1 °C and heating rates of 4 °C/s and cooling rates of 6 °C/s..

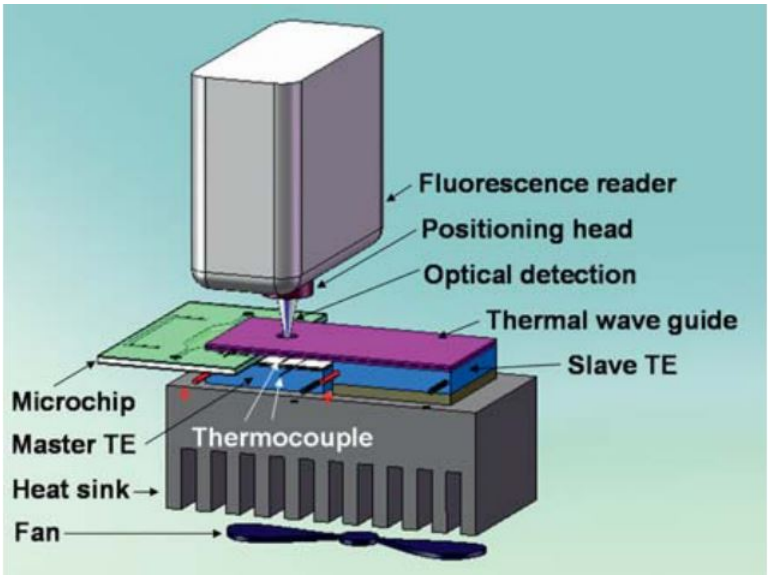

Figure 6: Schematic drawing of the real-time PCR platform with the microchip partly inserted [11]

2.1.2.2 Joule heating

Another way of heating an OoC is by using Joule heating. The principle of Joule heating is that when a current passes through an electrical conductor, thermal energy is produced [12]. Joule heating can be seen as the transformation of electrical energy into thermal energy [12]. This thermal energy can be used to heat the OoC.

Jr-Lung Lin et al. [13] have designed an integrated microfluidic perfusion cell culture system consisting of a microfluidic cell culture chip and an indium tin oxide (ITO) glass-based microheater. The layout of their design can be seen in Figure 7a. A top view of the chip can be seen in Figure 7b. The dimensions of the chip are 50.2mm x 20.7mm. The ITO glass microheater was created by first attaching a mask on the ITO-glass substrate. This was followed by print screening silver paste on top of it. After the mask was removed, the silver electrodes-patterned ITO glass was created. It was finished with a 15um thick insulation layer [13]. This process can be seen in Figure 8a. The ITO-glass microheater can be seen in Figure 8b. The ITO glass was bought from Ritek Corp., Taiwan. The system was able to provide pumping rates ranging from 15.4 to 120μL/min. With their system, they maintained a temperature of 37°C with a deviation of ± 0.3°C.

2.1.2.3 Heating by the use of water/air

A third way of heating the OoC is by using heated water or air. This heated water or air flows in channels surrounding the OoC. The heat from the water or air will then be dissipated to the OoC.

In the research of Jiu Yang Zhu et al. [14] a microfluidic system, integrated with commercially available polymer tubes for controlling the temperature of a sample under various static and dynamic conditions, was demonstrated. Two tubes, where heated water flows through, were placed under the microfluidic channel. Two configurations were used in their research, one where the tubes of water are parallel to the microfluidic channel and one where the tubes with water are perpendicular to the channels, as can be seen in Figure 9a. Their results can be seen in Figure 9b. For the parallel configuration, a flow rate of 60μL/min for the microfluidic channel and 500μL/min for the hot water was used, and the water had a temperature of 58°C. [14] A hot region was created which had a temperature of 37 ± 0.5°C and spend 70% of the microfluidic channel. They calculated that the heat consumption of this configuration is 0.48W, from which 12% was transferred to the microfluidic channel. For the cross configuration, the same flow rates were used, but a temperature of 56°C was used for the water. In the hot region, they were able able to reach the same temperature. The power consumption was calculated to be 0.34W, from which 17% was transferred to the microfluidic channel [14].

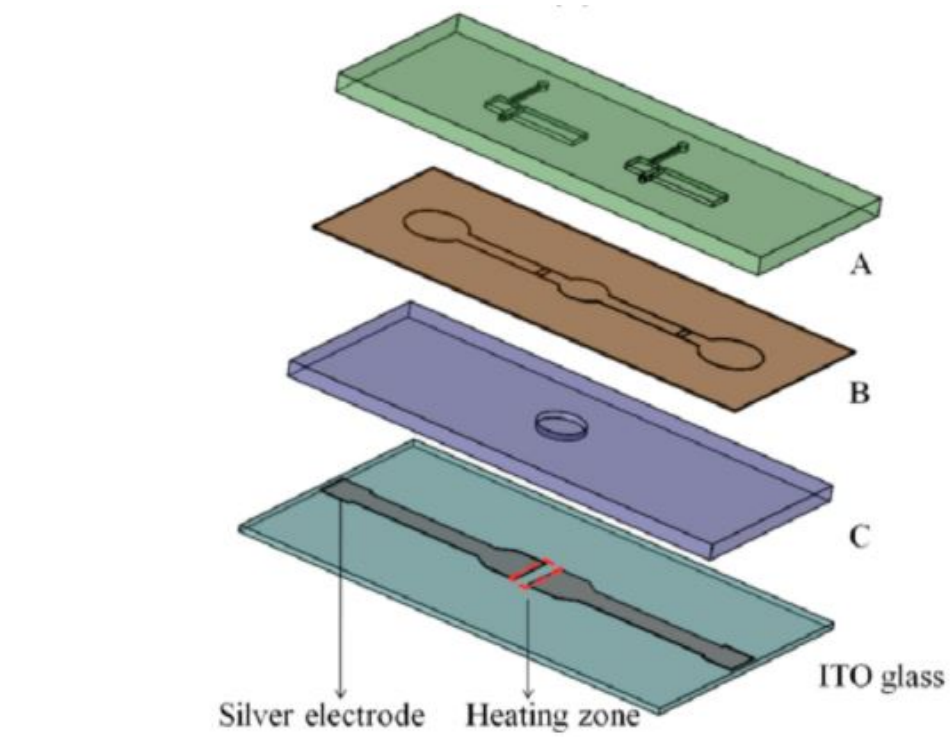

(a)

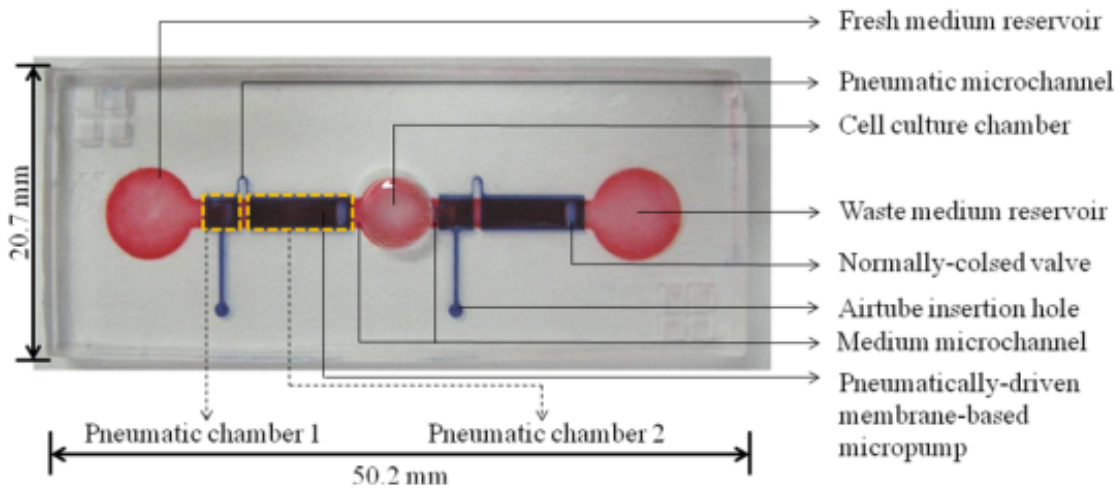

(b)

Figure 7: (a) A schematic drawing of the layout designed by Jr-Lung Lin. Where A, B and C are microfabricated PDMS plates. The last rectangular plate is a silver electrode-patterned ITO glass layer [13] (b) Top view of the microfluidic cell culture chip [13]

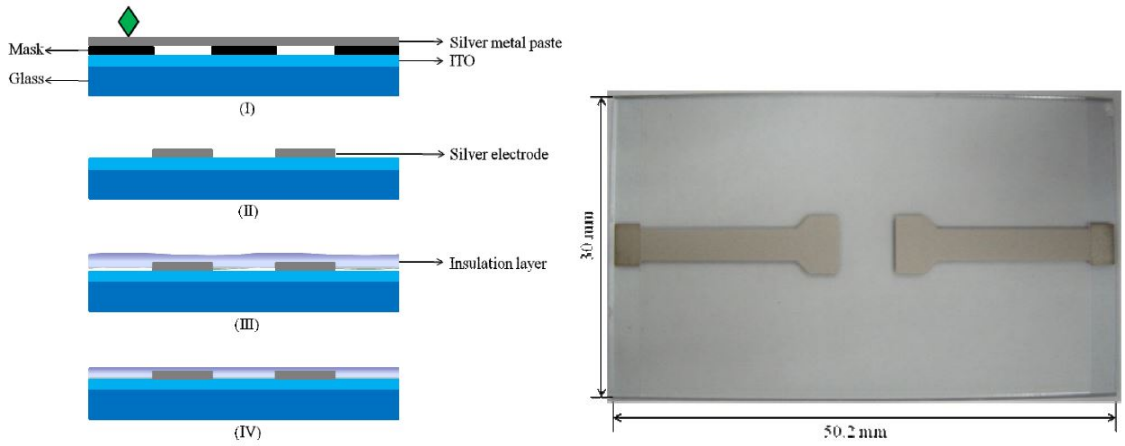

(a) (b)

Figure 8: (a) Process steps of the creation if the ITO-glass microheater [13] (b) ITO-glass microheater [13]

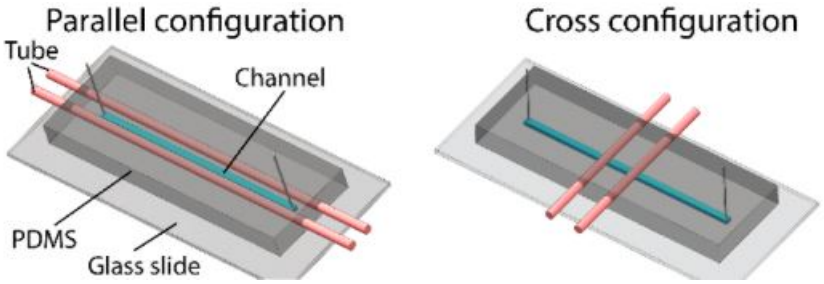

(a)

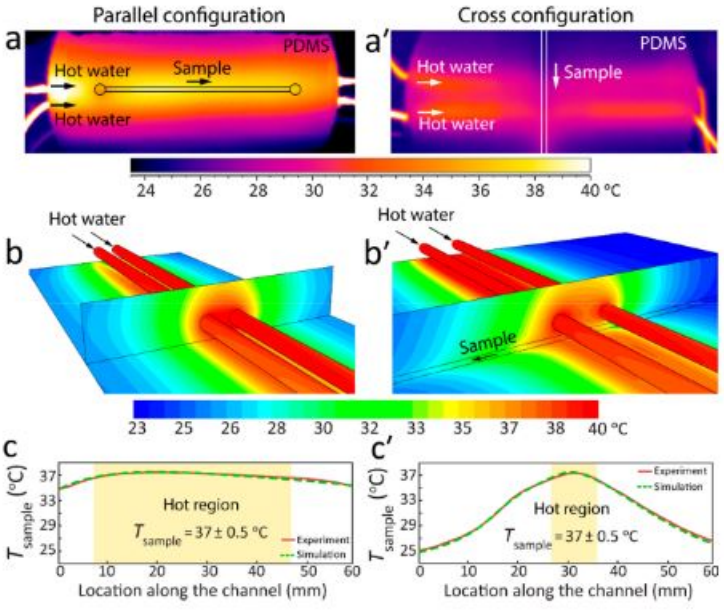

(b)

Figure 9: (a) Parallel and cross configuration of the design of Jiu Yang Zhu et al. [14] (b) Result that were obtained by Jiu Yang Zhu et al. [14]

2.1.3 Sensor

To know if the liquid and cells are correctly heated, a temperature sensor will be needed. In the following sub-chapters, several sensors will be discussed.

2.1.3.1 Thermocouple

A thermocouple exists of two dissimilar metals that are bonded to each other at one end of both wires [15]. This end is exposed to the environment you want to measure, and when there is a temperature difference between the end, where the two metals are bonded, and the other end, a voltage will appear between the two wires where they are not connected [15]. This working principle can be seen in Figure 10.

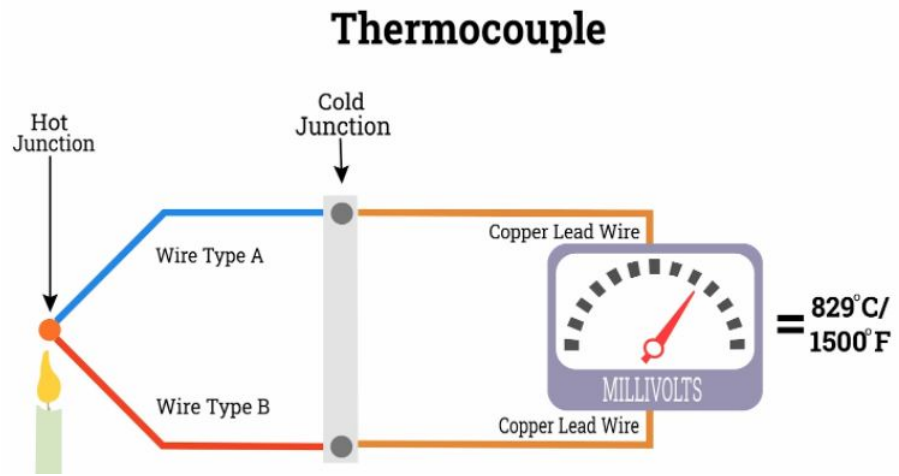

Figure 10: Principle of a thermocouple [16]

2.1.3.2 RTDs

Resistance Temperature Detectors (RTDs) work on the principle of the change in electrical resistance in pure metals due to heat. They are characterized by a positive temperature coefficient [15]. A schematic drawing of an RTD can be seen in Figure 11.

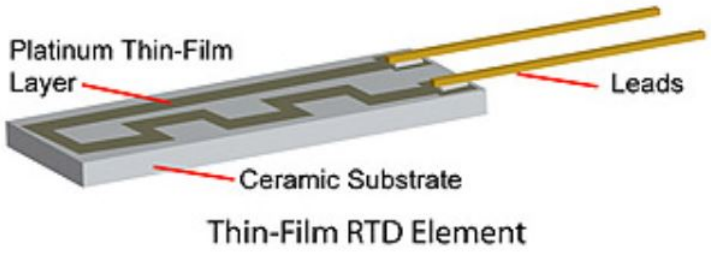

Figure 11: Schematic drawing of an RTD [17]

2.1.3.3 Thermistor

The concept of a thermistor is the same as that of the RTD. The only difference is that instead of metals, polymers or ceramics are used. See Figure 12 for a schematic drawing.

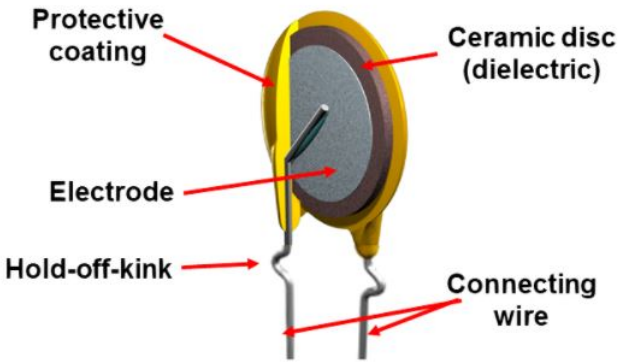

Figure 12: Schematic drawing of a thermistor [18]

2.1.4 Controllers

For the OoC, the temperature must be regulated around 37 °C. To be able to do that, a controller is needed. Three different types will be discussed in this design proposal.

2.1.4.1 On-Off controller

An On-Off controller works as follows. A setpoint is set to a specific temperature. When that temperature is exceeded, the controller will turn the heater off [19]. Until the temperature has dropped down to a specific point (below the hysteresis), the heater is turned on again [19]. A graph of the controller can be seen in Figure 13.

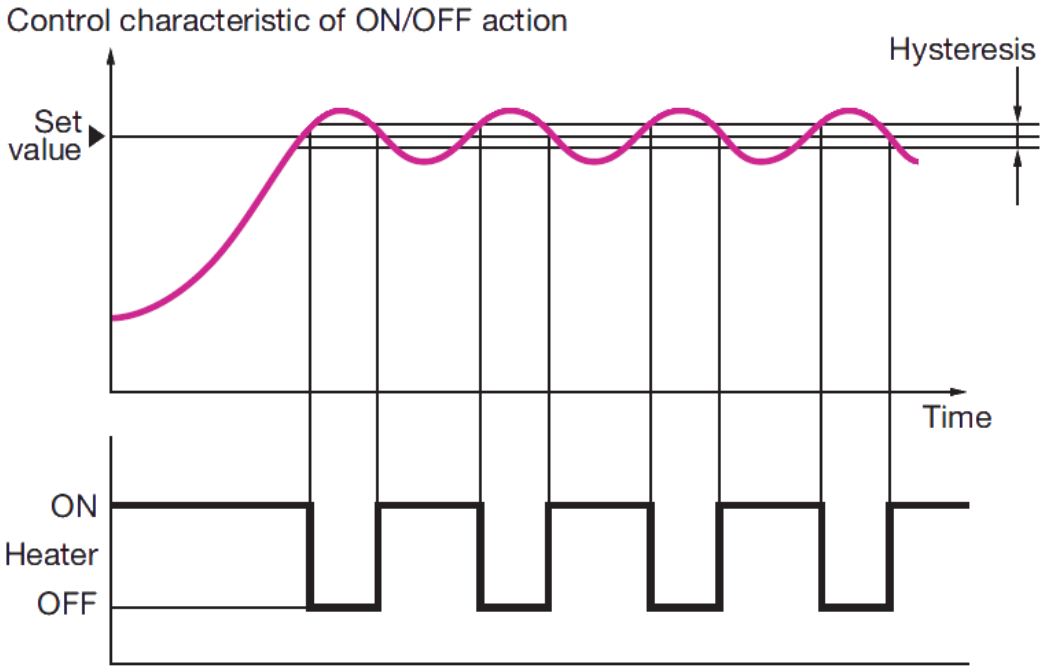

Figure 13: Graph of an On-Off controller [20]

2.1.4.2 Proportional controller

A proportional controller creates a proportional band around the setpoint [21]. When the measured temperature is inside this band, it changes the amount of power provided to

the heater [21]. It slows down the heater as it approaches the setpoint, which reduces the overshoot in comparison to the ON-Off heater [21]. A graph of how the proportional controller works is visible in Figure 14.

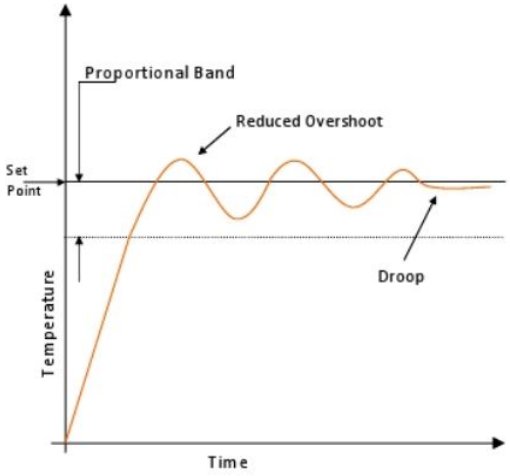

Figure 14: Graph of the proportional controller [21]

2.1.4.3 PID controller

A PID controller is a combination of a proportional, integral and derivative controller. The derivative turns the heater off if the setpoint is approached too fast [21]. The interval compensated for the droop caused by the proportional controller [21]. A graph of the PID can be seen in Figure 15.

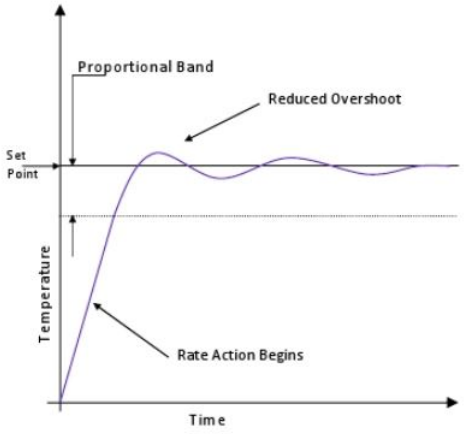

Figure 15: Graph of a PID controller [21]

2.1.5 Bubble Trap

When a fluid is heated up, the concentration of dissolved gasses that the medium can hold changes which cause bubbles to appear, the problem with these bubbles is that they can damage the cells due to shear stresses caused by the surface tension of the bubbles. A bubble trap is needed to remove these bubbles. In Figure 16, a schematic drawing of a bubble trap is visible. In the bubble trap, the fluid containing the bubble enters the inlet of the bubble trap and passes along a micro-porous membrane. The bubbles can escape

the fluid through this membrane and go out of the bubble trap via the back outlet [22]. The fluid, containing no bubbles, exits the bubble trap through the outlet. There are two types of bubble traps: active bubble trap and passive bubble trap. The difference between an active and a passive one is that a vacuum pump is used to suck out the air bubbles for an active one. For the passive, no vacuum pump is used [22].

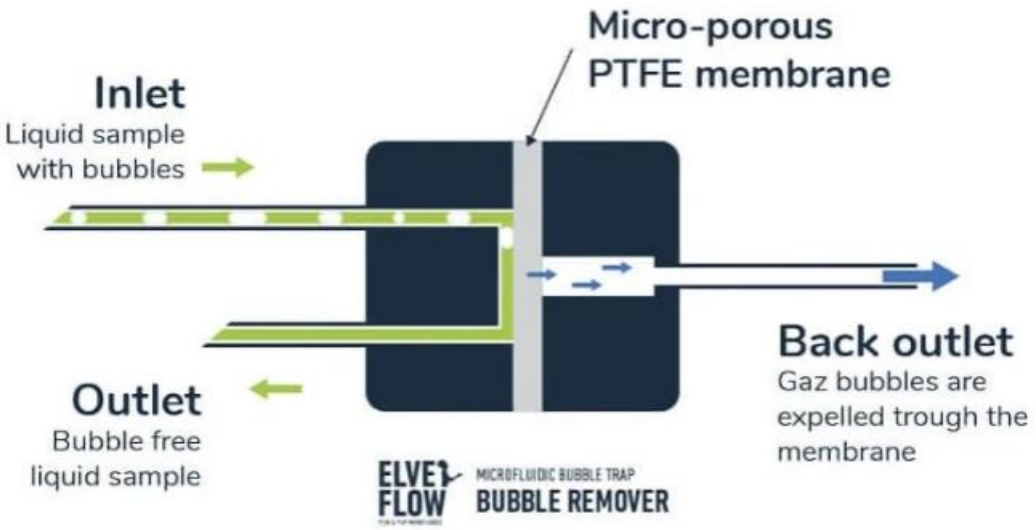

Figure 16: A schematic drawing of a bubble trap [22]

2.2 Design Approach

In this chapter, the decision for the components is made.

2.2.1 Heater

Three types of heaters have been discussed in the previous chapter: Peltier element, joule heating, and heating by the use of water/air. A comparison between the types is made here.

As seen from the previous chapter, each heater used in the research was precise enough to keep the deviation from the preferred temperature to be no larger than ± 0.5°C. This means that any of the heaters can follow the requirement that the temperature of the fluid and cells should be 37 ± 0.5°C. The precision of the controller will mainly influence the accuracy of the heaters. To be able to make a decision, the advantages and disadvantages should be taken into consideration.

The advantage of using a Peltier element is that when the OoC is overheated, you can switch the current to cool the OoC down. There are also Peltier elements having a hole in the middle, which makes using a microscope possible. A disadvantage is that Peltier elements might have a large power consumption. It will also increase the thickness of the holder.
An advantage of using joule heating is that there are transparent heaters. An example is an ITO heating film. Another advantage is that these films are thin and will not increase the thickness of the holder much. A disadvantage is that when the OoC is heated up too much, the only way to bring down the temperature is by turning off the heater which will take some time to cool down.
An advantage of using heated water/air is that it can be easily integrated into the holder's design. A disadvantage is that a separate reservoir and fluid/air pump will be needed.
These advantages and disadvantages are summarized in Table 3.

Table 3: Advantages and disadvantages of the heater types

Heater	Potential advantages	Potential disadvantages
Peltier	• Hole for optics • Cooling when too hot	• Thick • Might need a lot of power
Joule heating	• Transparent options • Thin	• No cooling
Water/Air	• Easily to integrate into a design	• Several components needed • moving components

Since the water/air heater will need several separate components, which might complicate the OoC platform, this option will not be chosen. To decide between the Peltier element and Joule heating, some simulations to know if the Peltier element will use much power will be made. The final decision will be made in the next step according to the results of the simulations. However, Peltier might be preferred since it could cool down the chip rapidly, which makes it possible to preserve the state of the cells in a specific condition.

2.2.2 Temperature sensor

Three types of sensors have been discussed in the previous chapter. To chose a sensor type, a comparison will be made.
In Table 4 an overview of the general specs of the components is given. From this table, it can be seen that the accuracy of the thermocouple is not enough. This would mean that the thermocouple would not be able to be an option. Both RTD and thermistor have an accuracy that is high enough. The thermistor has the fastest response time. When looking at all these points, the thermistor would be the best choice. However, if the advantages and disadvantages of each type are taken into account, which is visible in Table 5, it would be more beneficial to choose the RTD since it is almost linear. However, it has the slowest response time. However, thin film RTDs have a better response time. The thin film RTD (Pt100 Elements, Thin Film (100Ω)) provided by Farnell has a thermal response time of 0.1s [23]. Another advantage of choosing RTD over thermocouple and thermistor is that an RTD is flat. The thin film versions of a thermocouple and the thermistor are not entirely flat due to a ball at the end of the thermocouple/thermistor. This will make it hard to guarantee that the thermocouple or thermistor is connected to the OoC. Images of a flat RTD, Thermistor and thermocouple can be seen in the Figures 17a-17c

Table 4: Comparison of the sensors

Specifications	Thermistor	RTD	Thermocouple
Temperature range	-100 to 450°C	-250 to 900°C	-270 to 1800°C
Accuracy [24]	± 0.1°C	± 0.01°C	± 0.5°C
Output type [24]	Resistance	Resistance	Voltage
Excitation [24]	Voltage source	Current Source	None required
Response time [25]	Fast (0.10 to 10s)	Generally slow (1 to 50s)	Fast (0.12 to 10s)

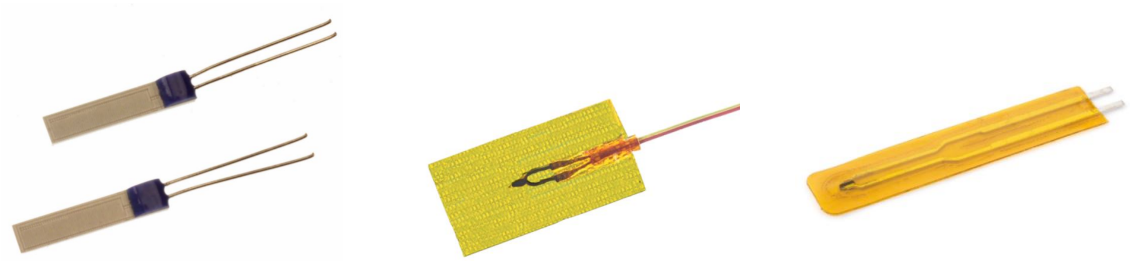

(a) (b) (c)

Figure 17: (a) Thin film RTD, smallest dimensions: 1.2x1.6mm [23] (b) Thin film thermocouple, dimensions: 20x12x0.13mm[26] (c) Thin film thermistor, dimensions: 15x75mm [27]

2.2.3 Controller

Three types of controllers have been discussed in the previous chapter. Now one type will be chosen. A comparison between the types will be made.
Though the On-Off controller is the most simple one of the three, it is also the least stable. As can be seen in Figure 13 there will always be an over-or undershoot. This is because the On-Off controller can only turn the heater on or off. This means that the setpoint will

Table 5: Advantages and disadvantages of the sensors [28]

	Advantages	Disadvantages
THERMOCOUPLES 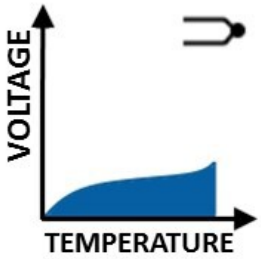	✓ Simple ✓ Rugged ✓ Inexpensive ✓ No external power ✓ Wide temperature range ✓ Variety of styles	× Nonlinear response × Small sensitivity × Small output voltage × Requires CJC × Least stable
RTD 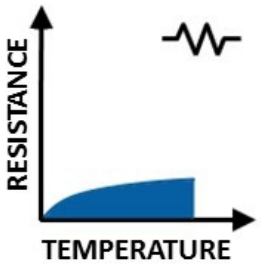	✓ Most stable ✓ Good Linearity ✓ Most accurate	× Low sensitivity × Externally powered × Costly × Small output resistance × Self-heating error
THERMISTOR 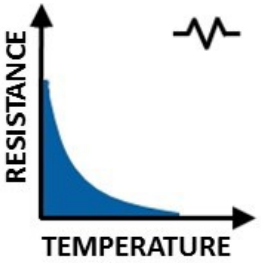	✓ Fast ✓ High output ✓ Minimal lead resistance error	× Limited temperature range × Externally powered × Nonlinear × More fragile × Self-heating error

not be reached.
The proportional controller is more stable than the On-Off controller, but it will not reach the setpoint just like the On-Off controller. This is due to the proportional controller creating a droop, which can be seen in Figure 14. Though it can reach a value that is close to the setpoint.
The PID is the most stable one of the three. Due to the integral and derivative controllers that are added in comparison to the proportional controller, the PID can reach the setpoint the best, as can be seen in Figure 15.
In Table 6 the advantages and disadvantages of each controller is summarized. Since the PID controller is the fastest, most stable, and acutely reaches the setpoint, it has been chosen for the design. Though it is the most complicated one, the advantages of the PID weigh heavier than the complexity since temperature control is critical.

Table 6: Comparison between the controllers

Controller	Potential advantage	Potential disadvantage
On-Off	• Simplest	• Least stable • Under- and Overshoot
Proportional	• Okay stability • Okay speed	• Droop
PID	• Fastest • Reaches setpoint the best • Most stable	• Most complicated

2.2.4 Materials

In this section, some materials that can be used as insulation is discussed. Insulation will be needed because by using insulation, it is possible to reduce the energy required to heat the chip and fluid. This is because less heat will be wasted by heat dissipation to the environment. The OoC material used in this project is glass, which has a thermal conductivity of 1.4 W/m K [7]. For the material that insulates it, the material must have low thermal conductivity. Granta Edupack was used to find materials with thermal conductivity of lower than 0.15 W/m K. The materials were also filtered for materials that can be 3D printed. This was done since 3D printing gives a lot of freedom in the form of the design. Another advantage is that it is ideal for prototyping. The list of materials that were obtained can be seen in Figure 18. The 3D printers that are available at the Departure of PME labs are Prusa and EnvisionTEC. For the start of the project, PLA will be used as an insulation material. The reason for this is that it has a low thermal conductivity of 0.13 W/m K.

2.2.5 Bubble trap

Since it is not the goal of this project to design a bubble trap, a commercially available one will be chosen. It will be a passive one to reduce the complexity of the design.
It is helpful to have an as small as possible bubble trap since that will require less heating. Some examples of bubble traps can be seen in Table 7. The last one should be chosen from the ones in the table since it is the smallest and which means it needs the least amount of heat to be heated.

Figure 18: List of materials that have a thermal conductivity lower than 0.15W/m K and are 3D printable, created by the use of Granta Edupack

Table 7: Specifications of some commercially available bubble traps

Bubble Trap	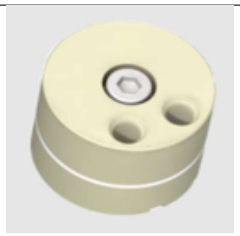		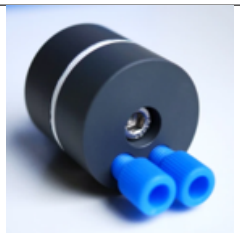	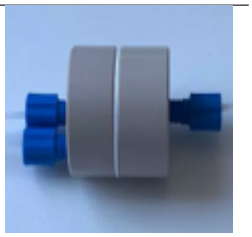
	[29]	[30]	[31]	[32]
Volume	115μL	32-362μL	44-320μL	25-300μL
Flow rate	up to 5mL/min	from 5μL/min	from 5μL/min	0-60ml/min
Max. Pressure	2bar	2.07bar	2.07bar	max. 2.07bar
Dimensions	3.2x3.2x2.2cm	47x34x28mm	30x30mm	30x28mm
Autoclave	No	Yes	No	No
Price	N/A	€137-147	€117-127	$93-138

2.2.6 Heating tubes

As mentioned in the requirements, the fluid/air must be heated before it enters the chip. A possible way is to heat the tubes before entering the holder. This can be done by a resistive wire spiralled around the tube that heats up when a current is applied. A temperature sensor will be needed to measure the temperature. One commercially available option is the heated tubing by Watlow [33]. These heated tubes have a temperature sensor inside of them. The smallest inner diameter is 0.8mm [33]. An image of the tubes can be seen in Figure 19a. If the distance between the bubble trap and the chip is small enough so that the fluid/air does not cool down, there is only a need for heated tubes before the bubble traps. Another option is to use heating plates and stick the tubes and bubble trap on top of it. An example of this idea can be seen in Figure 19b. This plate pre-heats and post-heats the fluid and a microfluidic chip.

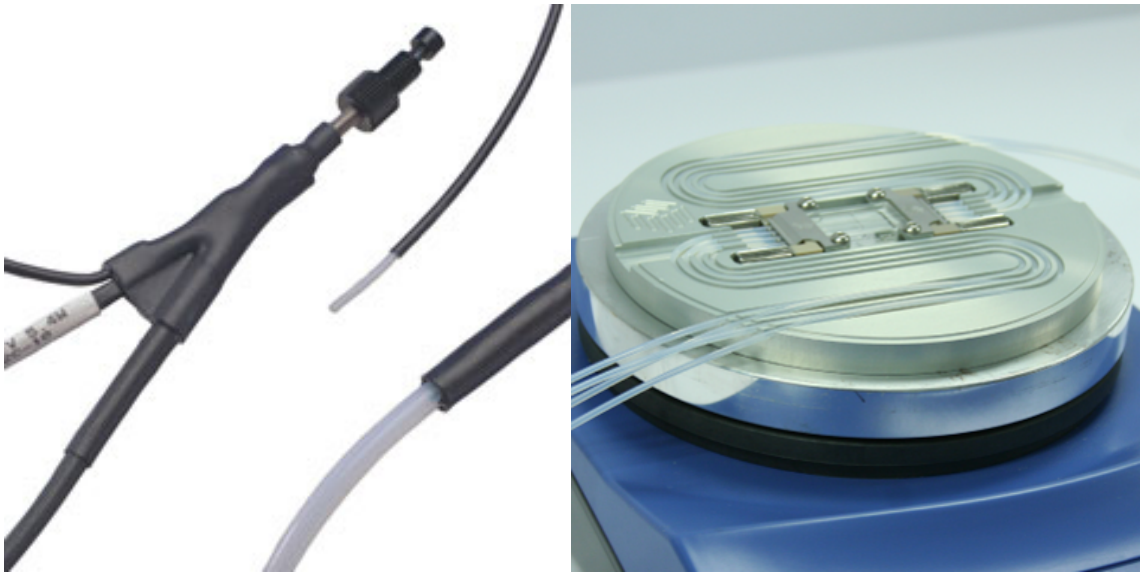

(a) (b)

Figure 19: (a) Heated tubes by Watlow [33] (b) A hotplate which pre and post heats the fluid and a microfluidic chip [34]

2.3 Designs

In this chapter, some concepts will be explained as well as the overall design.

2.3.1 Design concepts

The four design ideas can be seen in Figure 20. All four designs have a viewing hole. The function of this hole is that the cells can be seen when a microscope is used. This hole could be covered/modified with glass or another type of material that is transparent. If another material is used for insulation that is transparent in a later stage of the design project, no hole will be needed. Another point of attention is that no heat sinks are added in any of the designs. A heatsink might be required, but that will be determined later in the design project. In all the designs, the sensor is placed on top of the OoC, directly above the cells. This is done so that the temperature can be measured as accurately as possible. The inlet and outlet of the fluid/air are shown in all four designs. No electrical connections are drawn in these designs.
The first design (Figure 20a) is a design where a Peltier element is used. This Peltier element is one where a hole is in the middle so that the cells can be seen using a microscope. This means that this is one Peltier element. The red part of the Peltier element is the hot side of the Peltier element. The blue part of the Peltier element is the cold side of the Peltier element. If the current is reversed, the cold and hot sides will switch, which causes the chip to cool down. In this design, the holder and the insulation material are not the same. This design can be used if the insulation material itself is not strong enough to clamp the OoC.
The second design (Figure 20b) is almost the same as the first design. The main difference is that in this design, the holder and insulation material is the same. This design can be used if the insulation material is strong enough to clamp the OoC platform.
The third design (Figure 20c) is a design where a Joule heating thin film is used. As an example, this thin film could be ITO but does not need to be the case. The thin film is a bright green line in the image. The bright blue colour is glass to support the thin film. If the thin film is strong enough to hold the OoC, this glass might not be needed. In this design, the holder and the insulation material are not the same. This design can be used if the insulation material itself is not strong enough to clamp the OoC.
The second design (Figure 20d) is almost the same as the third design. The main difference is that in this design, the holder and insulation material is the same. This design can be used if the insulation material is strong enough to clamp the OoC platform.

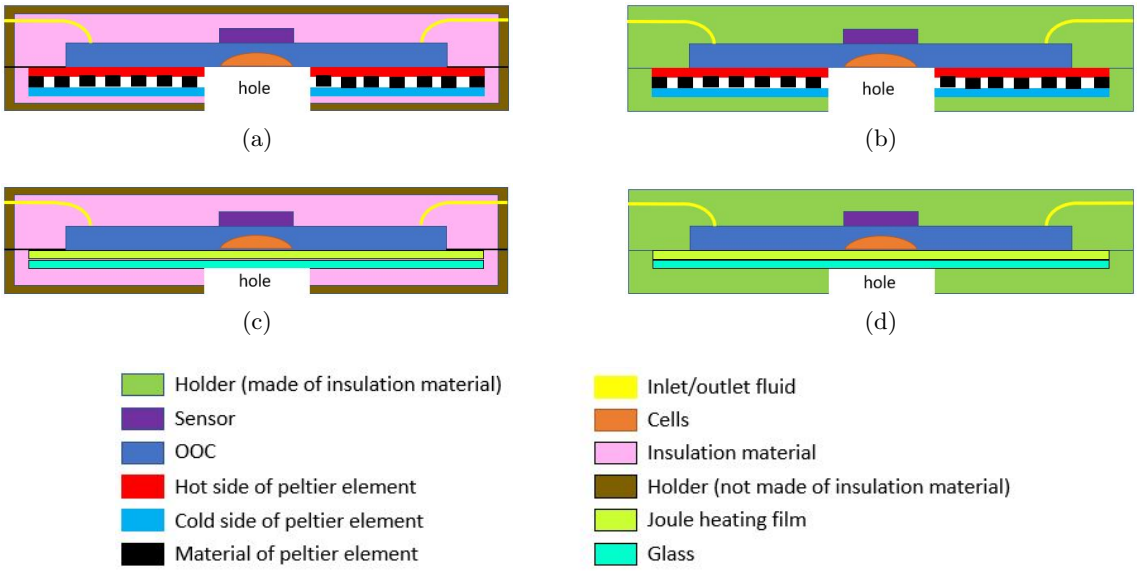

Figure 20: (a) Peltier design where the holder and insulation material are not the same (b) Peltier design where the holder and insulation material are the same (c) Thin film Joule heating design where the holder and insulation material are not the same (d) Thin film Joule heating design where the holder and insulation material are not the same (e) Legend

2.3.2 Overall Design

The holder for the chip with the temperature control system is a part of a bigger picture. In Figure 21 a schematic drawing is given of the OoC platform. This picture is an adaptation of the schematic illustration made by Haoyu Zhu [2]. In this figure, the Oxygenator is visible. This Oxygenator is being designed by Matthijs Reeuwijk [4]. This device lowers the concentration of oxygen in the medium [4]. This Oxygenator could create bubbles, so the Oxygenator must be placed before the bubble trap. To ensure that the oxygen concentration inside the medium is correct at the right temperature, the Oxygenator and the liquid should be heated at 37°C. The next point where heating is of great importance, before the chip, is at the bubble trap. The temperature of the medium and the bubble trap should be 37°C. This is because when a medium is heated, the concentration of gasses that it can hold changes which cause bubbles to appear. The temperature from the bubble trap to the chip should approximately stay at 37°C. Though if it cools down a bit, it will not be a big problem since, in the chip, the liquid has some time to heat up again before it reaches the cells. But this can only be done for minor deviations. More research will be done on this in the next step of the design project. The Oxygenator will not be taken into account in future steps since the main goal of this research is the temperature control of the chip.

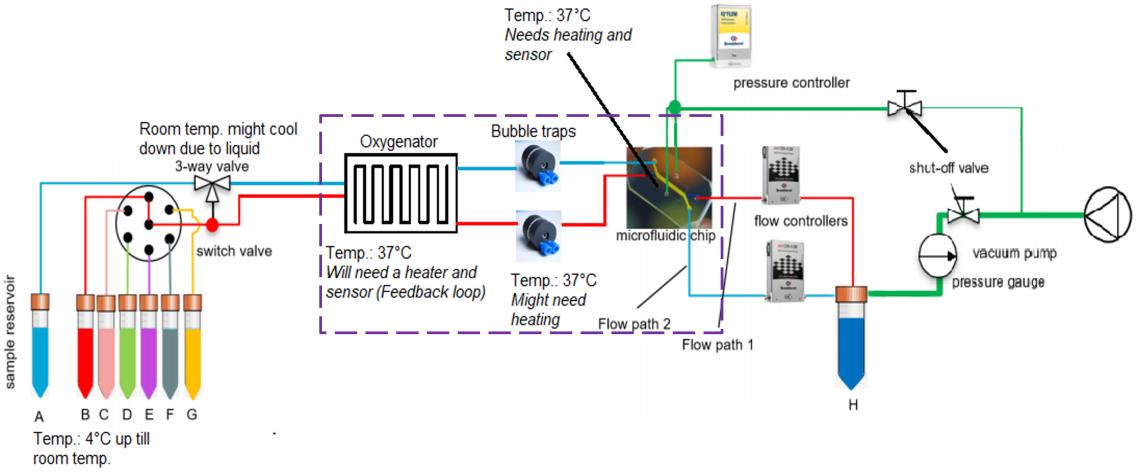

Figure 21: Schematic drawing of the OoC platform. The purple dashed line shows where the temperature control system will be used. This image is an adaptation of the image created by Haoyu Zhu [2]

3 Temperature Control System For Organ-on-a-Chip applications

A temperature control system for Organ-on-a-Chip applications

Abstract- An Organ-on-a-Chip (OoC) is a microfluidic device that mimics an organ function on a chip. The goal of the OoC technology is to create disease models of various organs and use them to minimise animal testing. One of the important parameters to maintain the cells/tissues on the OoC is the temperature, typically at 37 °C. Usually, cell culture incubators are used to maintain the temperature of cells on the OoC. However, it is inconvenient for external flow control instrumentation to interface with OoC inside the incubator, and other temperatures being not possible. Therefore, an on-chip temperature controller is needed. In this report, a temperature control system for an OoC is designed, implemented and tested. To cover a wide temperature range, multiple peltier elements are chosen to confine the temperature control only at the region close to cell chambers in the OoC. A resistive temperature detector (RTD) is used as feedback to control the temperature by a proportional-integral-derivative (PID) controller. To avoid any heat loss beyond the Organ-on-a-Chip, a 3D-printed polylactic acid (PLA) holder with good thermal insulating properties is used. The holder is designed for four chips to accommodate control chips along with test chips. A dedicated PCB with control electronics is designed and implemented to control the temperature on all four chips powered by a battery. A temperature uniformity of +/- 0.7 °C of 19 mm at 68 L/min and 23 mm at 10 L/min along a total microfluidic channel length of 40 mm (from inlet to outlet), a width of 5 mm, and a depth of 0.3 mm before compression, was achieved. The response time to recover from changes in the temperature is approximately 2 minutes. With a power consumption of 0.84 Watts per chip to maintain 37 °C, four chips can function on a 20000 mAh battery for a minimum of 4.5 hours (only cooling at a minimum of 18 °C) and a maximum of 8.3 hours (only heating at 37 °C) before recharge. The temperature control system was tested on Hepatocytes and Cholangiocytes for liver-on-a-chip applications, which showed that the oxygen disappearance rate is 9.87 times faster when maintained at 37 °C compared to room temperature.

1 Introduction

An Organ-on-a-Chip is a microfluidic chip that simulates the microenvironment of organs in terms of tissue interfaces, and mechanical stimulation [1]. This is done by perfusing media that mimics blood or other substances inside of the body. By doing this, the stresses that the cells feel are similar to those inside the human body. A schematic drawing of an OoC can be seen in Figure 1, where the cells are placed at the bottom of the OoC. A fluid flows through the channel, which creates shear stresses. The benefit of OoC is that human cells can be used when new drugs are tested, which means that animals are no longer needed for drug testing, and thus less harm will be done to these animals [2]. The animal cells that were used do not represent human cells well [2]. In addition, it will help with creating personalized medicine by using cells similar to that of the patient [3]. Another benefit of OoCs is that it can help with the acceleration of developing medicines [3]. Since OoCs are relatively cheap to make with in-house components [3, 4]. To use these OoCs, a system is needed to perfuse medium and air through these chips. One system that is able to do this is the OoC platform designed recently by Zhu et al. (2022), which can be seen in Figure 2a. This platform can hold eight reservoirs and have flow rates from 1.5 to 68 $\mu L/min$ for liquids, and 1.3 to 20.7 mL/min for vacuum [5]. The system is portable and can be used under a microscope. One aspect that this system is missing is temperature control. The average body temperature of a human is 37 °C [6]. Thus, when these experiments are done at room temperature, the cells might behave differently from how they would behave inside a human body [7]. The research question is: How to build a portable local temperature control system for Organ-on-a-Chip applications?

There are several design considerations to set up this heating system. The first one is the holder design being able to hold four chips simultaneously so that multiple experiments can be done simultaneously. The idea is that all chips can be accessed without interfering with other chips. Next, the heater and sensor components are placed outside of the chip to prevent direct contact with the medium. Also, the components of the sensor or heater could be toxic to the cells.

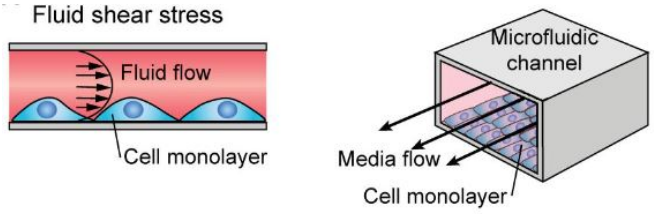

Fig. 1: *Schematic drawing of OoC where fluid shear stress can be seen as an active biomechanical stimulus [8]*

The system response time is considered as 2-3 minutes since cells do not immediately respond to small temperature changes [10]. The system should try to keep the cells at 37±0.5 °C to be at the optimum temperature. Another requirement is that the system should have a viewing window so that the cells

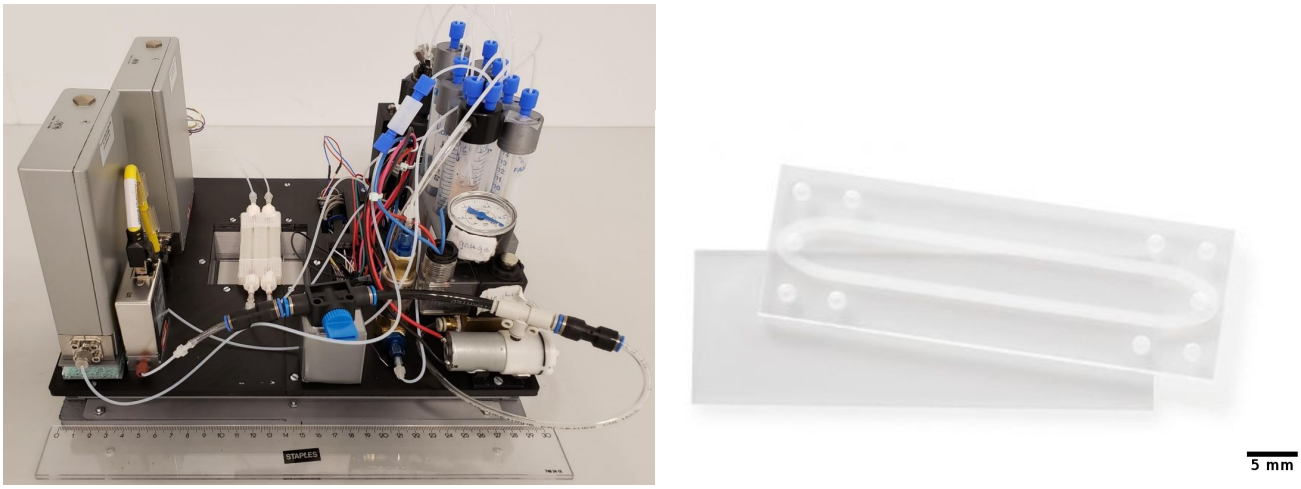

(a) **(b)**

Fig. 2: *(a) OoC platform with dimensions of: 290 mm x 240 mm x 220 mm [5] (b) Micronit chip dimensions: 45 mm x 15 mm x 2.1 mm [9]*

TABLE I: *Required specifications and components used in the system*

Components	Variety	Specifications	Type	Brand	Model key
Heater	Temperature at the cells and medium Precision	37 ± 0.5 °C 0.1 °C	Peltier	Artic Tec Tegnologies	MTEC-0.2-1.2-0.12-71-3/5
Temperature sensor	Resolution Interference with cells Response time	0.1 °C No 2-3 min	RTD	TE Connectivity Measurement Specialties	NB-PTCO-058
Battery	Duration heating Max power consumption	0.5 hour(s) 24.28 W	Powerbank	GRIXX	-
Controller	Response time	2-3 min	PID (Arduino)	Arduino	ATmega2560
Holder	Number of chips Chip dimensions Transparent Clamping	2 45x15x2.1mm (Micronit) One side No leakage	-	-	-

can be monitored via a microscope. The portability of the system is another important aspect so that the experiments can continue while transferring OoCs from one lab to an other lab. As mentioned above, in the literature survey, the duration of the battery should be 30 minutes. It is preferred to be able to cool down the cells to a temperature of 4 °C so that a particular state of the cells can be preserved [11]. In Table I, the requirements can be seen.

2 Materials and Method

2.1 Materials

A list of the used components can be seen in Table I. For the complete list, see Appendix B, where also the costs of the components are shown.

2.1.1 Chip: For this project, the OoC of Micronit is used. The design is made for this chip but can be modified for other chips. The Micronit chip with dimensions 15 mm x 45 mm x 2.1mm consists of two glass slides [9]. One of the two glass slides has holes for the inlet and outlet and a layer of elastomer attached to it [9]. This elastomer defines the flow path of the chip and functions as a seal for the top glass [9]. By compressing the two glass slides against each other the fluid can flow into the flow path. An image of the chip can be seen in Figure 2b. It is preferred that the channel of the chips, where the cells rest, can easily be monitored with a microscope.

2.1.2 Peltier: For heating the chip, peltier elements were used. They were chosen because they can cool the system as well. The peltier elements used are from ArticTec Technologies and have the dimensions 2.8 mm x 4.4 mm x 2.4 mm [12]. The peltier element can handle a maximum voltage of 0.2 V, and a maximum current of 1.2 A [12]. The maximum temperature difference it can create is 80 °C if the hot side has a temperature of 50 °C, and the cold side -30 °C [12]. To power the peltiers, a 10 channel transistor amplifier was used. A separate power supply can be connected to this device. This is required since the Arduino cannot handle the current needed to power the peltiers. By connecting the Arduino to this device, the Arduino can control how much current can flow to the peltier from the power supply. It was initially decided to connect the peltiers in parallel to control every peltier. This would mean that the maximum voltage is 0.2 V,

and the maximum current is 9.6 A for one chip. The problem with this is that the 10 channel transistor amplifier cannot handle voltages this low. Therefore, another power supply and a relay to achieve low voltages would be needed. Furthermore, one 10 channel transistor amplifier can be used for one chip in this case, which would mean that four 10 channel transistor amplifiers will be needed for four chips. Another problem is that the Arduino runs the code line by line, which means that the peltiers will not work simultaneously but one after the other. The Arduino will also likely not have the computational power to control eight peltiers in parallel which means several Arduinos will be needed. Besides, the number of connections needed for one chip will be 16. This will complicate the system. Therefore peltiers connected in series is preferred. For a series connection, the maximum voltage for one chip will be 1.6 V and a maximum current of 1.2 A. This voltage is high enough to work with the 10 channel transistor amplifier. The number of connections per chip will be reduced to only two, which means that one 10 channel transistor amplifier is needed to connect all four of the chips. A comparison can be seen in Table II.

2.1.3 Sensor and PID: The NB-PTCO-058 RTD sensor was chosen because this sensor has a wide temperature range of -30 °C to 200 °C, a quick response time of 0.2 s in water with a speed of 0.4 m/s and 10 s in air for a flow speed of 1 m/s, and has a flat surface to contact the surface of the chip [13]. This sensor measures the temperature by the change in resistance inside the sensor. To read out the sensor, a Wheatstone bridge was used to measure the voltage change produced by this sensor due to the change in resistance. This signal is amplified with an INA125P amplifier and read out with an Arduino Mega microcontroller. A PCB containing these electronics was designed in the EasyEDA software. This PCB is designed to be able to connect 12 sensors simultaneously. A schematic drawing of the connections and the PCB can be seen in Appendix C. The Arduino code to read out the sensor can be seen in Appendix D where the code for controlling the peltier elements is shown as well. The sensor was calibrated using a thermal camera to match the temperature at the bottom of the chip. For the PID control, the PID_v1 library from Brett Beauregard was used [14].

TABLE II: *A comparison between connecting the eight peltier elements in series and in parallel for one and four chips*

	Series	Parallel
Total max Voltage	1.6 V (1.6 V for 4 chips)	0.2 V (0.2 V for 4 chips)
Total max Current	1.2 A (4.8 A for 4 chips)	9.6 A (38.4 A for 4 chips)
Number of connections	2 (8 for 4 chips)	16 (64 for 4 chips)

2.2 Methods

To heat the microfluidic chip, a heater is needed. Uniformity and not interfering with the cells are important parameters for the heating mechanism. The cell chamber area should not be covered by the heater unless the heater is transparent. Peltier elements were chosen as the heating element because of their ability to cool down the chip, which was preferred. First, a numerical analysis was made to understand the thermal behaviour of the peltier element and the Micronit chip. Then a design was made, which, after several iterations, led to the final design. This design was tested to ensure no leakage occurred. Afterwards, the holder was tested with PID control. Finally, the chip was tested with Hepatocytes and Cholangiocytes.

2.2.1 Numerical Analyses: A numerical analysis was done to understand the heat distribution created by peltier elements on the chip. In the simulations, half of the chip was modelled to reduce the computation time, since the chip is symmetric. The model contained four peltiers and a simplified version of the chip. The model can be seen in Figure 3a. The flow rates were chosen as 1.5 μL/min, 35 μL/min, and 68 μL/min. 1.5 μL/min and 68 μL/min are the two extremes that the OoC platform, designed by Zhu et al. (2022), can provide. The flow rate of 35 μL/min was chosen since this is the flow rate used for the experiments with the liver cell line in the case study. In this simulation, the peltier elements were connected in parallel. The distance between the peltier elements was chosen so that a sensor could fit in between peltier elements. The distance between the peltier elements is 3.07 mm. The peltier element and the sensors are not placed on top of the channel to keep the channel viewable from the top and bottom. The peltier elements and the sensors are placed on top of the chip to provide enough space for the inverted microscope. For the data collection, 15 data points were placed on the bottom of the chip in the area where cells will be placed. The placement of these data points can be seen in Figure 3d.

2.2.2 Design: The final design of the temperature control system can hold four chips of various dimensions simultaneously. Each chip can be operated separately since the lids are opened and closed independently of each other. The holder can hold chips of dimensions up to that of a microscope slide (75 mm x 25 mm), see Figure 3b. Using a separate component, smaller chip sizes can be held. The one in Figure 3c is designed for the Micronit chip. The lid is designed for the Micronit chip (see Figure 2e). The lid design can be adjusted for several chip designs. The lid contains eight peltier heaters, a sensor, two sensor holders and two heatsinks. The peltiers are connected to the heatsink using adhesive carbon tabs. The peltiers are connected in series, as explained before. The sensors are connected to a 3D printed part that also functions as alignment for the peltiers. The sensor is connected to this part using double-sided tape. A cross-section of the lid containing these components can be seen in Figure 3g. A locking system ensures that peltiers touch the surface of the glass. This locking system can be seen in Figure 3f. The idea is that when the lid is rotated downwards, the locks are rotated into the lid and slid to the side. Due to its form, it will not be able to rotate backwards and thus locks the system. The lid

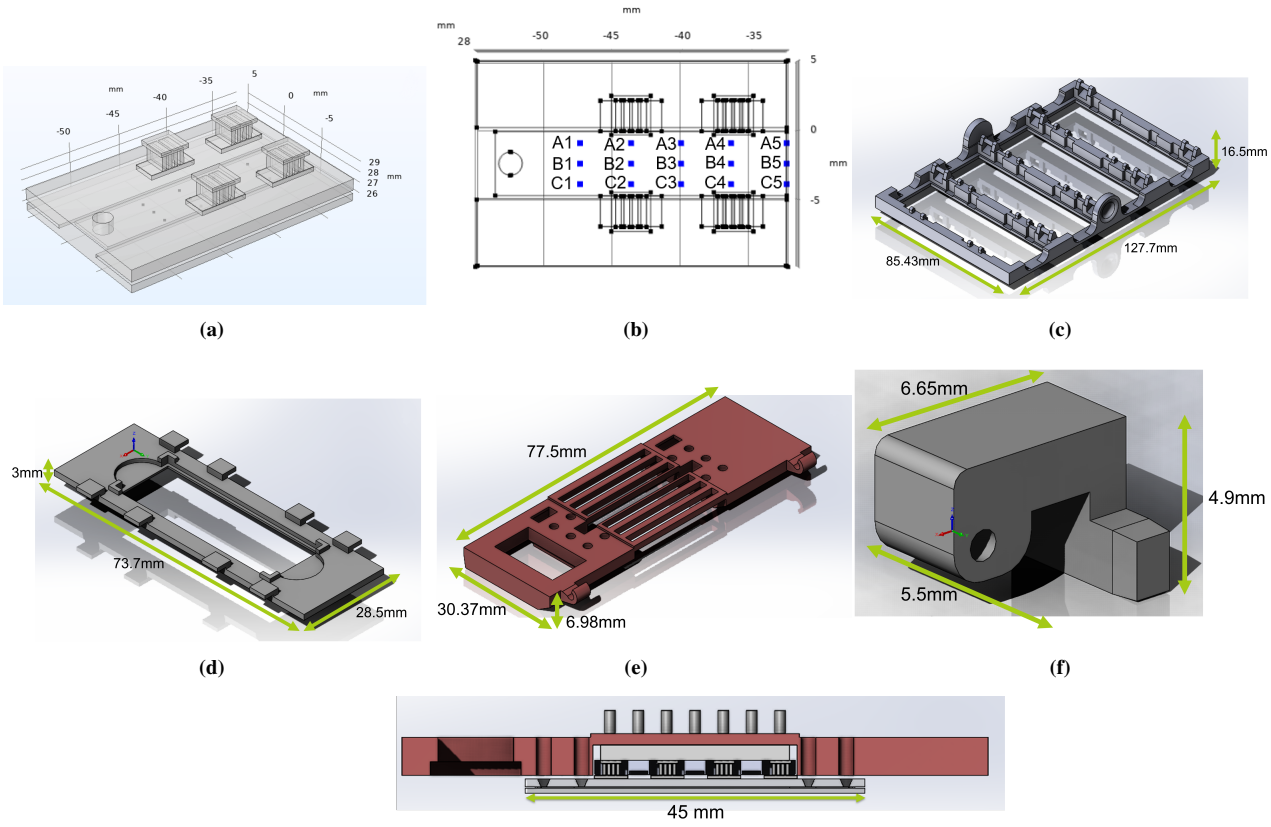

(a) **(b)** **(c)** **(d)** **(e)** **(f)** **(g)**

Fig. 3: *(a) Numerical model using COMSOL Multiphysics v5.6 (b) Data point position (c) Holder that can hold four chips simultaneously of a maximum size of 75mm x 25mm (glass slide) (d) Chip holder: hold the Micronit chip (e) Lid which will hold the heaters and sensor (f) Lock: which makes sure that the system does not open (g) Side cross-section lid with Micronit chip with a length of 45mm*

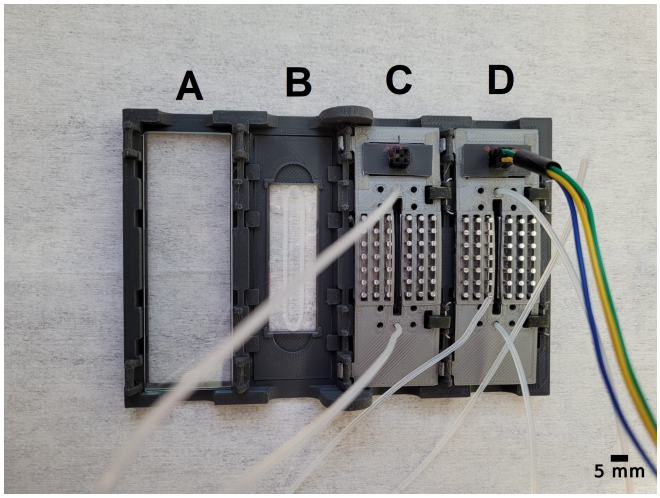

Fig. 4: *In area A a glass slide of the dimensions 75 mm x 25 mm is placed. In area B the chip holder and Micronit chip are placed inside of the holder. In area C the lid is placed with the fluidic connections connected to the lid. In area D a cable is connected to the lid for powering the peltier elements and to read out the sensor*

and the holder were 3D printed using poly lactic acid (PLA) material. As described as in Chapter 2: the literature review, PLA was chosen since it acts as an effective thermal insulator. It has a thermal conductivity of 0.13 W/mK, whereas wood, a well-known isolation material, has a thermal conductivity of 0.12 W/mK. Figure 4 shows what the system looks like when the system is closed. In Figure 5c a schematic drawing of the final setup can be seen. The holder has a mass of 16.92 grams. The lid has a mass of 11.12 grams. The chip holder has a mass of 2.05 grams. The box's design where all the electronics are placed can be seen in Appendix F. It has a mass of 1.37 kg. It has a 20000mAh battery to power the system.

2.2.3 Experimental Setup:

First, some experiments were done with only the peltier element to characterize its behaviour. Next, an experiment was done to check for leakage, and then an experiment was done to check if the heat was reaching the chip, and experiments were done combining the two. Finally, the system was tested with Hepatocytes and Cholangiocytes.

a) The heating and cooling performance of Peltier elements: In the first experiment, the sensor was placed against the peltier element to measure the temperature for heating and cooling. Afterwards, some experiments were done with

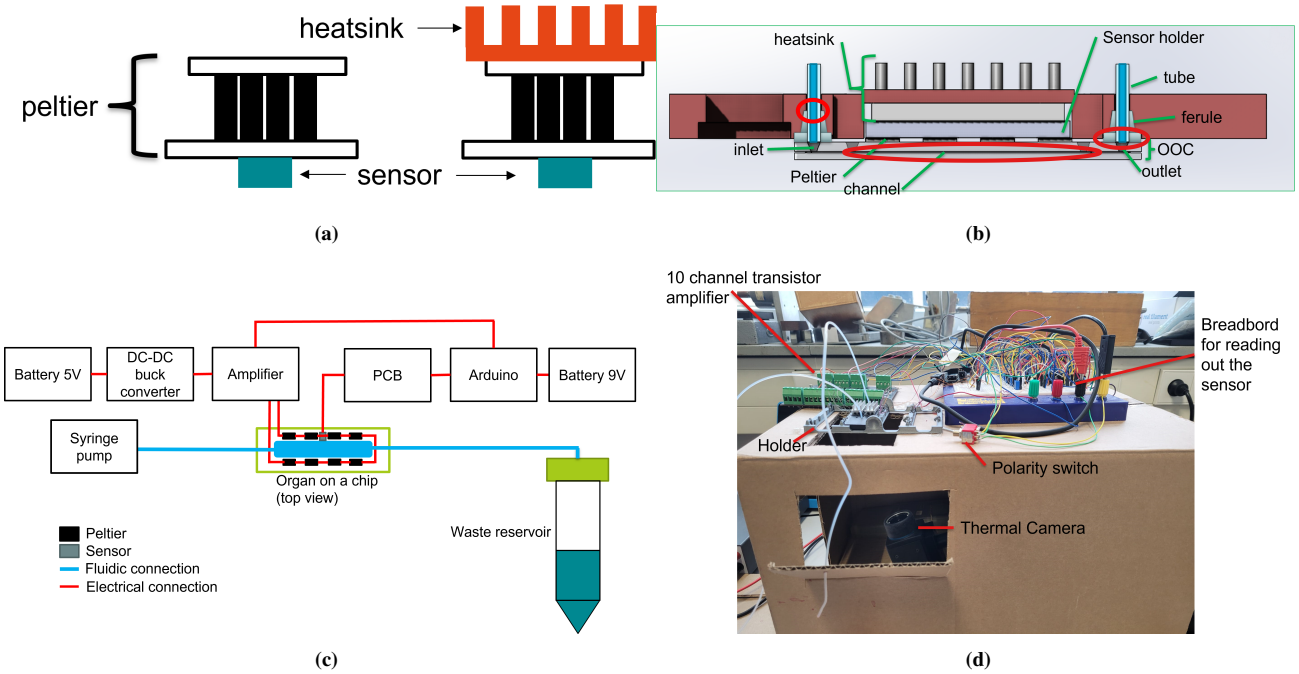

Fig. 5: *(a) Schematic drawing of the experimental setup for the understanding of the thermal behaviour of the peltier elements (b) Side view with ferrules and tubings. The red circle shows the areas of possible leakage (c) Schematic drawing of the electronic connection and the fluid connections (d) experimental setup for heating and cooling, the syringe pump and reservoir are not visible but are used during the experiments*

a heatsink to see the influence of the heatsink on the temperature. Hence the sensor was not calibrated at this point. These experiments were mainly used to understand the peltier's increasing and decreasing temperature properties. However, the formula used was obtained from the sensor's datasheet, which can be seen in the following equation:

$$R_{(T)} = R_{(0)} * (1 + aT + bT^2)[13] \quad (1)$$

Where $R_{(T)}$ is the resistance at a certain temperature in Ohm, $R_{(0)}$ is the resistance of the sensor when the temperature is 0 °C in Ohm, T is the temperature in °C, a is a coefficient with a value of $3.9083e^{-3}$ and b is a coefficient with a value of $-5.775e^{7}$ [13]. This equation was rewritten for the temperature. Thus, most likely, the temperature was not too far from the actual temperature. A schematic drawing of the experimental setup can be seen in Figure 5a. The first experiment that was done was for checking the heating performance for 5 minutes with and without heatsink. The second experiment was cooling from room temperature for 5 minutes with and without a heatsink. At last, the system was heating up for 5 minutes and then cooling down for 5 minutes by switching the current direction. In all the experiments the voltage applied to the peltier element is approximately 0.2 V, which is the maximum voltage that the peltier elements can handle.

b) Leakage: To test for leakage, a dyed DI water was used as liquid. To test this, first, the tube must be placed through the lid's holes from the top. Then the ferrule from Micronit can be slid onto the tubes from the bottom of the lid and pressed into the lid's hole. The chip holder was placed inside the holder to hold the Micronit chip. After placing the chip, the lid can be rotated until the ferrules touch the glass. Then the lid can be locked with the locking system. A syringe pump (kdScientific, LEGATO 111) was used to push the dyed DI water into the Micronit chip. Places where leakage could occur, are between the two glass slides, between the ferrule and the glass slide and between the tube and the ferrule. These areas are shown in Figure 5b. Flow rates of 10, 35 and $68\mu L/min$ and higher were tested until leakage occurred.

c) Influence of PID: The lid was closed in the same way as described above to test the heating system. A thermal camera (FLIR Ax5) was used to see what happens when the

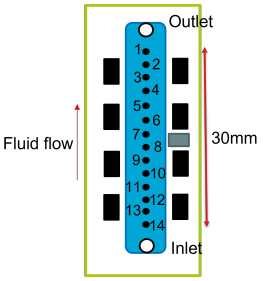

Fig. 6: *A schematic drawing of the chip, where the blue rectangle represents the channel, the black rectangles represent the peltier elements and the green rectangle between the peltier elements represents the sensor. Points 1 to 14 are a representation of the locations where the data was collected by the thermal camera. These points were spread over an area a length of 30 mm, which is the length over which the cells will be placed*

lid is closed. This thermal camera was pointed at the bottom of the chip. By switching on the peltiers, the heating process can monitored by the camera. At 14 points along the channel data was collected using the thermal camera. These points can be seen in Figure 6. These points were placed over a length of 30 mm. This is the same length over which the cells will be placed. This was done with and without PID to understand the influence of PID control with a flow rate of 35 $\mu L/min$. An image of the experimental setup can be seen in Figure 5d.

d) Influence of fluid flow: The temperature profile for the different fluid flows can be seen using the thermal camera. Experiments were done for 1 hour to see how stable the system was over a more extended period, for different flow rates, 10, 35, 68 $\mu L/min$, and 0 $\mu L/min$ (no flow and no liquid). The purpose of the experiment is to understand the influence of fluid flow on the uniformity of the heat.

e) Influence to air turbulence around the chip: After some time, by blowing air against the glass side, the influence of air turbulence is measured. This is done to see how fast the system will respond to temperature changes due to the environment. To check the performance of heating under external air flow, a case study of blowing air in two different periods was realized. After the first 10 minutes of undistributed heating cycle, a 10 second air flow is applied along the chip. Then a second air flow of 1 minute is applied after 10 minutes of undistributed heating cycle. The flow rate was adjusted to 35 $\mu L/min$.

f) Cooling: For cooling, a polarity switch was used. After 15 minutes of heating, the polarity was switched, so the system started cooling, which was done for 10 minutes. Cooling from room temperature was also done for 20 minutes at a flow rate of 35 $\mu L/min$.

g) Hepatocytes and Cholangiocytes: The system was also tested with cells. Two types of cells were used: Hepatocytes (liver cells) and Cholangiocytes (bile duct cells). These cells are differentiated from the HepaRG cell line. These cells were prepared in Erasmus MC at the department of anesthesiology. The cells were placed at the bottom glass slide of the Micronit chip. Then the top glass side was placed on top and inside the holder. The holder was then closed, as described before. The 20,9% O_2 around 150 mm Hg media flushed throughout the system with a flow rate of 35 $\mu L/min$. Using a tunable Opolette 355-I, Opotek, Carlsbad laser [15], the oxygen was measured in the center of the chip when the heater was turned on. After some time, the fluid flow was stopped, and the oxygen was measured. This was done three times. Hereafter the heater was turned off. The oxygen was measured at room temperature with and without fluid flow. The purpose was to see how the heat influences the oxygen consumption of cells. An image of the experimental setup can be seen in Appendix A.

3 Results and Discussion

3.1 Numerical analysis

The results from the numerical analyses can be seen in Figure 7. Figure 7a shows the temperature over time plot at a fluid flow of 10$\mu L/min$. From this graph, it can be seen that the majority of points (A2, A3, A4, A5, B2, B3, B4, B5, C2, C3, C4, C5) are between 35.6 °C and 37.9 °C, which is a temperature difference of 2.3 °C. The greatest temperature difference is 6.3 °C. Figure 7b shows the temperature over time plot at a fluid flow of 35 $\mu L/min$. From this graph, it can be seen that the majority of points (A2, A3, A4, A5, B2, B3, B4, B5, C2, C3, C4, C5) are between 33.6 °C and 37.2 °C, which is a temperature difference of 3.6 °C. The greatest temperature difference is 8.3 °C. Figure 7c shows the temperature over time plot at a fluid flow of 68 $\mu L/min$. This graph shows that the majority of points (A2, A3, A4, A5, B2, B3, B4, B5, C2, C3, C4, C5) are between 30.8 °C and 35.8 °C, which is a temperature difference of 5.0 °C. The greatest temperature difference is 11.1 °C.
Apparently, the fluid flow influences the uniformity of the heat distribution. With a higher flow rate, the uniformity of the heat decreases. This is probably because the higher the fluid flow, the more heat is removed from the system, and the less fast the fluid will increase in temperature. The fluid that flows in with a temperature of 20 °C will take longer to heat up. It needs to be noted that in these simulations, no heatsink was applied. According to the simulations, the power consumption is about 0.15 W.

3.2 The heating and cooling performance of Peltier elements

In Figure 8, the results from the experiments done on the peltier elements can be seen. In Figure 8a, the heating of the

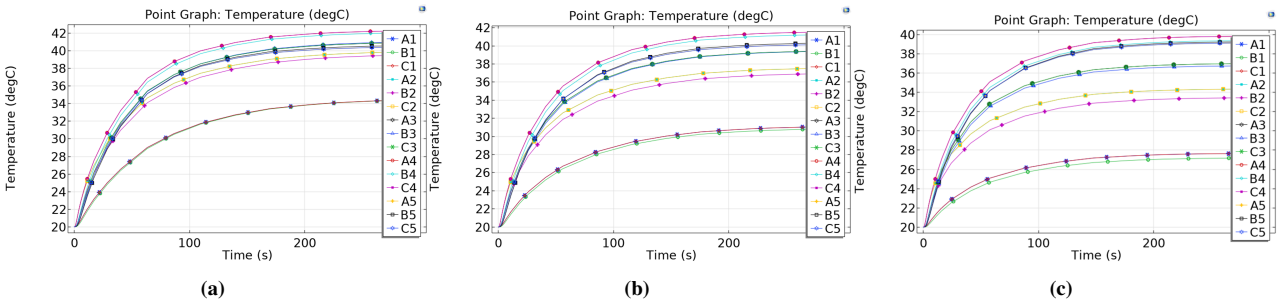

Fig. 7: *(a) Temperature profile for 10 $\mu L/min$ (b) Temperature profile for 35 $\mu L/min$ (c) Temperature profile for 68 $\mu L/min$*

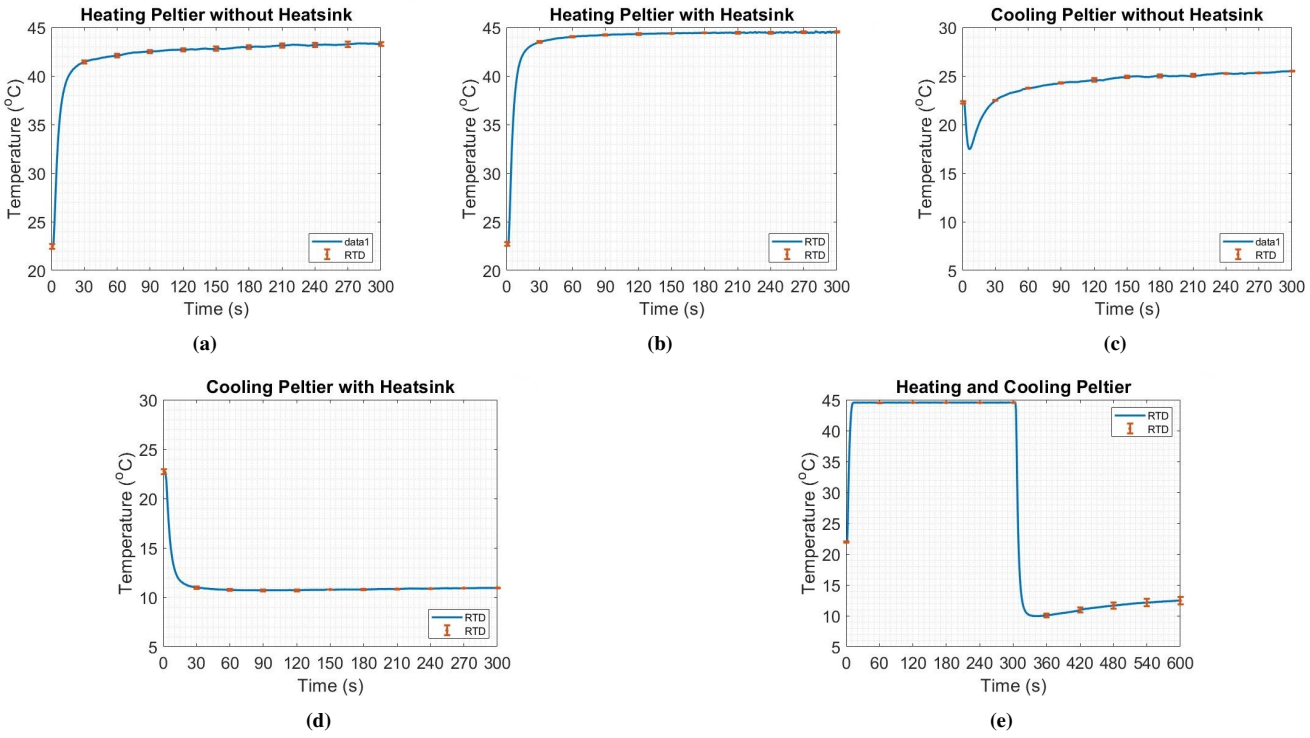

Fig. 8: *For the schematic drawing of the experiments see Figure 5a (a) Peltier heating without heatsink for five minutes (b) Peltier heating with heatsink for five minutes (c) Peltier cooling without heatsink for five minutes (d) Peltier cooling with heatsink for five minutes (e) Peltier first 5 minutes of heating than 5 minutes cooling*

peltier element without heatsink is seen. It can be seen that the maximum temperature reached is 43.44 °C, and it took approximately 22s before the system started stabilising. For heating with a heatsink, the maximum temperature is 44.44 °C, and it took approximately 22s to stabilise, see Figure 8b. It seems that the influence of the heatsink for heat is that with a heatsink, the system can reach a high temperature. Also, it stabilises better than without a heatsink. For cooling without a heatsink minimum temperature of 17.47 °C was reached. It took 7s to get to this temperature. The maximum temperature after cooling is 25.49, see Figure 8c, which is an increase of 8.03 °C. When a heatsink is placed against the Peltier element, a minimum temperature of 10.76 °C was reached, see Figure 8d. It took 54 s to reach this temperature. The maximum temperature after cooling is 10.94 °C, which means that there is a temperature increase of 0.18 °C. A noticeable difference is that the temperature stays low when a heatsink is applied. In contrast, when cooling without a heatsink, the temperature increases again. This increase is most likely because the heat cannot dissipate fast enough, which will cause the heat to flow back into the peltier itself, thus heating itself. Lastly, when switching from heating to cooling with a heatsink, as seen in Figure 8e, a maximum temperature of 44.55 °C was reached after 14 s. The minimum temperature reached was 9.965 °C in 40 seconds, which gives a temperature difference of 34.585 °C. This temperature difference is smaller than expected since, according to the datasheet, there should be a temperature difference between 70 and 80 °C for a voltage of 0.2 V. This voltage corresponds to the maximum voltage that the peltier elements can handle. The current that should be seen is 1.2 A but during the experiments, a lower current was seen. The current during the experiments is between 0.7 A and 0.8A. This difference might be because the heatsink is not able to remove the heat fast enough.

3.3 Leakage

The system has been tested for several fluid flows to measure at which fluid flow leakage would occur. The system started to leak at 70 $\mu L/min$, between the ferrule and the tube during infusion. This should not be a problem since for the Liver-on-a-chip, a flow rate is needed of 35 $\mu L/min$. For withdrawal (vacuum), no visible leakage was seen.

3.4 Influence of PID Control

The results of heating without control is shown in Figure 9a. The lines sp1 to sp14 are the points where the temperature was measured by the camera. These points and their placements can be seen in Figure 6. After 15 minutes, the system does not stabilise. The maximum temperature that was reached was 43.3 °C. In Figure 9b, the results of heating with PID control can be seen. The temperature does stabilise after 110 s. This shows that using PID is beneficial for the stability of the system.

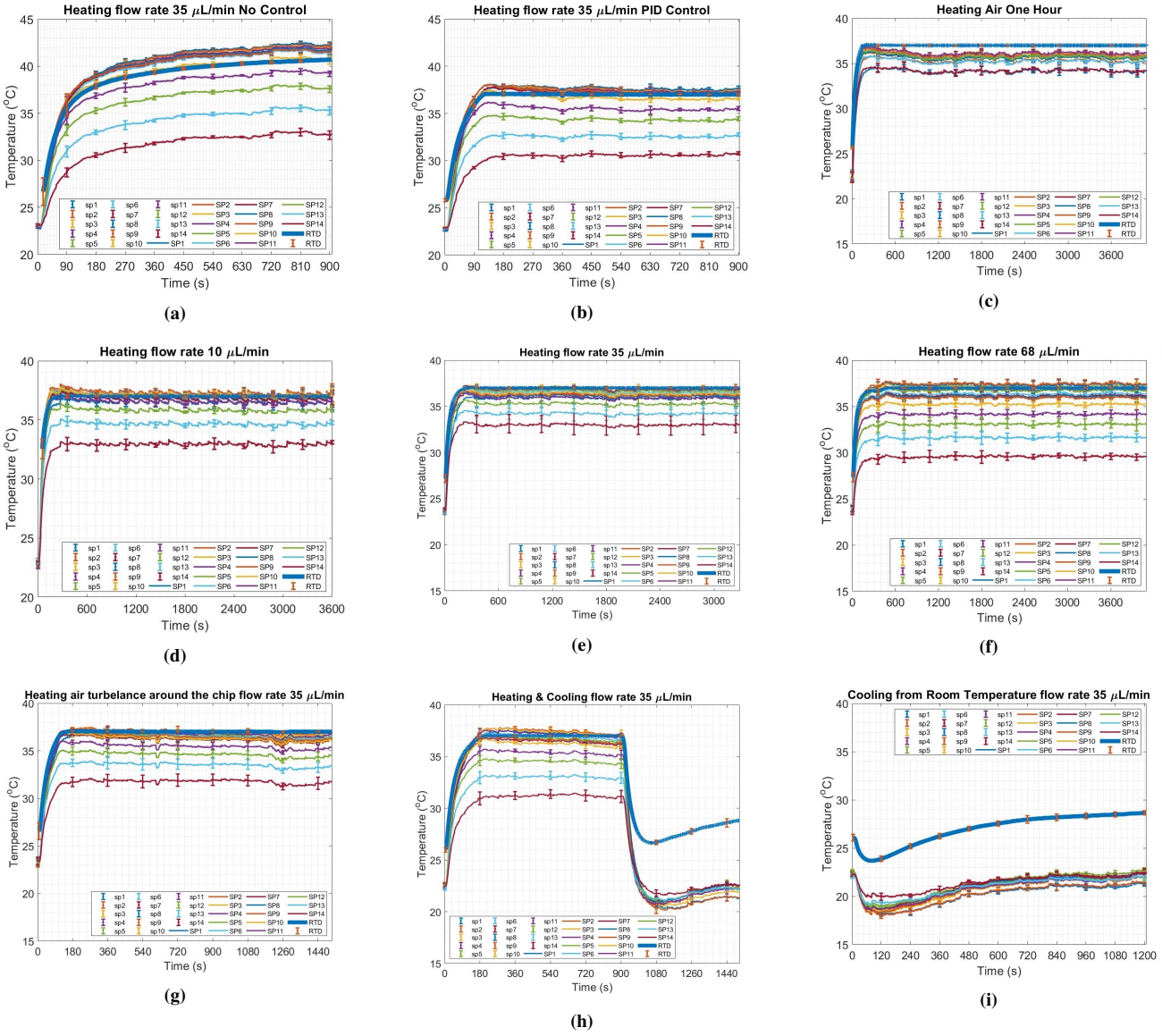

Fig. 9: *In Figure 6 a schematic drawing of the chip can be seen with the point placements that resemble sp1 to sp14 in the graphs (a) Heating without control for 15 minutes at a flow rate of 35 $\mu L/min$ (b) Heating with PID control for 15 minutes at a flow rate of 35 $\mu L/min$ (c) Heating for one hour without fluid flow, thus air in the channel (d) Heating for one hour with fluid flow of 10 $\mu L/min$ (e) Heating for one hour with fluid flow of 35 $\mu L/min$ (f) Heating for one hour with fluid flow of 68 $\mu L/min$ (g) Heating with air turbulence after 10 minutes for 10 seconds and then after 10 minutes for one minute around the chip at a flow rate of 35 $\mu L/min$ (h) Heating and cooling at a flow rate of 35 $\mu L/min$ (i) Cooling from room temperature for 20 minutes at a flow rate of 35 $\mu L/min$*

3.5 Influence of Fluid flow

The results for heating with no fluid flow (air in the channel), at 10, 35, and 68 $\mu L/min$ can be seen in Figures 9c,d,e and f. For no fluid flow, thus only air in the channel, most points (sp1 to sp13) are within a range of 0.97 °C. The total temperature difference is 2.01 °C. The response time was approximately 170 s. For a fluid flow of 10 $\mu L/min$, the majority of points (sp1 to sp11) are within a range of 0.83 °C. The total temperature difference is 4.38 °C. The response time was approximately 198 s. For a fluid flow of 35 $\mu L/min$, the majority of points (sp1 to sp11) are within a range of 1.02 °C. The total temperature difference is 3.88 °C. The response time was approximately 197 s. For a fluid flow of 68 $\mu L/min$, the majority of points (sp1 to sp9) are within a range of 1.59 °C. The total temperature difference is 7.87 °C. The response time was approximately 187 s. The influence of the fluid flow can be seen by comparing the four fluid flows. It is noticeable that the temperature uniformity gets less with higher fluid flow. This is most likely due to the fluid removing the heat. Another thing that can be seen is that it takes the system approximately 3 minutes to stabilise. There is a temperature difference between 0.83 and 1.59 °C for most points over a length of 19 mm at 68

$\mu L/min$ and 23 mm at 10 $\mu L/min$, meaning that the system is adequetly uniform.

3.6 Comparison numerical analysis and experimental results

By comparing the numerical results, shown in Figures 7a, b and c, and the experimental results, shown in Figures 9d, c and e, it can be seen that in both cases the temperature distribution decreases with a higher flow rate. In the numerical analyses, with a higher flow rate it took longer to stabilize while in the experiments it took approximately 3 minutes for all the fluid flows. This is most likely due to that in the experiments PID control was active and thus the power of the peltier elements could be adjusted while in the simulations a fixed power was used. Another difference between the numerical analyses and the experimental results is that in the numerical analyses, the temperature achieved when stabilised decreases with a higher flow rate. In the experimental setup, the stabilised temperature seems to be approximately the same for all three flow rates. This could be due to the PID control that is used in the experiments while there was no control in the numerical analysis. Though this could also be due to the sensor used during the experiments. At the time of the experiments, the cables of the sensor were connected to a breadboard, which caused the sensor values to change when the cables were moved around, which means that the sensor needed to be adjusted several times during the experiments. It could be possible that in case when the sensor is soldered to the lid that the same effect, that was seen in the numerical analyses, is seen in the setup as well, though it could be that the PID control can keep the temperature the same for different flow rates.

3.7 Influence of disturbances

In Figure 9g, the results of an airflow flows along the chip for 10 seconds and one minute is shown. It took the system 27 s to recover after the airflow of 10 seconds with a temperature dip of 0.4 °C. It took the system 307 s to recover after an airflow of one minute with a temperature dip of 0.76 °C. It would be preffered to decrease this temperature dip and the time needed to recover.

3.8 Cooling

In Figure 9h, you can see the results when the system is first heated up for 15 minutes and then cooled down for 10 minutes. It can be seen that the lowest temperature reached was 20.13 °C. Figure 9i shows the results of cooling down from room temperature. The lowest temperature that was reached was 18 °C. This indicates that the system is not able to cool the system down to 4 °C. This is most likely because when the peltier is cooling down, the heatsink is not able to remove the heat from the hot side fast enough, which causes the peltier element to heat up again.

3.9 Power consumption

For heating, the maximum voltage was 1.4 V, and the maximum current was 0.6 A, which gives a maximum power of 0.84 W for one chip. For cooling, the maximum voltage was 1.4 V, and the maximum current was 1.12 A, which gives a maximum power of 1.57 W for one chip. For four chips where the current is multiplying by four, the heating gives a maximum power of 3.36 W and cooling gives 6.27 W.
Using the maximum power, which is 6.27 W, which corresponds to a current of 4.48 A and the capacity of the battery, which is 20000 mAh, it is possible to calculate how long the system can stay on the battery. This would mean that the system can stay on for approximately 4.5 hours when only cooling is applied. The maximum power for only heating is 3.36 W, which corresponds to a current of 3.36 A, which would mean that the system can stay on for 8.3 hours.

3.10 Hepatocytes and Cholangiocytes

Figure 10 shows the results from the experiments with the cells. In Figure 10a, heat was applied to the cells and the fluid flow was turned off. A trendline was obtained from this graph which has the following function :

$$y_1 = -42.02t + 179.79 \tag{2}$$

Where y_1 is the PO_2 in mm Hg and t is the time in minutes. The measurements that were done are usually done at 37 °C, which means that the PO_2 values that were obtained need to be corrected for the measurements at room temperature

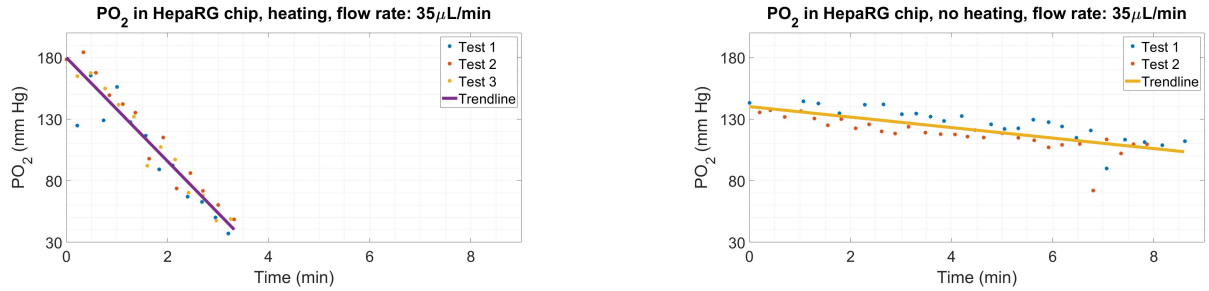

(a) **(b)**

Fig. 10: *(a) The PO_2 values of the cells measured when heat is applied. The flow rate of 35 $\mu L/min$ was stopped at the start of this graph, thus at t=0 s. (b) The corrected PO_2 values of the cells were measured when no heat was applied. The flow rate of 35 $\mu L/min$ was stopped at the start of this graph, thus at t=0 s.*

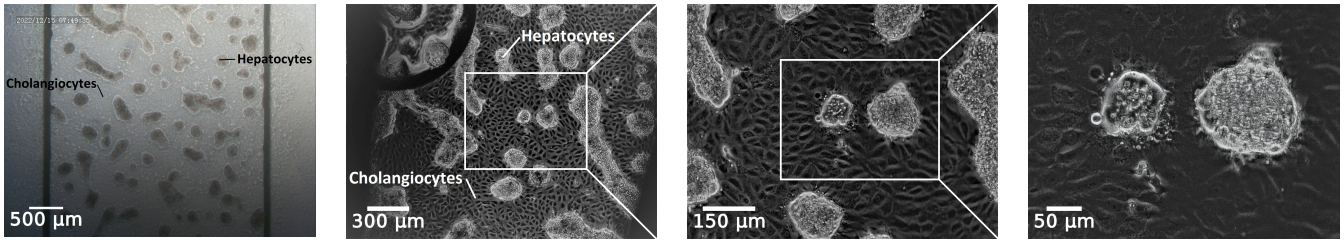

(a) **(b)** **(c)** **(d)**

Fig. 11: *(a) In this figure, the large islands are the Hepatocytes. The other cells are Cholangiocytes. Tissue culture microscope Zeiss Axiovert 40 Objective 2.5x was used. This is the image of the cells before the experiments (b) 4x magnification of the cells with the Olympus IX51 microscope. This image was taken after the experiments. In the left corner, a bubble is visible. (c) 10x magnification of the cells with the Olympus IX51 microscope(d) 20x magnification of the cells with the Olympus IX51 microscope*

(approximately 23 °C). To do this the Stern-Volmer equation was used [16]:

$$\frac{\tau_0}{\tau} = 1 + \tau_0 k_q' PO_2 \tag{3}$$

Where τ_0 is the decay time in the absence of oxygen in μs, τ is the decay time in μs and k_q' is equal to αk_q where α is the oxygen solubility coefficient in mm Hg/M and k_q is the Stern-Volmer quenching constant in $M^{-1}s^{-1}$ [16]. The τ_0 in the experiments at 37 °C is 550 μs. This value is lower than the one used in the paper by Sinaasappel and Ince (1996). τ_0 can be calculated by the following equation [16]:

$$\tau_0 = 719 - 3T - 0.02T^2 \tag{4}$$

Where T is the temperature. To correct the τ_0 for room temperature the factor between the τ_0 for 37 °C and 23 °C is taken from Sinaasappel and Ince (1996) and used to calculate τ_0 at 23 °C. This factor was 1.1 which gave a τ_0 of 605.70 μs. In this experiment k_q' is equal to 3.56x10^{-4} $Hg^{-1}s^{-1}$ for 37 °C. For room temperature the value of k_q' needs to be corrected. This was done by takening the factor between the k_q' values for 37 °C and 23 °C from Sinaasappel and Ince (1996), which was 0.769. This gives a k_q' value of 2.74x10^{-4} $Hg^{-1}s^{-1}$. By rewriting equation 3 for PO_2 and using the corrected values for τ_0 and k_q' the corrected values for PO_2 for room temperature can be calculated. Figure 10b shows the results after correction where the fluid flow was turned off at t=0s. A trendline was obtained from this graph which has the following function:

$$y_2 = -4.2595t + 140.1 \tag{5}$$

Where y_2 is the PO_2 in mm Hg and t is the time in minutes. From the start of the graphs, where the fluid flow was stopped, the cells consumed a lot of oxygen, hence the decrease in PO_2. Taking the derivative of the Equations 2 and 5, gives the oxygen disappearance rate (ODR) which are -42.02 mm Hg/min and -4.2595 mm Hg/min respectively. Thus, when heat is applied the oxygen disappeared 9.87 times faster than when no heat is applied, and thus more oxygen is consumed. This would mean that the temperature does influence the oxygen consumption of the cells. In Figure 11a, the cells before the experiments are visible. Tissue culture microscope Zeiss Axiovert 40 Objective 2.5x was used. The large islands are the Hepatocytes. The other cells are Cholangiocytes. In Figures 11a,b and c, the cells can be seen with a magnification of 4x, 10x and 20x after the experiments were done with the Olympus IX51 microscope. In Figure 10a, in the right corner, a bubble is visible. Multiple bubbles were seen inside the chip. This is most likely because warm liquids can hold less gas than cold fluids, which causes these bubbles to expand when heated up.

4 Conclusion

An overview of the obtained specifications can be seen in Table III. The system is able to hold four chips simultaneously. The system's response time is approximately 2 minutes, and the sensor's resolution is 0.05 °C. The system is able to create temperatures from 18 °C to 45 °C. The maximum flow rate that the system is able to achieve is 70 $\mu L/min$, and the maximum power consumption is between 0.84 W and 1.57 W for one chip and between 3.36 W and 6.27 W for four chips. For heating and cooling, respectively. The system is able to stay on for approximately from 4.5 hours (only cooling) to 8.3 hours (only heating) and is thus portable. The results with the cells showed that when heat is applied, the oxygen disappeared 9.87 times faster than when no heat was applied. This research has successfully shown an option to create a portable temperature control system for Organ-on-a-Chip applications.

TABLE III: *Obtained specifications*

Variety	Specifications
Response time system	2 min
Sensor resolution	0.05 °C
Temperature range	18 °C - 45 °C
Cooling	down to 18 °C
Temperature distribution	0.83 °C - 1.59°C
Area of uniformity	19-25 mm
Leakage	from 70 $\mu L/min$
Interference with cells	No
Duration heating	4.5 hours
Max power consumption	6.27 W (4 chips)
Number of chips	4
Chip dimensions	45mm x 15 mm x 2.1 mm (Micronit)
Transparent	One side

4.1 Recommendation

4.1.1 Heat distribution: A copper layer can be placed between the peltier elements and the glass slide to improve the heat distribution. This could improve the heat distribution because copper transfers heat well.

Another option could be to use ITO heating as the heater and keep the peltier elements mainly for cooling. This ITO heater can heat from the bottom due to its transparency. The disadvantage would be that a distance between the cells and the microscope is added due to the thickness of the ITO heater, which might cause the distance between the cells and the microscope to be larger than the working distance of the microscope, which means that some amplifications might not work anymore.

Another option is to use parallel connections for the peltier elements. This way, it is possible to control every single peltier. Thus, it could make the heat distribution more uniform. This will only be possible if electronics are found that can work with low voltages and high currents, which was not possible during this project.

4.1.2 Cooling: To improve the cooling of the system, a fan can be added. The fan can improve the removal of heat from the heatsink, which may improve the cooling capabilities of the peltier elements. According to the datasheet, it should be possible to cool down to lower temperatures. Thus adding a fan could help with that.

4.1.3 Leakage: To improve the leakage, it is possible to change the inlet/outlet design so that the ferrule presses better against the tubing. A high-resolution printer might be needed. Another option is to add a thin layer of material at the inlet/outlet to create more pressure between the ferrule and tubing. This could be done by a thin layer of tape or by depositing a thin layer of material.

4.1.4 User Interface: The interface between the system and the end user could be improved by creating an interface where it is possible to fill in the setpoint that the end user wants and the flow rate that will be used. By doing some tests at different flow rates and creating a formula for these tests, the sensor could adapt to the speed to make it more accurate for a specific flow rate. An LCD screen can be used to visualize the temperature measured by the sensor.

4.1.5 Bubbles: To remove the bubbles, the fluid should be preheated and go through a bubble trap before it enters the chip. This way, the bubbles created due to gas expansion due to heat can be removed before they enter the chip.

References

[1] Qirui Wu et al. "Organ-on-a-chip: recent breakthroughs and future prospects". In: *BioMedical Engineering OnLine volume* 19:9 (2020). DOI: https://doi.org/10.1186/s12938-020-0752-0. URL: https://biomedical-engineering-online.biomedcentral.com/articles/10.1186/s12938-020-0752-0.

[2] Q. Wu et al. "Organ-on-a-chip: recent breakthroughs and future prospects". In: *BioMed Eng OnLine* 19 (9 (2020)). DOI: https://doi.org/10.1186/s12938-020-0752-0. URL: https://biomedical-engineering-online.biomedcentral.com/articles/10.1186/s12938-020-0752-0#citeas.

[3] Alex Ede Danku et al. "Organ-On-A-Chip: A Survey of Technical Results and Problems". In: *Frontiers in Bioengineering and Biotechnology* 10 (2022). ISSN: 2296-4185. DOI: 10.3389/fbioe.2022.840674. URL: https://www.frontiersin.org/articles/10.3389/fbioe.2022.840674.

[4] Sadeq Abu-Dawas et al. "Design and Fabrication of Low-Cost Microfluidic Chips and Microfluidic Routing System for Reconfigurable Multi-(Organ-on-a-Chip) Assembly". In: *Micromachines* 12.12 (Dec. 2021), p. 1542. ISSN: 2072-666X. DOI: 10.3390/mi12121542. URL: http://dx.doi.org/10.3390/mi12121542.

[5] Haoyu Zhu et al. "Portable and Integrated Microuidic Flow Control System Using Off-the-shelf Components Towards Organs-on-chip Applications". In: (Oct. 2022). DOI: https://doi.org/10.21203/rs.3.rs-2166950/v1. URL: https://assets.researchsquare.com/files/rs-2166950/v1_covered.pdf?c=1666722414.

[6] V.E. Del Bene. "Clinical Methods: The History, Physical, and Laboratory Examinations". In: Walker HK, Hall WD, Hurst JW, editors, 3rd edition. Boston: Butterworths, 1990. Chap. 218 Temperature. URL: https://www.ncbi.nlm.nih.gov/books/NBK331/.

[7] Essen BioScience and Sartorius. *Effects of Temperature and Atmospheric Perturbation During Cell Culture: The Silent Variables*. URL: https://www.essenbioscience.com/en/resources/articles/temperature-atmospheric-perturbation-cell-culture/. (accessed: 06.01.2023).

[8] Clare L. Thompson et al. "Mechanical Stimulation: A Crucial Element of Organ-on-Chip Models". In: *Frontiers in Bioengineering and Biotechnology* 8 (2020). ISSN: 2296-4185. DOI: 10.3389/fbioe.2020.602646. URL: https://www.frontiersin.org/articles/10.3389/fbioe.2020.602646.

[9] Micronit. "Resealable flow cell-topconnect". In: (n.d.). URL: https://store.micronit.com/resealable_flow_cell.html.

[10] Tobias R Kießling et al. "Thermorheology of living cells—impact of temperature variations on cell mechanics". In: *New Journal of Physics* 15.4 (Apr. 2013), p. 045026. DOI: 10.1088/1367-2630/15/4/045026. URL: https://dx.doi.org/10.1088/1367-2630/15/4/045026.

[11] L. Mocé-Llivina and J. Jofre. “A method to maintain mammalian cells for days alive at 4 degrees C”. In: *Cytotechnology* 46(1) (2004), pp. 57–61. DOI: https://doi.org/10.1007/s10616-005-2106-y. URL: https://www.ncbi.nlm.nih.gov/pmc/articles/PMC3449471/pdf/10616_2005_Article_2106.pdf.

[12] Arctic Tec Technologies. “MTEC-0.2-1.2-0.12-71-3/5”. In: (n.d.).

[13] TE Connectivity. “PTF Family, PLatinum Thin Film (PFT) Temperature Elements”. In: (11-2022). URL: https://www.te.com/commerce/DocumentDelivery/DDEController?Action=showdoc&DocId=Data+Sheet%5C%7FPTF-FAMILY%5C%7FA5%5C%7Fpdf%5C%7FEnglish%5C%7FENG_DS_PTF-FAMILY_A5.pdf%5C%7FNB-PTCO-058.

[14] Brett Beauregard. “GitHub - br3ttb/Arduino-PID-Library”. In: *GitHub* (20-06-2017). URL: https://github.com/br3ttb/Arduino-PID-Library.

[15] Matthijs van Reeuwijk. “Design of a miniature gas exchanger for oxygen control in microfluids”. Master Thesis. 2021. URL: https://repository.tudelft.nl/islandora/object/uuid%5C%3Af13f7d0d-7179-4908-9f26-cf317a95f281.

[16] M. Sinaasappel and C Ince. “Calibration of Pd-porphyrin phosphorescence for oxygen concentration measurements in vivo”. In: *Journal of applied physiology (Bethesda, Md. : 1985)* 81(5) (1996), pp. 2297–2303. DOI: https://doi.org/10.1152/jappl.1996.81.5.2297. URL: https://journals.physiology.org/doi/full/10.1152/jappl.1996.81.5.2297?rfr_dat=cr_pub++0pubmed&url_ver=Z39.88-2003%5C&rfr_id=ori%5C%3Arid%5C%3Acrossref.org.

4 Conclusion and Recommendations

4.1 Conclusion

Table 8: Obtained specifications

Variety	Target Specifications	Obtained Specifications
Response time system	2-3 min	2 min
Sensor resolution	0.1 °C	0.05 °C
Temperature range	4 °C - 37.5 °C	18 °C - 45 °C
Cooling	down to 4 °C	down to 18 °C
Temperature distribution	1 °C	0.83 °C - 1.59 °C
Area of uniformity	30 mm	19-25 mm
Leakage	No leakage	from 70 $\mu L/min$
Interference with cells	No	No
Duration experiments	0.5 hour(s)	4.5 - 8.3 hours (4 chips)
Max power consumption	24 W	6.272 W (4 chips)
Number of chips	2	4
Chip dimensions	45 mm x 15 mm x 2.1 mm (Micronit)	45 mm x15 mm x 2.1 mm (Micronit)
Transparent	One side	One side

In this thesis, a portable temperature control system for Organ-on-a-Chip applications is presented. This thesis contains a literature review on Organ-on-a-Chip, several heaters, sensors and controllers. This literature review also includes the design approach, components selection, and initial design. This thesis contains the final design, the numerical and experimental setup and the results. See Table 8 for the target and achieved specifications.

4.2 Recommendations

In this section, some ideas for improving the system are given.

4.2.1 Heat distribution

A copper layer can be placed between the peltier elements and the glass slide to improve the heat distribution. This could improve the heat distribution because copper transfers heat well. Figure 22 shows some examples of the copper layer.
Another option could be to use ITO heating as the heater and keep the peltier elements mainly for cooling. This ITO heater can heat from the bottom due to its transparency. The disadvantage would be that a distance between the cells and the microscope is added due to the thickness of the ITO heater, which might cause the distance between the cells and the microscope to be larger than the working distance of the microscope, which means that some amplifications might not work anymore.
Another option is to use parallel connections for the peltier elements. This way, it is possible to control every single peltier. Thus, it could make the heat distribution more uniform. This will only be possible if electronics are found that can work with low voltages and high currents, which was not possible during this project.

Figure 22: Four designs of a copper layer

4.2.2 Cooling

To improve the cooling of the system, a fan can be added. The fan can improve the removal of heat from the heatsink, which may improve the cooling capabilities of the peltier elements. According to the datasheet, it should be possible to cool down to lower temperatures. Thus adding a fan could help with that.

4.2.3 Leakage

To improve the leakage, it is possible to change the inlet/outlet design so that the ferrule presses better against the tubing. A high-resolution printer might be needed.
Another option is to add a thin layer of material at the inlet/outlet to create more pressure between the ferrule and tubing. This could be done by a thin layer of tape or by depositing a thin layer of material.

4.2.4 User Interface

The interface between the system and the end user could be improved by creating an interface where it is possible to fill in the setpoint that the end user wants and the flow rate that will be used. By doing some tests at different flow rates and creating a formula for these tests, the sensor could adapt to the speed to make it more accurate for a specific flow rate. An LCD screen can be used to visualize the temperature measured by the sensor.

4.2.5 Bubbles

To remove the bubbles, the fluid should be preheated and go through a bubble trap before it enters the chip. This way, the bubbles created due to gas expansion due to heat can be removed before they enter the chip.

5 Reflection

5.1 Research goal and scheme

When I started this project, the idea at first was that the holder should hold two chips and that an area of the chip was visible to the microscope. For this idea, I ordered larger peltier elements. However, later on, in the project, it was noted that it was preferred to have the whole chip viewable and should hold four chips simultaneously, which as a result, changed my design drastically. I had to look for the smallest peltier elements, which was a task force since peltier elements are not usually made in these sizes, which resulted in a delay. In the meantime, I did some simulations, but the project could not take off without the heater since this was the main component of the design. The peltier element arrived five months after ordering, which meant that from that point, it was possible to start doing experiments. This showed me that it is important to have the requirement as correct as possible at the beginning of the project to try to make a project go as smoothly as possible.
Furthermore, I wanted to connect the peltier elements in parallel to control each one to improve the heat distribution. Due to the 10-channel amplifier not being able to go too low values, this was not possible. It took time to figure out the precise cause before we reached this conclusion. To prevent this, I should have changed to series earlier when it seemed parallel was not working instead of trying to make the system more complicated with additional components.
The experiment for the oxygen consumption was done three times but for an unknown reason, the last test was not saved. In appendix G the raw data can be seen. The temperature plot shows that the experiment continued for a while and that the heater was turned on again but this data is missing from the PO_2 plot, though the third test did look like the other two tests. It was not possible to redo this experiment because there were no more cells available. I should have made sure that the data was saved properly before leaving the experimental setup at Erasmus.

5.2 Component selection and purchase

Ordering components through the university was new to me. I first expected that when you order, most components could be shipped immediately and arrive within a few days. I learned this was not the case, which caused several delays in this project. One of the components that caused the most delay was the peltier element and the cables for the PCB. For both, there were some logistic problems with the financial team, resulting in delays. Furthermore, the idea was to solder connection pins to these cables, but they were too small, which meant that these cables were only useful if additional components were ordered. Since time was tight, I immediately soldered the cables on the PCB itself.

5.3 COVID-19 Related Issue

During my thesis, there were several corona restrictions for universities during the COVID-19 pandemic, such as the lockdown and having corona, due to both not being able to go to the university.

5.4 Conclusion

During this project, I learned that having a clear project goal with all its requirements is essential. This will save time. It is also important to take the lead time of components into account and make sure to update myself after an order is placed to be sure that an order will not be cancelled.

5.5 Acknowledgement

I would like to thank the following people: My supervisors, Murali Ghatkesar, Gürhan Özkayar and Joost Lötters, for their supervision and insight during this project.
Harold Raat for his feedback on the project.
Bradley But for his help during this project. He helped me a lot with the electronics part of this project. The lab technicians as well for their help during the project.
My family and friends for their support during the project. They helped me to stay positive and reduce my stress throughout the project.

5.6 Timeline

In Figure 23, you can see the Gantt chart set up at the beginning of the project. The design and fabrication part took much longer than first was anticipated. This was due to the delays described above.

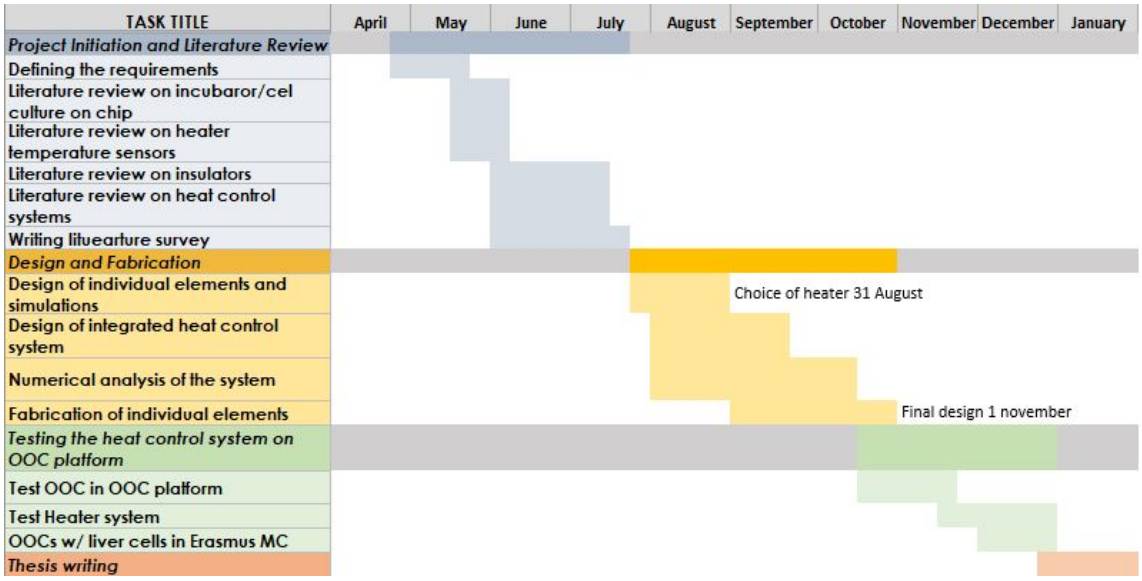

Figure 23: Gantt Chart

References

[1] Clare L. Thompson, Su Fu, Hannah K. Heywood, et al. "Mechanical Stimulation: A Crucial Element of Organ-on-Chip Models". In: *Frontiers in Bioengineering and Biotechnology* 8 (2020). ISSN: 2296-4185. DOI: 10.3389/fbioe.2020.602646. URL: https://www.frontiersin.org/articles/10.3389/fbioe.2020.602646.

[2] Haoyu Zhu, Gürhan Özkayar, Joost Lötters, et al. "Portable and Integrated Microuidic Flow Control System Using Off-the-shelf Components Towards Organs-on-chip Applications". In: (25-20-2022). DOI: https://doi.org/10.21203/rs.3.rs-2166950/v1. URL: https://assets.researchsquare.com/files/rs-2166950/v1_covered.pdf?c=1666722414.

[3] V.E. Del Bene. "Clinical Methods: The History, Physical, and Laboratory Examinations". In: Walker HK, Hall WD, Hurst JW, editors, 3rd edition. Boston: Butterworths, 1990. Chap. 218 Temperature. URL: https://www.ncbi.nlm.nih.gov/books/NBK331/.

[4] M.P. van Reeuwijk. "Oxygen Measurement at Hypoxia and Oxygen Control on Organ Chips". MA thesis. Delft: TU Delft, 2021.

[5] Garret Dunlap. "Organs-on-Chips: A promising future for therapeutic drugs". In: (June 2018). URL: https://sitn.hms.harvard.edu/flash/2018/organs-chips-promising-future-therapeutic-drugs/.

[6] Tugba Kilic, Fatemeh Navaee, Francesca Stradolini, et al. "Organs-on-chip monitoring: sensors and other strategies". In: *Microphysiological Systems* 2.0 (2018). ISSN: 2616-275X. URL: https://mps.amegroups.com/article/view/4689.

[7] Jr-Lung Lin, Min-Hsien Wu, Chun-Yen Kuo, et al. "Application of indium tin oxide (ITO)-based microheater chip with uniform thermal distribution for perfusion cell culture outside a cell incubator". In: *Biomedical microdevices* 12.3 (June 2010), pp. 389–398. ISSN: 1387-2176. DOI: 10.1007/s10544-010-9395-4. URL: https://doi.org/10.1007/s10544-010-9395-4.

[8] *Convert mAh (milliamphours) to time in hours*. URL: https://convert-formula.com/mah-hours.

[9] Science Struck. *Pros, Cons, and Applications of the Peltier Effect Explained*. June 2015. URL: https://sciencestruck.com/peltier-effect-explained.

[10] Andrés Fonys Sanata. "Characterization of a Peltier module working as a thermoelectric generator". In: (2015). URL: http://diposit.ub.edu/dspace/bitstream/2445/67389/1/TFG-Fonts-Santana-Andres.pdf.

[11] Xianbo Qiu, Michael G. Mauk, Dafeng Chen, et al. "A large volume, portable, real-time PCR reactor". In: *Lab Chip* 10 (22 2010), pp. 3170–3177. DOI: 10.1039/C0LC00038H. URL: http://dx.doi.org/10.1039/C0LC00038H.

[12] SimScale. *What Is Joule Heating?: SimWiki Documentation*. May 2021. URL: https://www.simscale.com/docs/simwiki/heat-transfer-thermal-analysis/what-is-joule-heating/.

[13] Jr-Lung Lin, Shih-Siou Wang, Min-Hsien Wu, et al. "Development of an Integrated Microfluidic Perfusion Cell Culture System for Real-Time Microscopic Observation of Biological Cells". In: *Sensors* 11.9 (2011), pp. 8395–8411. ISSN: 1424-8220. DOI: 10.3390/s110908395. URL: https://www.mdpi.com/1424-8220/11/9/8395.

[14] Jiu Yang Zhu, Ngan Nguyen, Sara Baratchi, et al. "Temperature-Controlled Microfluidic System Incorporating Polymer Tubes". In: *Analytical Chemistry* 91.3 (2019), pp. 2498–2505. DOI: 10.1021/acs.analchem.8b05365. eprint: https://doi.org/10.1021/acs.analchem.8b05365. URL: https://doi.org/10.1021/acs.analchem.8b05365.

[15] Boris Boris, Zeljko Hocenski, and Ljubivoj Cvitas. "Optimal Approximation Parameters of Temperature Sensor Transfer Characteristic for Implementation in Low Cost Microcontroller Systems". In: *2006 IEEE International Symposium on Industrial Electronics*. Vol. 4. 2006, pp. 2784–2787. DOI: 10.1109/ISIE.2006.296055.

[16] IQS Directorty. *Thermocouples*. URL: https://www.iqsdirectory.com/articles/thermocouple.html.

[17] John R. Gyorki. *Designing with RTD Temperature Sensors*. July 2012. URL: https://www.designworldonline.com/designing-with-rtd-temperature-sensors/.

[18] *A guide to temperature sensor design*. URL: https://es.farnell.com/a-guide-to-temperature-sensor-design#.

[19] Ian Parnell. *Understanding On-Off Temperature Controllers*. Jan. 2014. URL: https://www.west-cs.com/news/understanding-on-off-temperature-controllers/#:~:text=An%20on-off%20temperature%20controller,changed%20to%20make%20it%20fall..

[20] Fuji Electric. *Digital Temperature Controller*. Mar. 2021. URL: https://americas.fujielectric.com/products/instrumentation/temperature-controllers/digital-temperature-controller/.

[21] Engineering360. *Temperature Controllers Information*. URL: https://www.globalspec.com/learnmore/manufacturing_process_equipment/process_controllers/temperature_controllers.

[22] Christelle Angely. *How to avoid air bubbles in your microfluidic chip?* Nov. 2020. URL: https://darwin-microfluidics.com/blogs/tutorials/how-to-avoid-air-bubbles-in-your-microfluidic-chip.

[23] Franell. *Platinum Sensing Resistors - Thin Film (Pt100 Pt1000 Ohm)*. URL: http://www.farnell.com/datasheets/1918818.pdf.

[24] Janet Heath. *RTD vs. Thermocouple vs. thermistor in temperature sensors*. Oct. 2020. URL: https://www.analogictips.com/temperature-sensors-thermocouple-vs-rtd-vs-thermistor-vs-semiconductor-ic/.

[25] Omega Engineering. *OMEGA Engineering*. URL: https://www.omega.co.uk/temperature/z/thermocouple-rtd.html.

[26] TC Driect. *Cement On Polyimide Thin Film Thermocouple - Aerostructure Grade*. URL: https://www.tcdirect.co.uk/Default.aspx?level=2&department_id=180/25.

[27] Selco. *TF Series: Thin Film Thermistors*. URL: https://www.selcoproducts.com/products/tf-series.

[28] National Instruments. June 2020. URL: https://www.ni.com/nl-nl/innovations/white-papers/06/overview-of-temperature-sensors.html.

[29] Fluigent smart microfluidics. *bubble trap to remove air bubbles in case of microfluidic application*. Aug. 2019. URL: https://www.fluigent.com/product/microfluidic-components-3/bubble-trap/.

[30] *In-line Bubble remover : detection and trap*. Dec. 2020. URL: https://www.elveflow.com/microfluidic-products/microfluidics-accessories/bubble-remover/.

[31] Darwin Microfluidics. *Bubble Trap for Microfluidics*. URL: https://darwin-microfluidics.com/products/microfluidic-bubble-trap?variant=37424727681.

[32] PreciGenome. *Inline Bubble Trap, Air Bubble Remover, PEEK, Microfluidic/HPLC, Standard Ver.* URL: https://www.precigenome.com/product-page/inline-bubble-trap-fluidic-bubble-remover-peek-for-microfluidic-hplc.

[33] Watlow. *FREEFLEX® Heated Tubing*. URL: https://www.watlow.com/products/heaters/fluid-delivery-heaters/freeflex-heated-tubing.

[34] Dolomite. *Hotplate Adapter*. Mar. 2021. URL: https://www.dolomite-microfluidics.com/product/hotplate-adapter/.

A Test Setup Oxygen

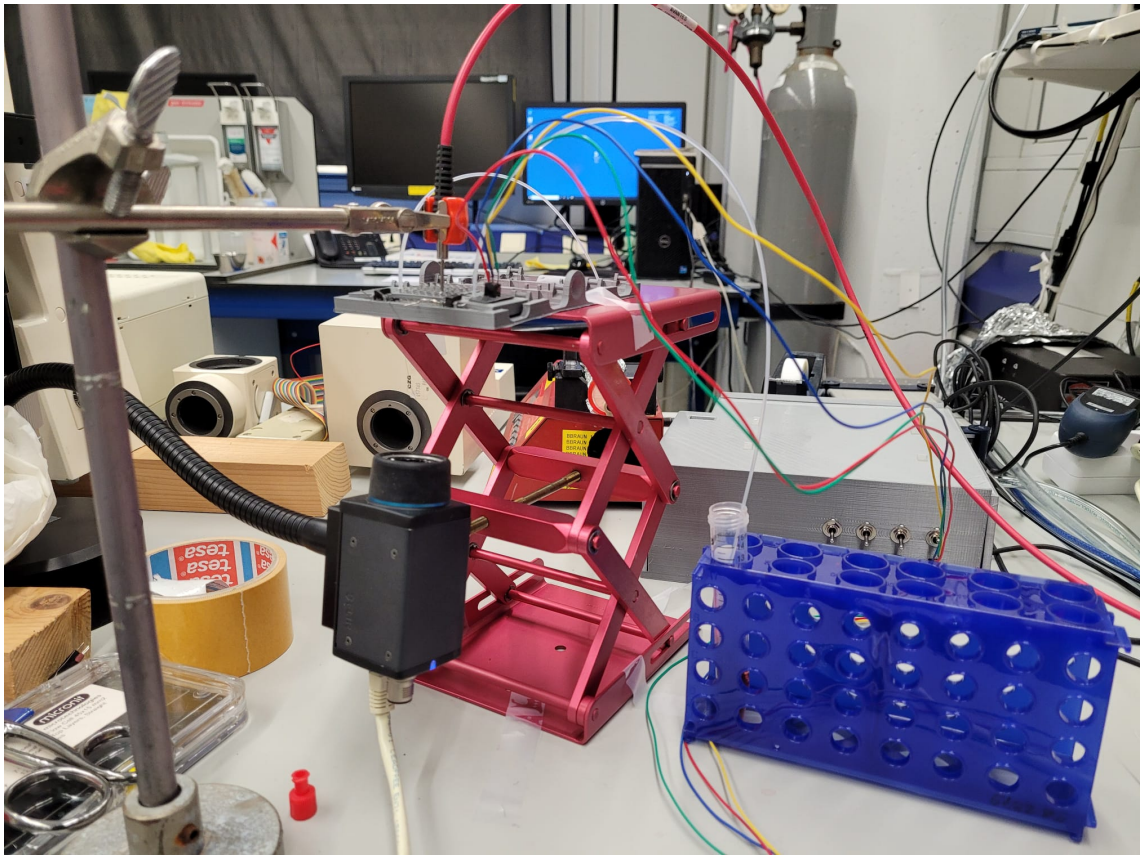

Figure A2: Test setup for Oxygen measurements

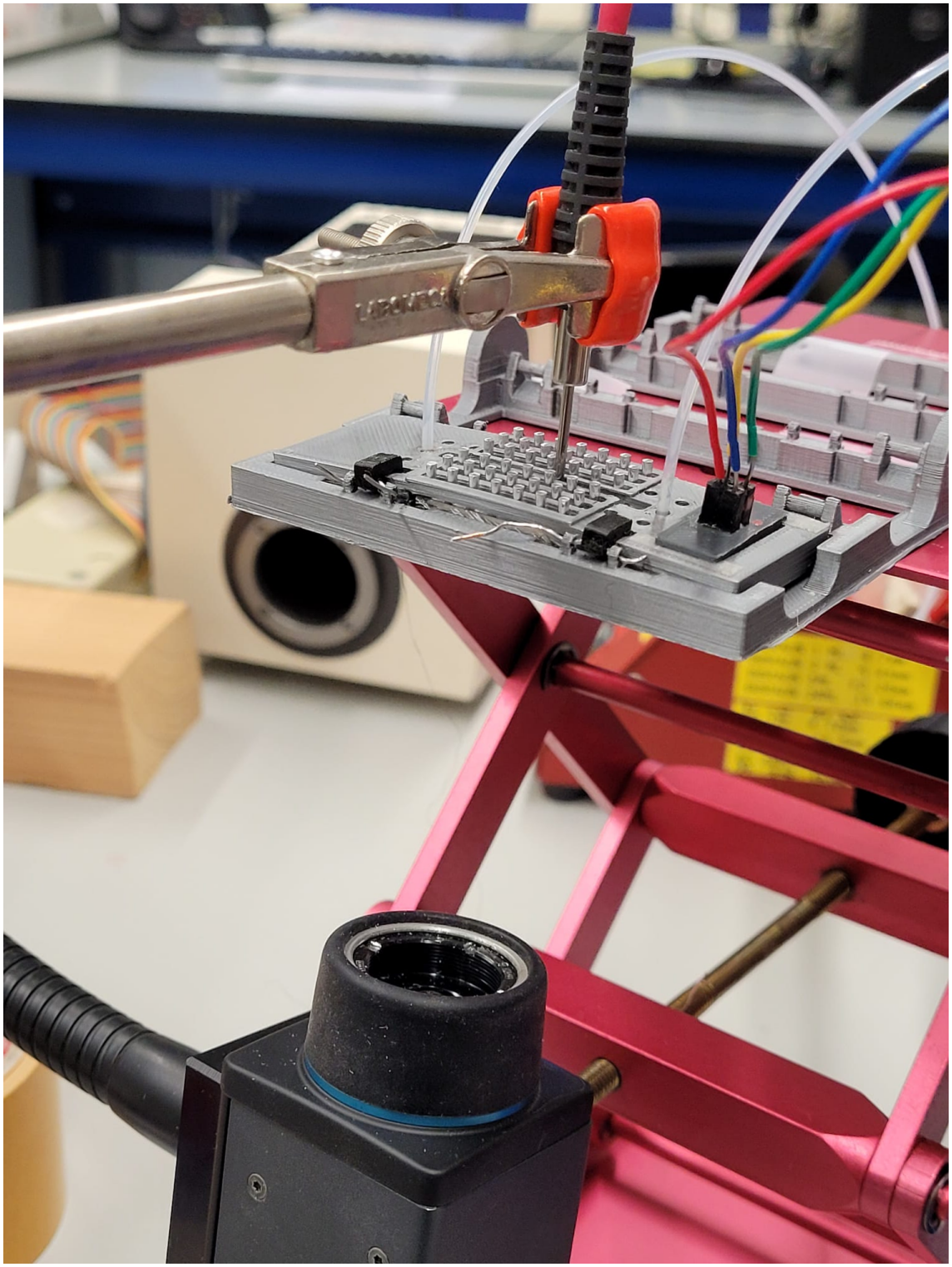

Figure A3: Test setup for Oxygen measurements close up

Figure A4: Test setup for Oxygen measurements, view from the bottom of the chip

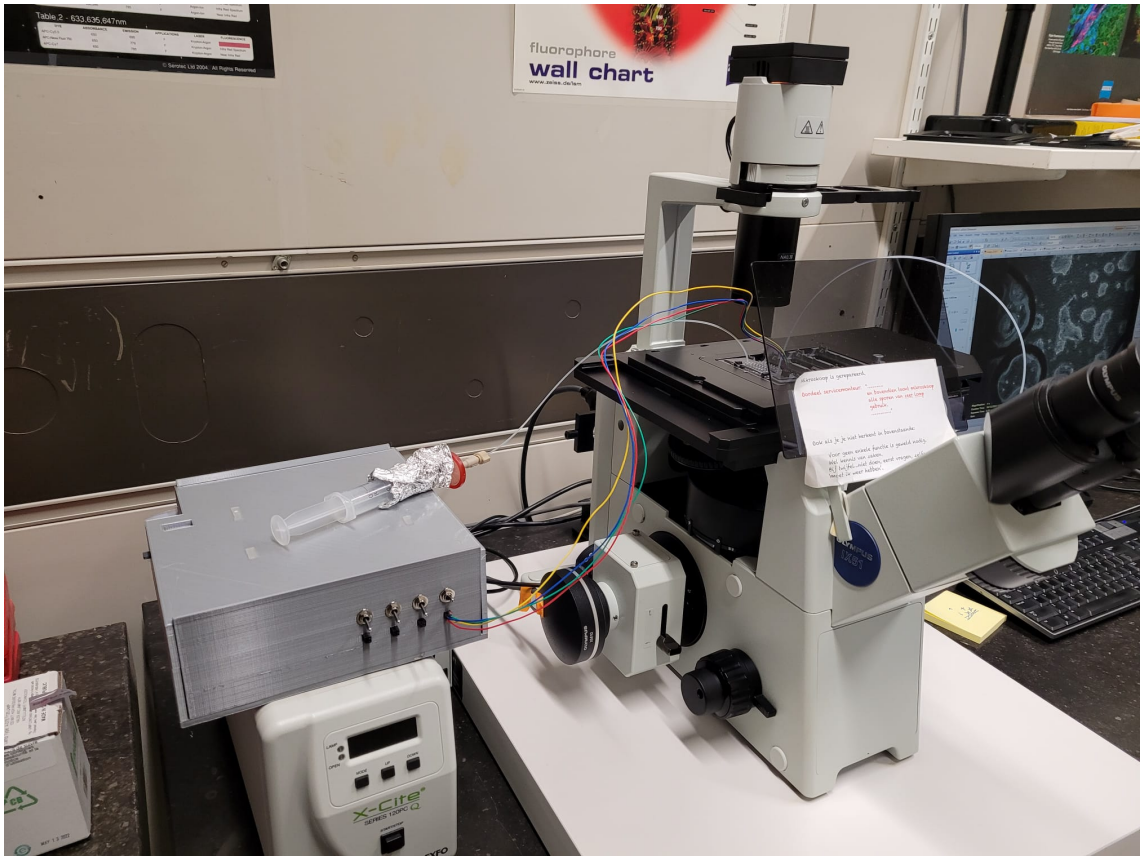

Figure A5: Setup in combination with microscope

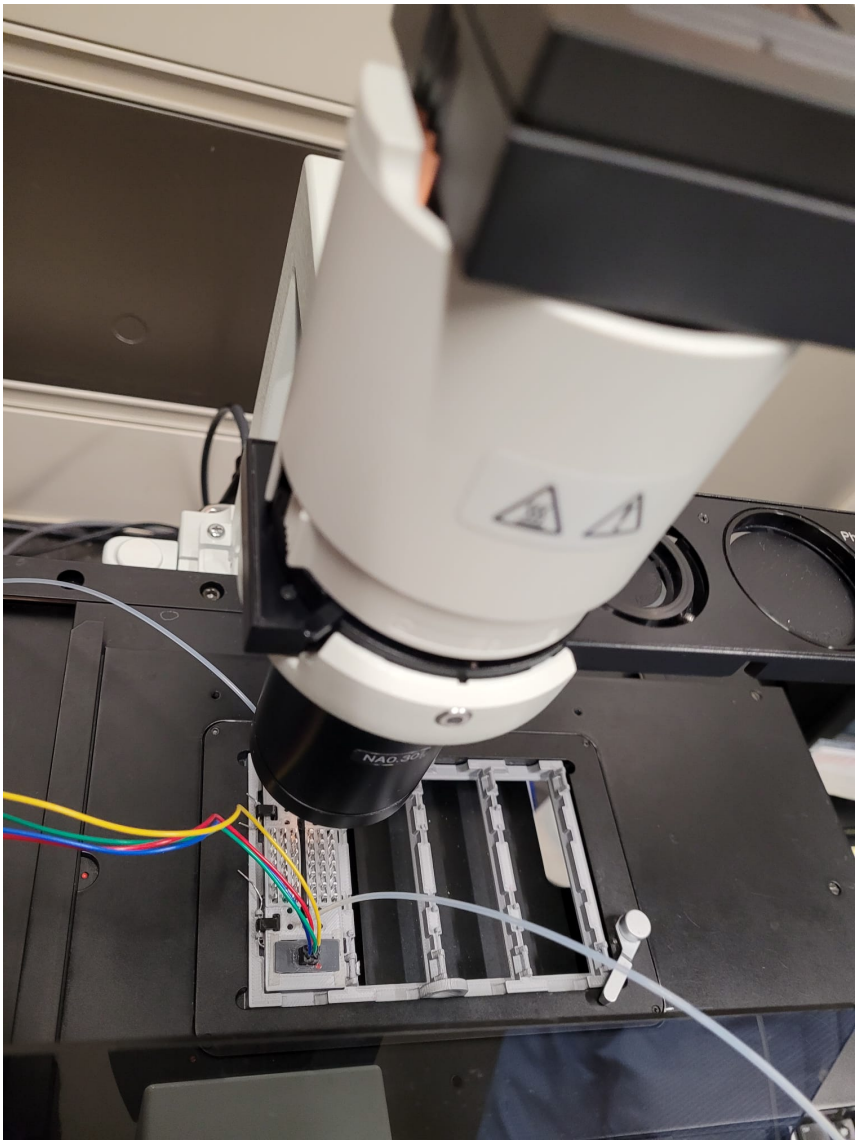

Figure A6: Setup in combination with the microscope, top holder

B Costs

Table B1: Prices of the components used in the Setup

Component	Brand	Model Key	Quantity	Price €
Peltiers	Artic Tec Tegnologies	MTEC-0.2-1.2-0.12-71-3/5	8	60
RTD	TE Connectivity Measurement Specialties	NB-PTCO-058	1	6,35
Heatsink	FISCHER ELEKTRONIK	ICK S 25 X 25 X 6,5	1	6,80
adhesive carbon tabs	-	-	2	Free
DC-DC buck converter	DFROBOT	DFR0379	2	9,72
PCB	-	-	1	9,91
Potentiometer	BOURNS	PV36W201C01B00	1	2,74
Amplifier	Texas Instruments	INA125P	1	8,24
Arduino	Arduino	ATmega2560	1	42
Battery	GRIXX	-	1	20
Switch	Eledis	Similar to 1A43-NF1STSE	4	39,72
Connector heads	-	-	1	4,30
M3 x 16 bolts	-	-	6	Free
M3 x 35 bolts	-	-	2	Free
M3 nuts	-	-	10	Free
Double sided tape, width = 19.6 mm, thickness = 0.2 mm	-	-	-	Free
Double sided tape, width = 6.1 mm, thickness = 0.8 mm	-	-	-	Free
PLA	-	-	-	Free
Cables	-	-	-	Free
USB cable	-	-	1	1
Total				210,78

Note that the components that say Free were already available at the university.

C PCB

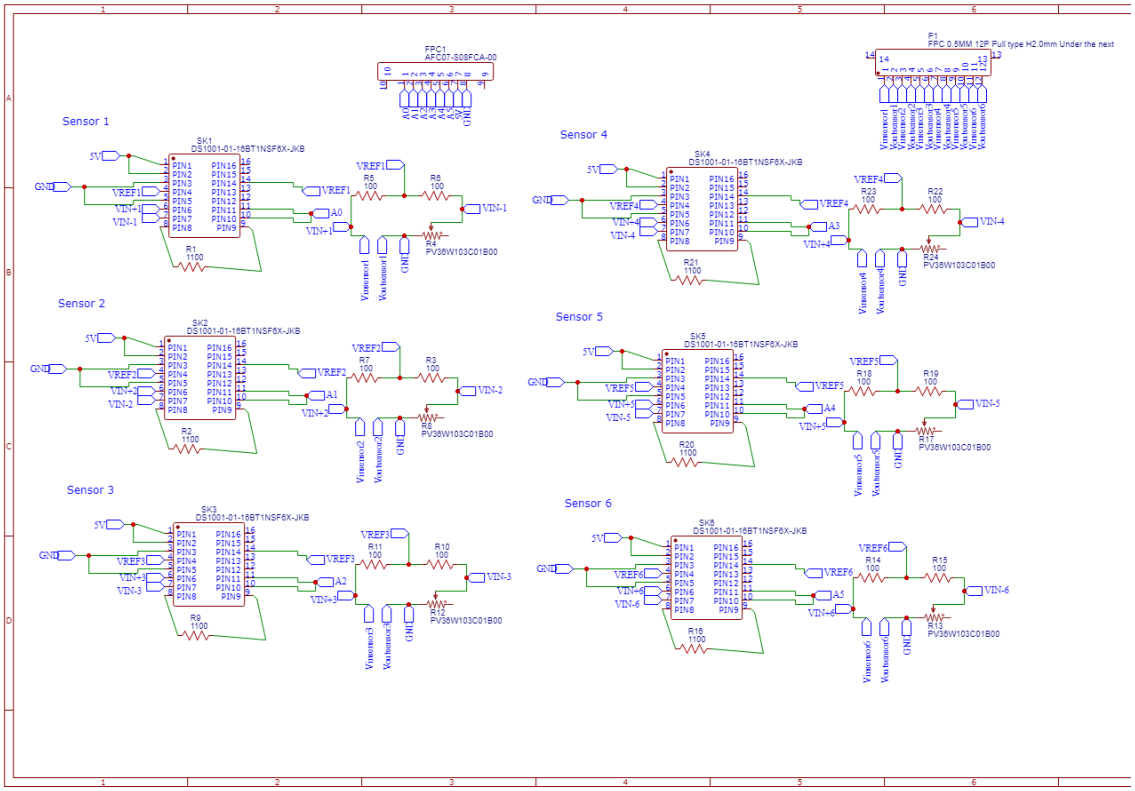

Figure C2: Schematic drawing of half of the connections of PCB

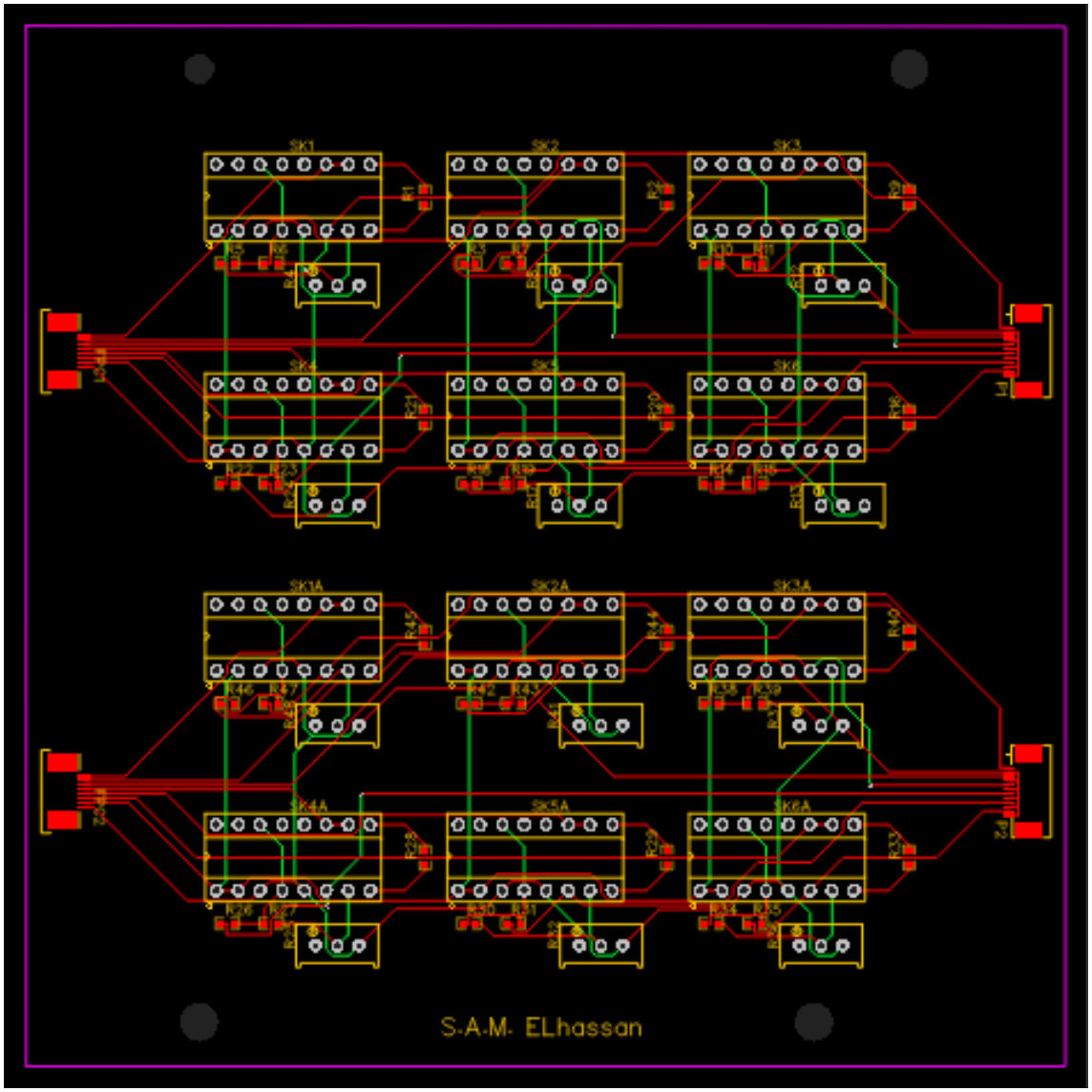

Figure C3: Layout PCB, green are the bottom connection, red the top connections

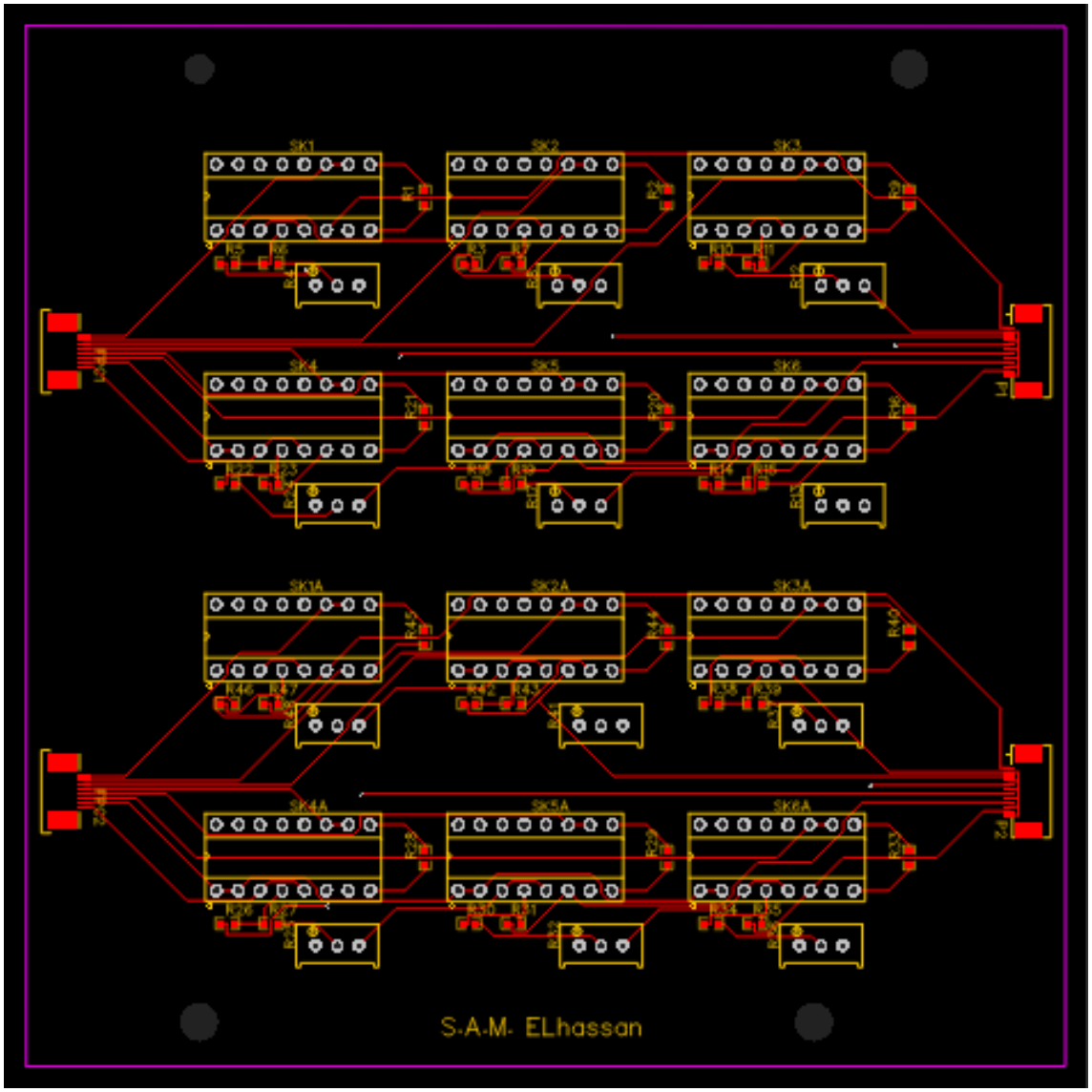

Figure C4: Layout PCB, top connections

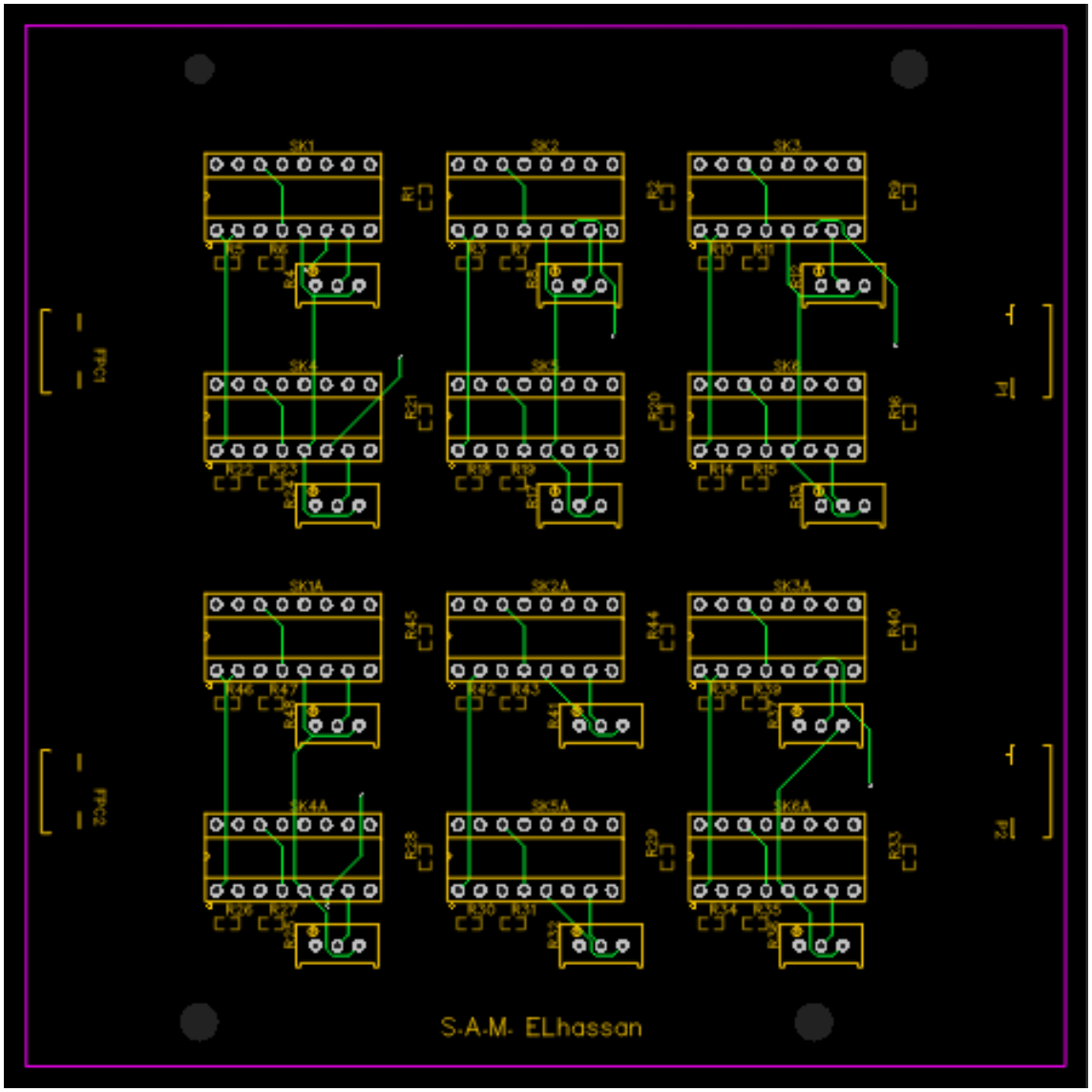

Figure C5: Layout PCB, bottom connections

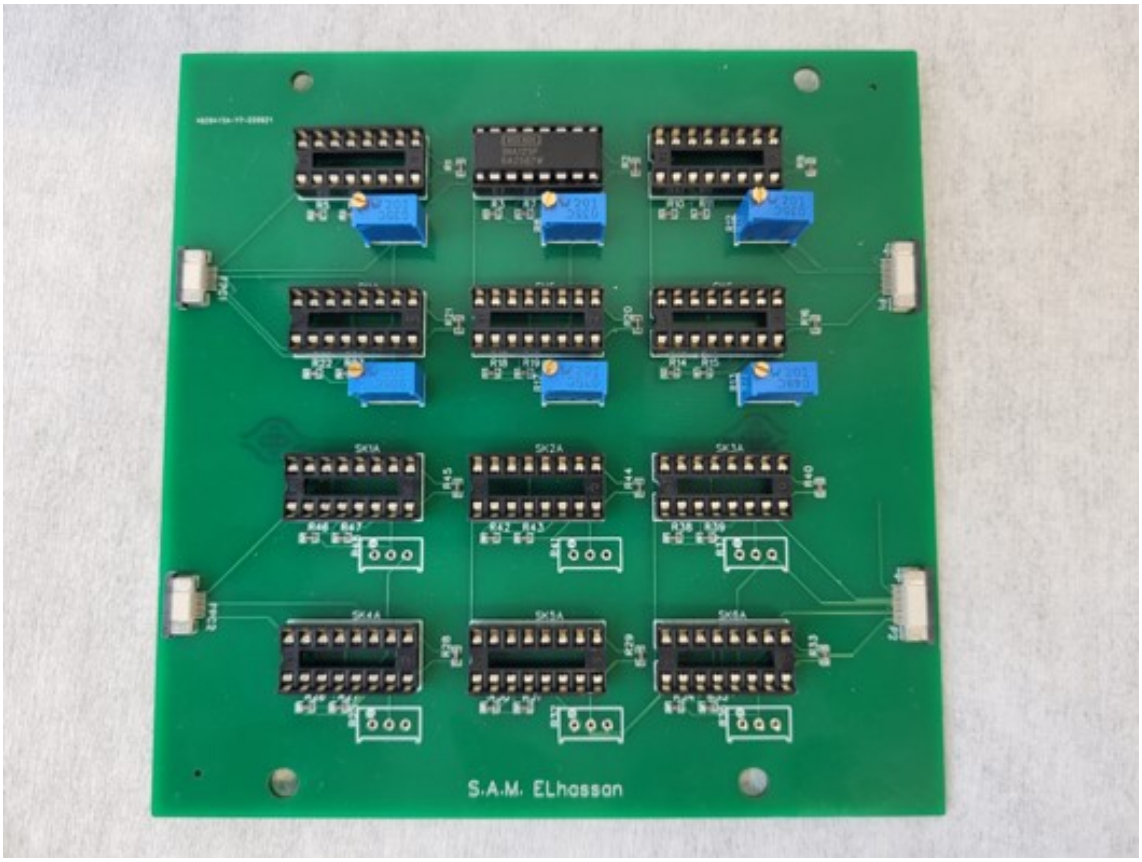

Figure C6: Image of the PCB

D Arduino Code

```
#include <PID_v1.h>

#define PIN_INPUT1 A0
#define PIN_INPUT2 A1
#define PIN_INPUT3 A2
#define PIN_INPUT4 A3
#define PIN_OUTPUT1 9
#define PIN_OUTPUT2 2
#define PIN_OUTPUT3 3
#define PIN_OUTPUT4 4
#define PIN_OUTPUT5 5
#define PIN_OUTPUT6 6
#define PIN_OUTPUT7 7
//#define PIN_OUTPUT 9

int Vo1,Vo2,Vo3,Vo4,Vo5,Vo6;
//float R1 = 446.8;
float R3,R7,R11,R15,R19,R23;
float Tc1,Tc2,Tc3,Tc4,Tc5,Tc6;
float Vout1,Vout2,Vout3,Vout4,Vout5,Vout6;
float G1,G2,G3,G4,G5,G6;
float R0=100;
float a= 3.9083e-03, b= -5.775e-07;
float R1=100, R2=100, R4=100, V1=1.551;
float R5=99.8, R6=99.6, R8=100 ,V2=1.463;
float R9=99.8, R10=99.6, R12=100 ,V3=1.463;
float R13=99.6, R14=99.7, R16=100 ,V4=1.463;
float R17=99.6, R18=99.7, R20=100 ,V5=1.463;
float R21=100.0, R22=100.1, R24=100 ,V6=1.463;

//Define Variables we'll be connecting to
double Setpoint, Input1, Output1, Input2, Output2, Input3,
Output3, Input4, Output4;
//double Input2, Output2,Input3, Output3, Input4, Output4,
Output5, Output6, Output7, Output8;


//Specify the links and initial tuning parameters
double Kp=400, Ki=3 , Kd=1;
PID myPID1(&Input1, &Output1, &Setpoint, Kp, Ki, Kd, DIRECT);
```

```
PID myPID2(&Input2, &Output2, &Setpoint, Kp, Ki, Kd, DIRECT);
PID myPID3(&Input3, &Output3, &Setpoint, Kp, Ki, Kd, DIRECT);
PID myPID4(&Input4, &Output4, &Setpoint, Kp, Ki, Kd, DIRECT);
//PID myPID7(&Input5, &Output5, &Setpoint, Kp, Ki, Kd, DIRECT);
//PID myPID8(&Input6, &Output6, &Setpoint, Kp, Ki, Kd, DIRECT);

void setup()
{
 Serial.begin(9600);
 //initialize the variables we're linked to
 Input1 = Tc1;
 //Input2 = Tc2;
 //Input3 = Tc3;
 //Input4 = Tc6;
 Setpoint = 37;

 //turn the PID on
 myPID1.SetMode(AUTOMATIC);
 //myPID2.SetMode(AUTOMATIC);
 //myPID3.SetMode(AUTOMATIC);
// myPID4.SetMode(AUTOMATIC);
// myPID5.SetMode(AUTOMATIC);
// myPID6.SetMode(AUTOMATIC);
// myPID7.SetMode(AUTOMATIC);
// myPID8.SetMode(AUTOMATIC);
}

void loop()
{
 //sensor1
 Vo1 = analogRead(A0);
 Vout1 = Vo1 * (5.0 / 1023.0);
 G1 = Vout1/58.8947849954;//58.545;//31.18227848;
 R3 =
(-(G1/V1)*R1*R2-(G1/V1)*R1*R4-R1*R4)/((G1/V1)*R4+(G1/V1)*R2-R2);
 Tc1=((-a+sqrt(sq(a)-4*b*(R0/R3-1)))/(2*b));
 // sensor 2
 Vo2 = analogRead(A1);
 Vout2 = Vo2 * (5.0 / 1023.0);
 G2 = Vout2/58.844606947;//58.545;//31.18227848;
```

```
 R7 =
(-(G2/V2)*R5*R6-(G2/V2)*R5*R8-R5*R8)/((G2/V2)*R8+(G2/V2)*R6-R6);
 Tc2=((-a+sqrt(sq(a)-4*b*(R0/R7-1)))/(2*b));
 // sensor 3
 Vo3 = analogRead(A2);
 Vout3 = Vo3 * (5.0 / 1023.0);
 G3 = Vout3/58.8947849954;//58.545;//31.18227848;
 R11 =
(-(G3/V3)*R9*R10-(G3/V3)*R9*R12-R9*R12)/((G3/V3)*R12+(G3/V3)*R10-R
10);
 Tc3=((-a+sqrt(sq(a)-4*b*(R0/R11-1)))/(2*b));
 //sensor 6
 Vo6 = analogRead(A3);
 Vout6 = Vo6 * (5.0 / 1023.0);
 G6 = Vout6/58.8947849954;//58.545;//31.18227848;
 R23 =
(-(G6/V6)*R21*R22-(G6/V6)*R21*R24-R21*R24)/((G6/V6)*R24+(G6/V6)*R2
2-R22);
 Tc6=((-a+sqrt(sq(a)-4*b*(R0/R23-1)))/(2*b));
 Input1 = Tc1;
 Setpoint = 37;
 myPID1.Compute();
 //myPID2.Compute();
 //myPID3.Compute();
 //myPID4.Compute();
 //myPID5.Compute();
 //myPID6.Compute();
 //myPID7.Compute();
 //myPID8.Compute();

 analogWrite(PIN_OUTPUT1, Output1);
 //analogWrite(PIN_OUTPUT2, Output2);
 //analogWrite(PIN_OUTPUT3, Output3);
 //analogWrite(PIN_OUTPUT4, Output4);
 //analogWrite(PIN_OUTPUT5, Output1);
 //analogWrite(PIN_OUTPUT6, Output1);
 //analogWrite(PIN_OUTPUT7, Output1);
 //analogWrite(PIN_OUTPUT8, Output1);
 //Serial.print("Sensor6:");
 Serial.print(Tc1,4);
```

```
 Serial.print(",");
 //Serial.print("Sensor1:");
 Serial.print(Tc2,4);
 Serial.print(",");
 //Serial.print("Sensor2:");
 Serial.print(Tc3,4);
 Serial.print(",");
 //Serial.print("Sensor3:");
 Serial.print(Tc6,4);
 Serial.print(",");
 Serial.println( );
 delay(100);
}
```

E Box

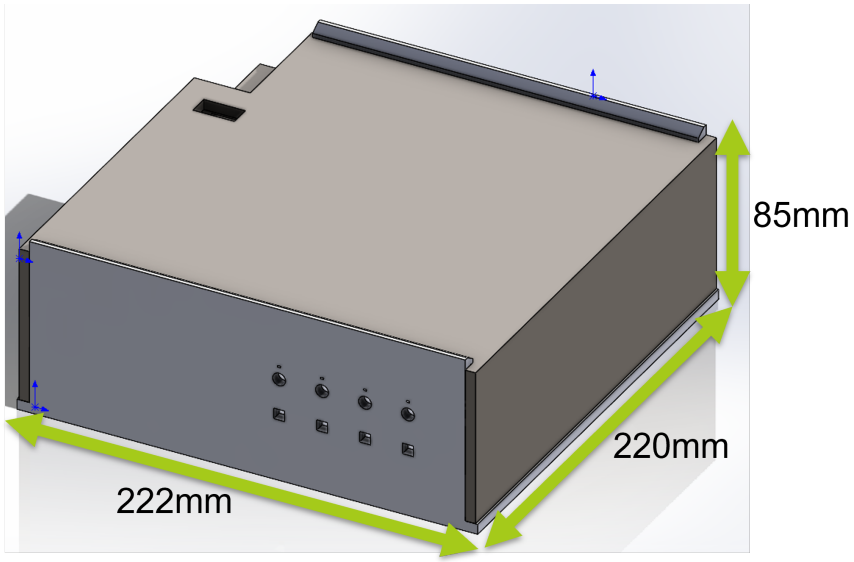

Figure E2: Assembly of the box the circles are for the switches, and the small rectangular holes underneath it are for the cables. The large hole on top is a viewing window for the percentage of the battery

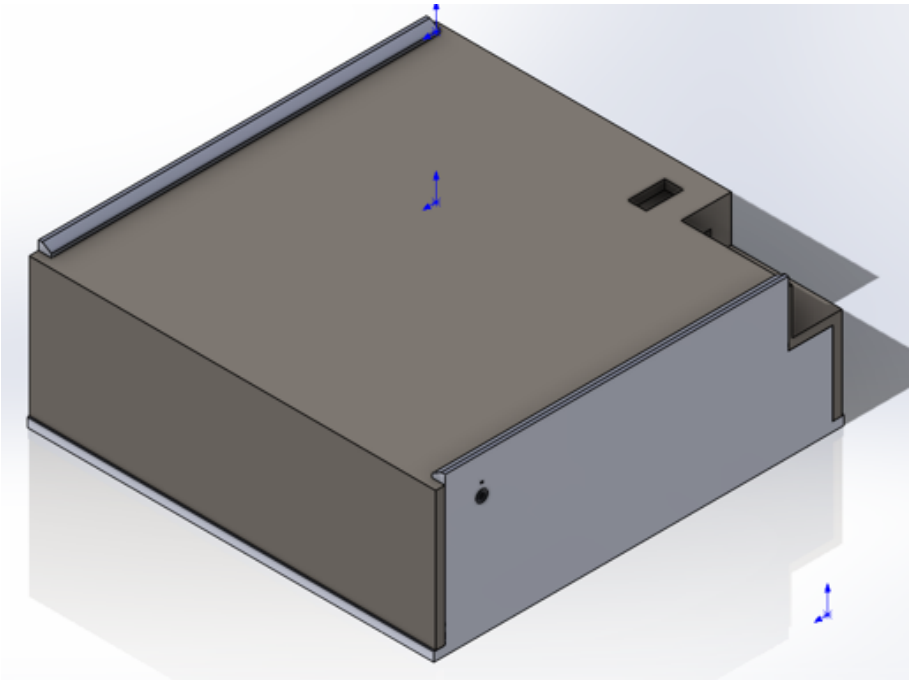

Figure E3: Assembly of the box the circles are for the switches, and the small rectangular holes underneath it are for the cables

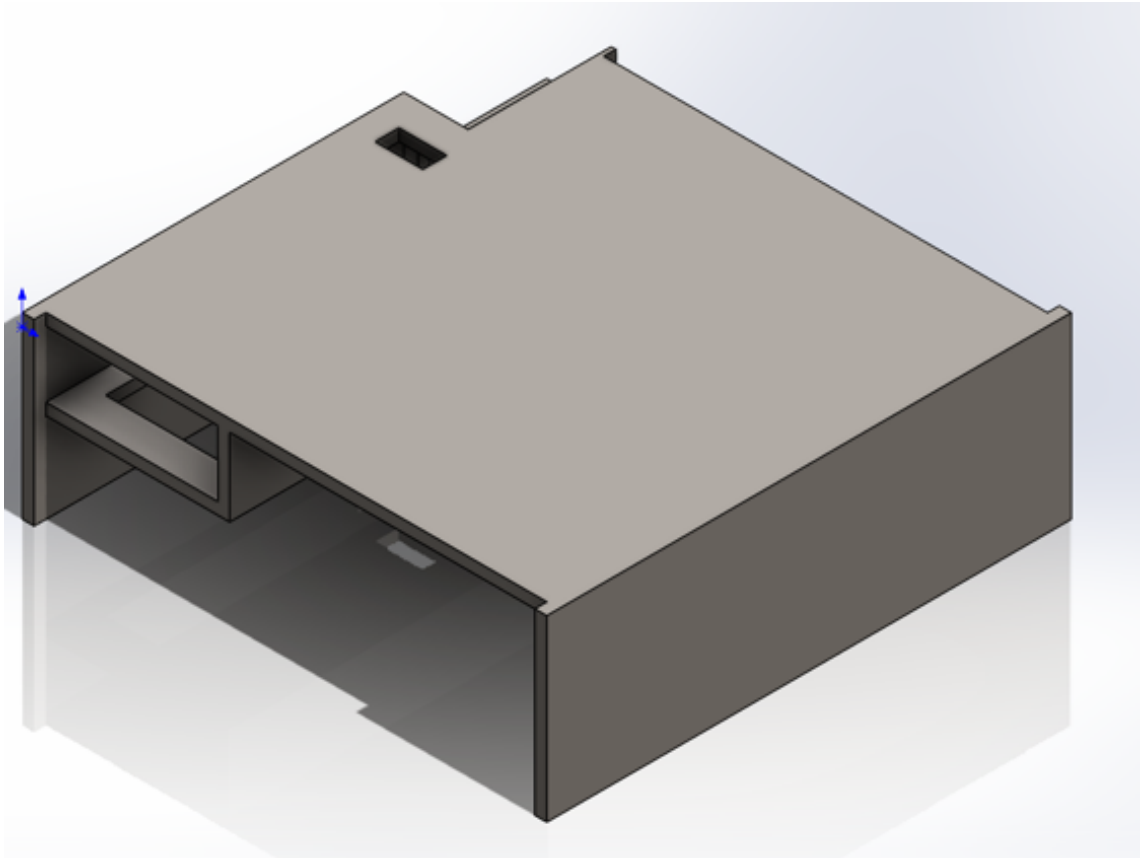

Figure E4: Lid of the box

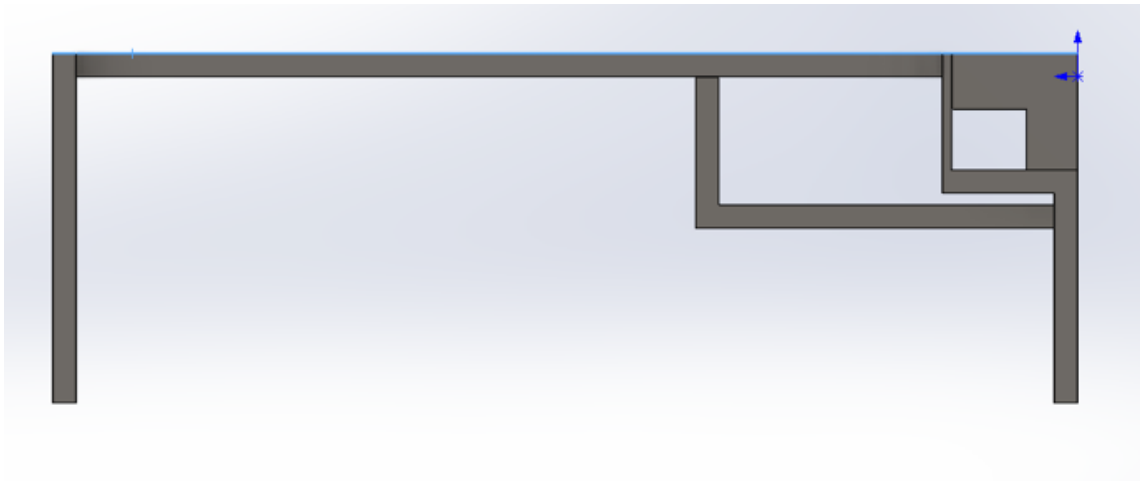

Figure E5: Side view Lid. The rectangular part is to hold the battery

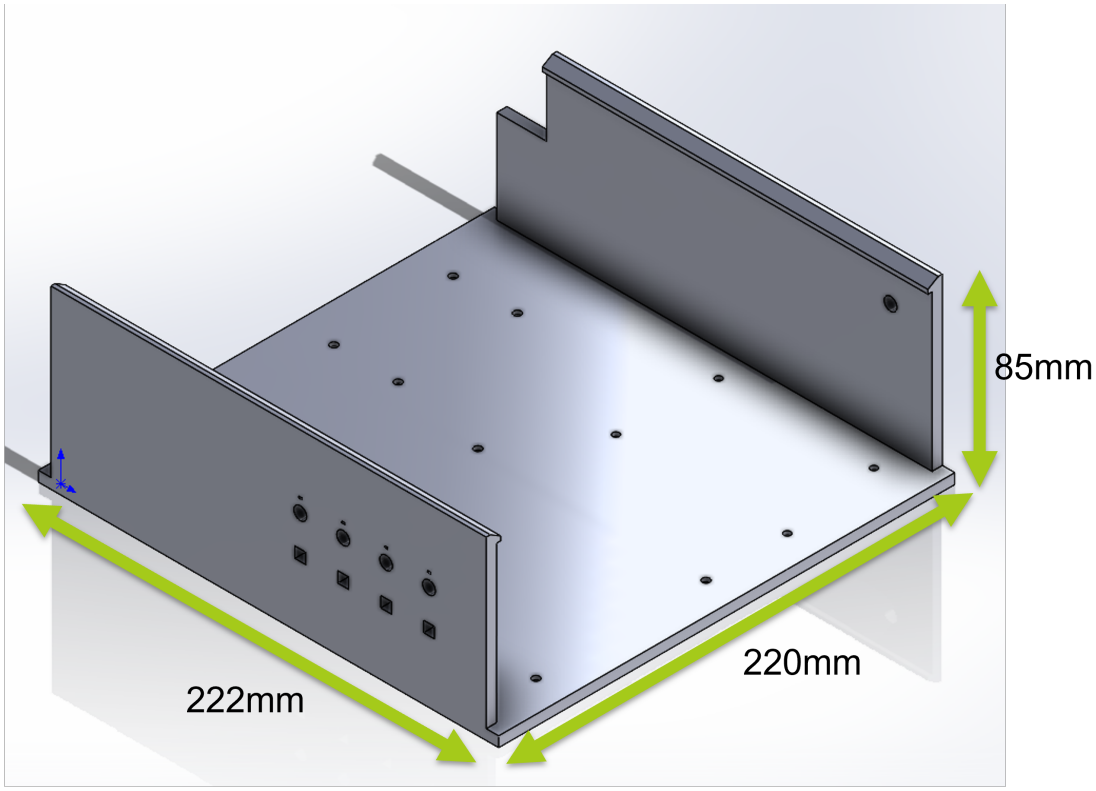

Figure E6: bottom part of the box, holes on the bottom are used to secure the electronic. They can be secured with M3 bolts and screws

Figure E7: Final version box

Figure E8: A close-up of the switches and cable connectors. Switching up is heating, down is cooling and in the de middle is off

Figure E9: The percentage of the battery is visible on the top of the box.

Figure E10: On the side is the on/off button. Pressing once turns the device on. Pressing twice shortly after each other turns the device off

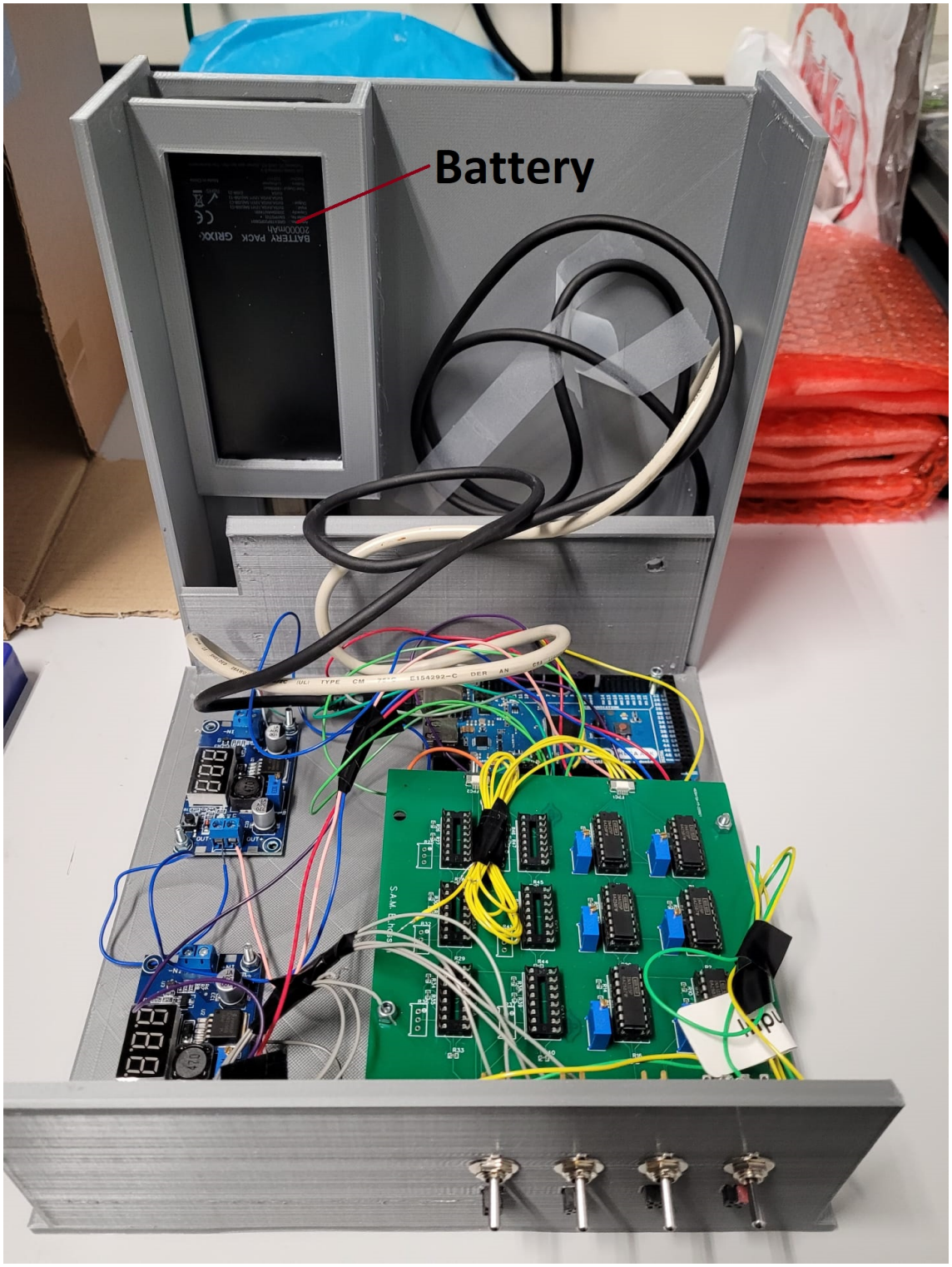

Figure E11: Inside of the box with the electrical components

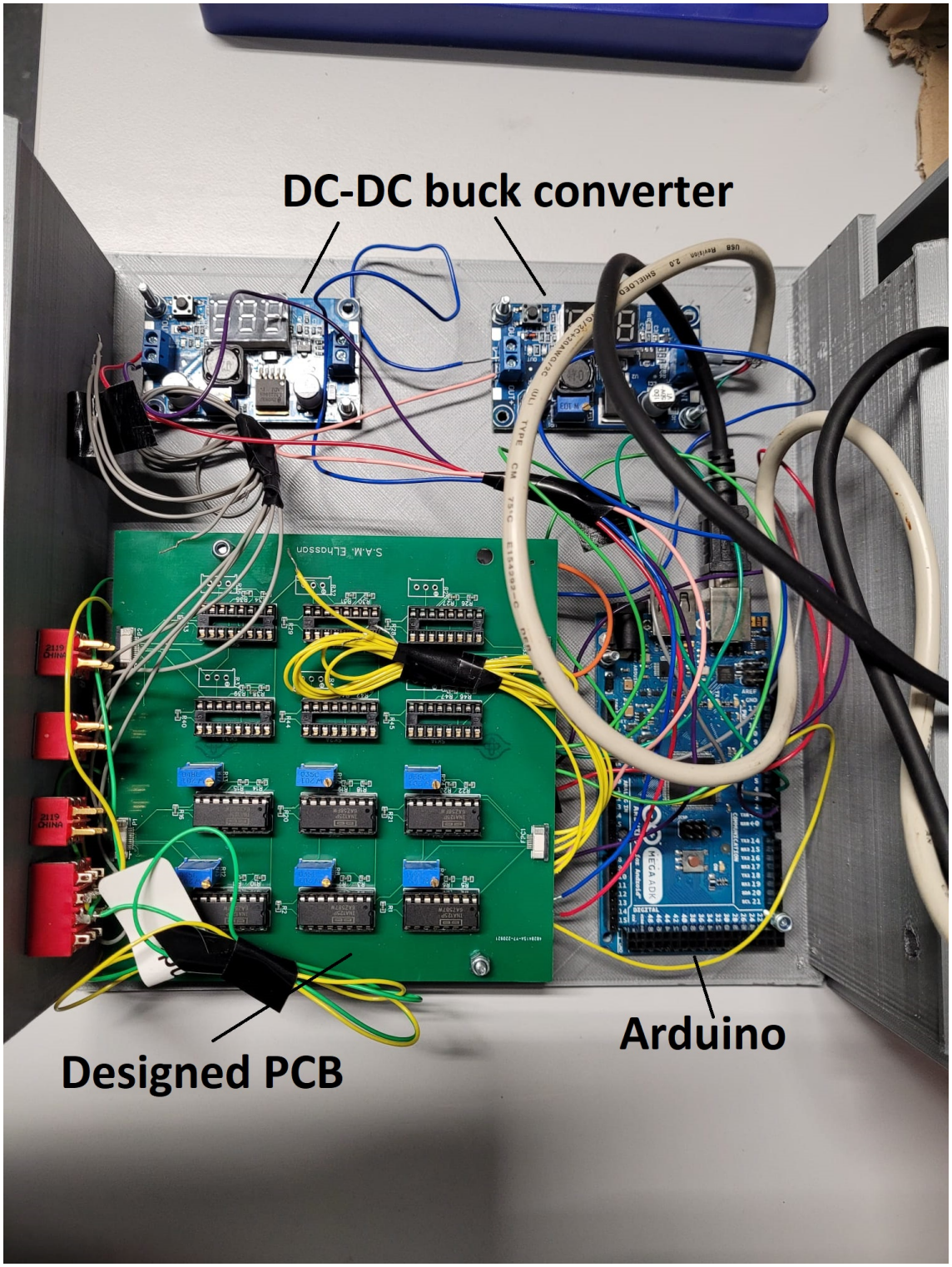

Figure E12: Top view of the electrical components with the PCB for the sensors, the two dc-dc buck converters and the Arduino

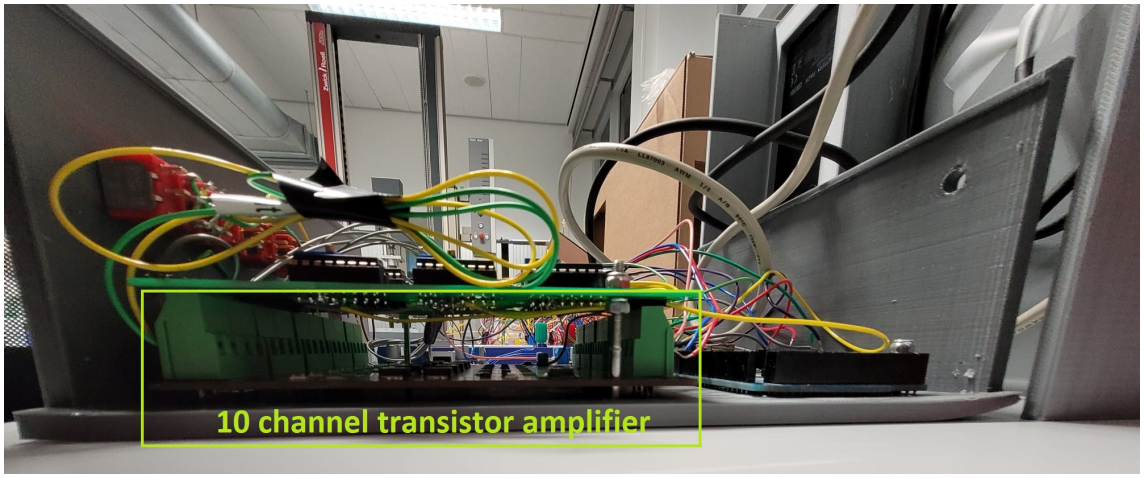

Figure E13: Underneath the PCB for the sensors is the 10 channel transistor amplifier

F Assembly Lid

 	Step 1: Cut the heatsink such that each part has three columns.
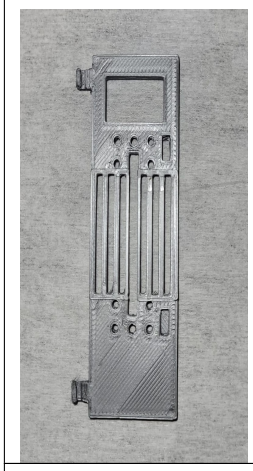  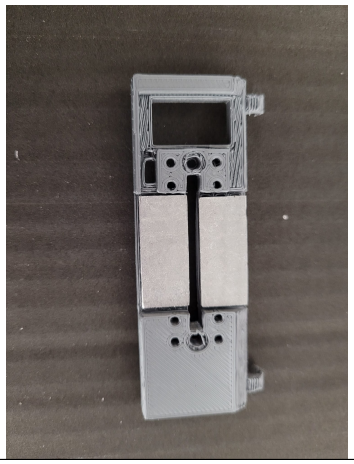	Step 2: Place the heatsink inside the lid. Use double-sided tape to stick the heatsink to the lid
	Step 3: Stick the sensor holder to the heatsink using double-sided tape. Do this for both sides.

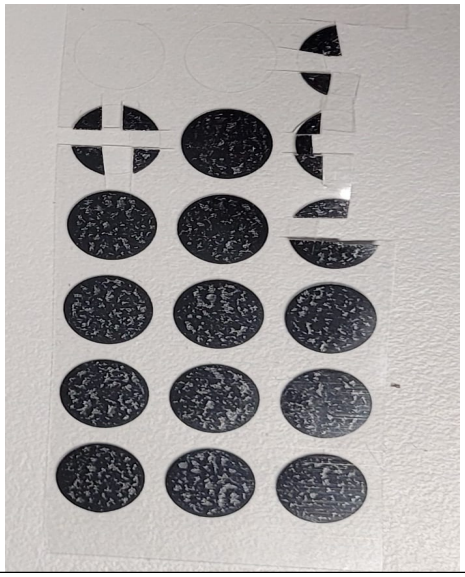 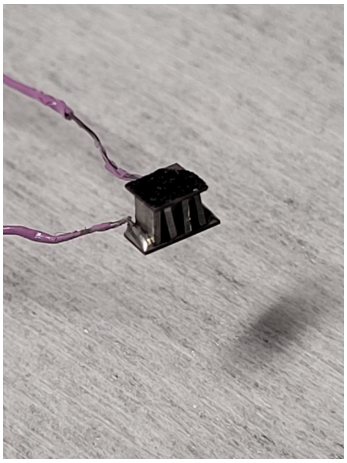	Step 4: Cut the adhesive carbon tabs into small pieces to fit on top of the heater and stick this to the peltier element.
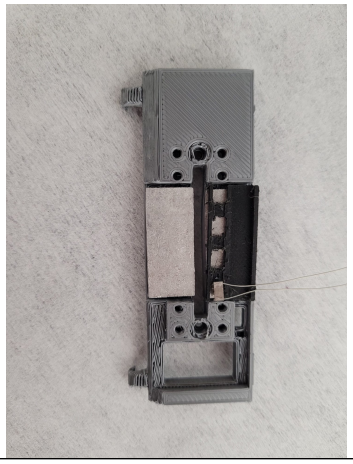	Step 5: stick the peltier element to the heatsink in the space left open by the sensor holder. Do this eight times.
 	Step 6: Cut the pin header into small pieces so four pins can be connected.

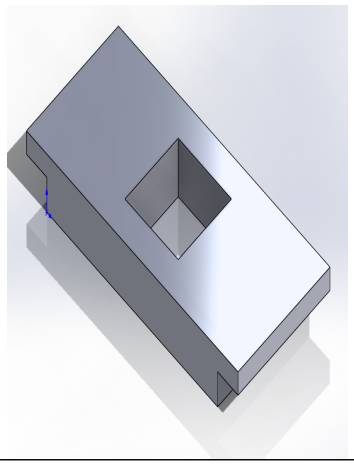 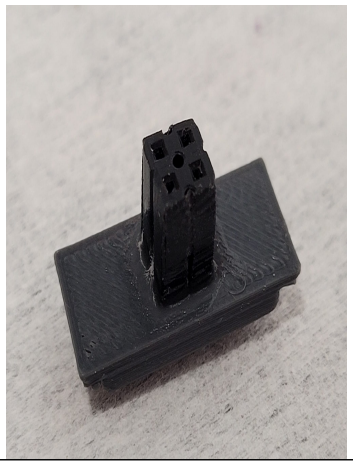	Step 7: Stick the header to the connection holder using glue.
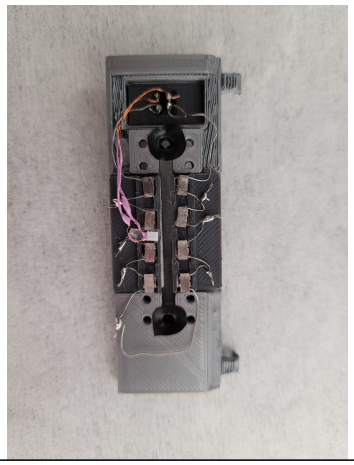	Step 8: Solder all the cables of the peltier elements to each other in a series connection and to the pin header. Place the sensor in the middle. The lid is finished.

Table F1: Assembly lid

G Additional results

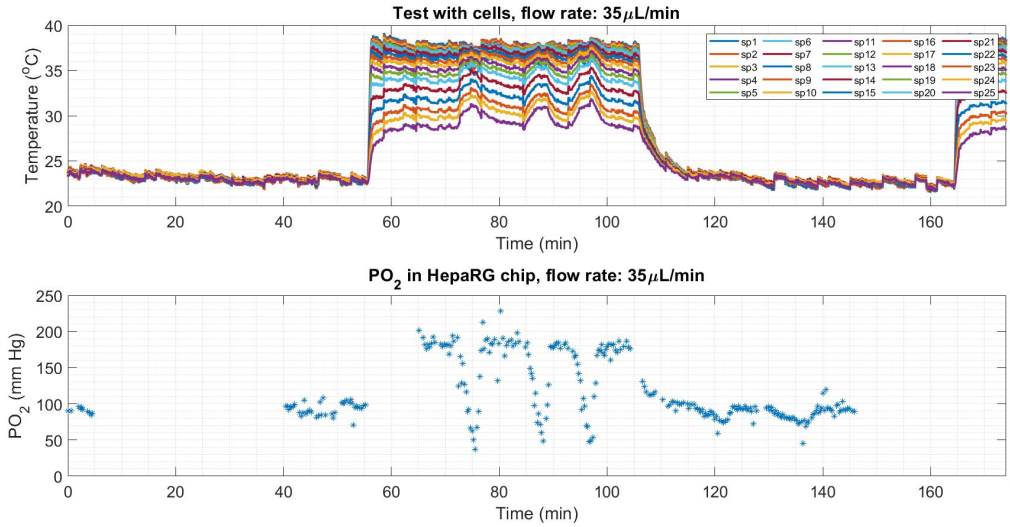

(a)

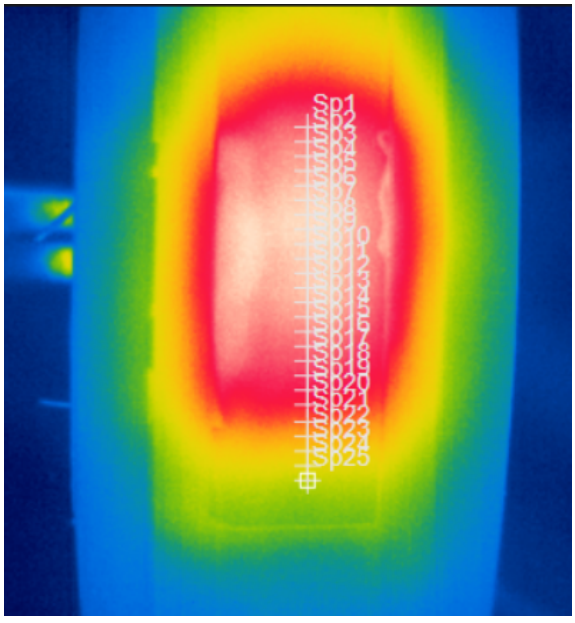

(b)

Figure G1: Raw test data with cells and the corresponding temperature plot. The oxygen consumption was measured up to the point where the last temperature increase is seen in the figure. For an unknown reason, the last part of the data went missing (b) Data point placement seen in the thermal camera software FLIR Tools

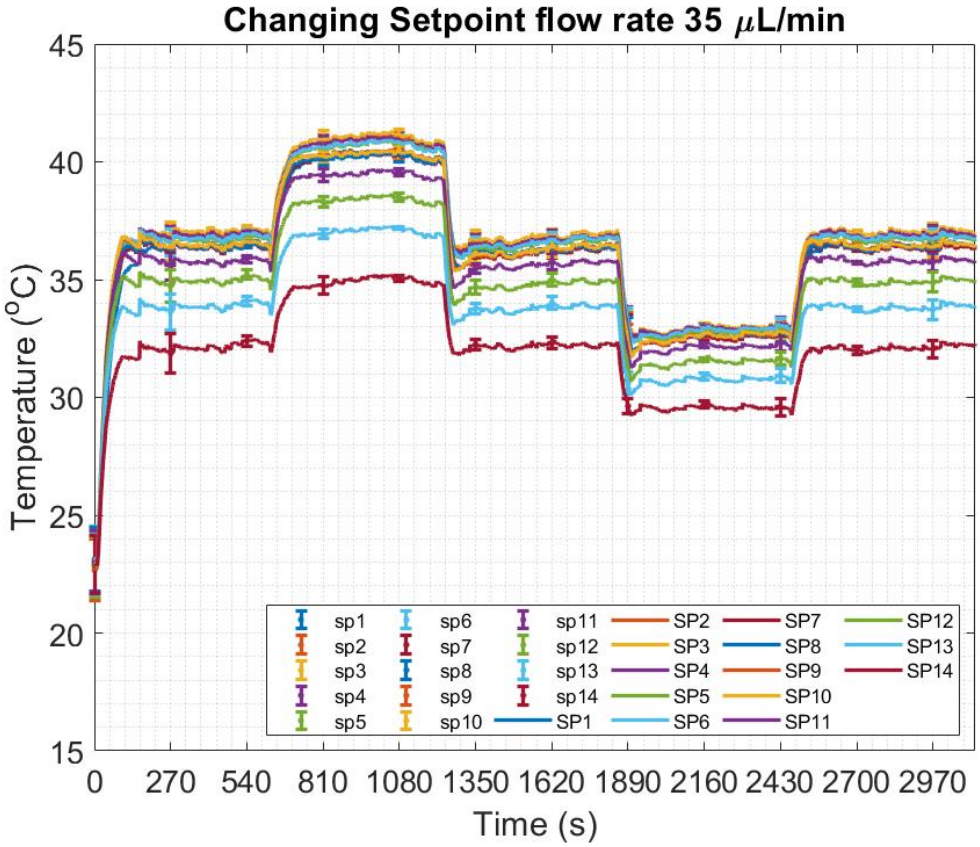

Figure G2: Changing the setpoint from 37 °C to 40 °C back to 37 °C to 34 °C and then back again to 37 °C

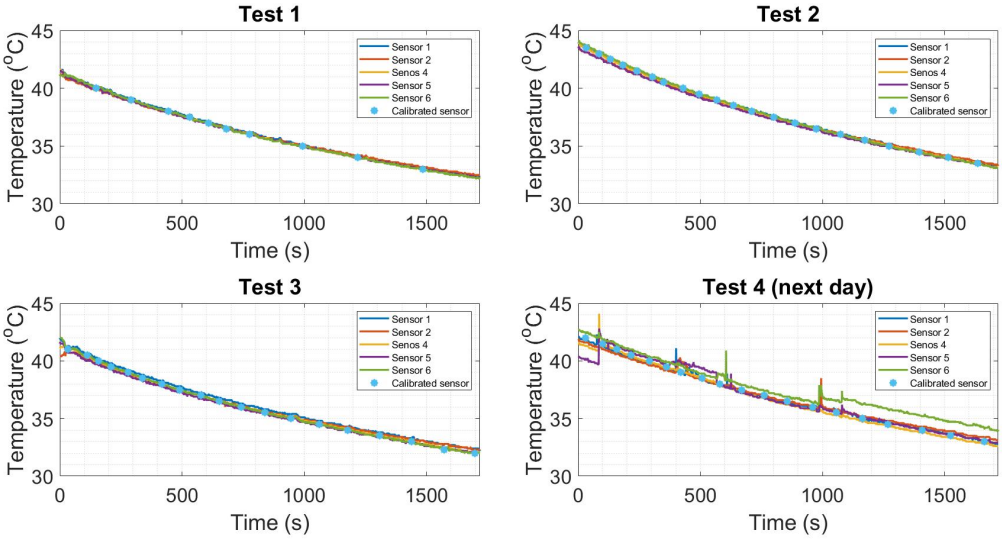

Figure G3: Four experiments with 5 RTD sensors and one calibrated sensor. The calibrated sensor is a thermometer (similar to Medisana, Medisana TM-700) used to measure the temperature of a human. The fourth experiment was done on the next day. This shows that the sensor values can change over time. This wos mostlikely due to the fact that the cables were connected to a breadboard which was unstable, which changed the value of the resistance of the RTD sensors

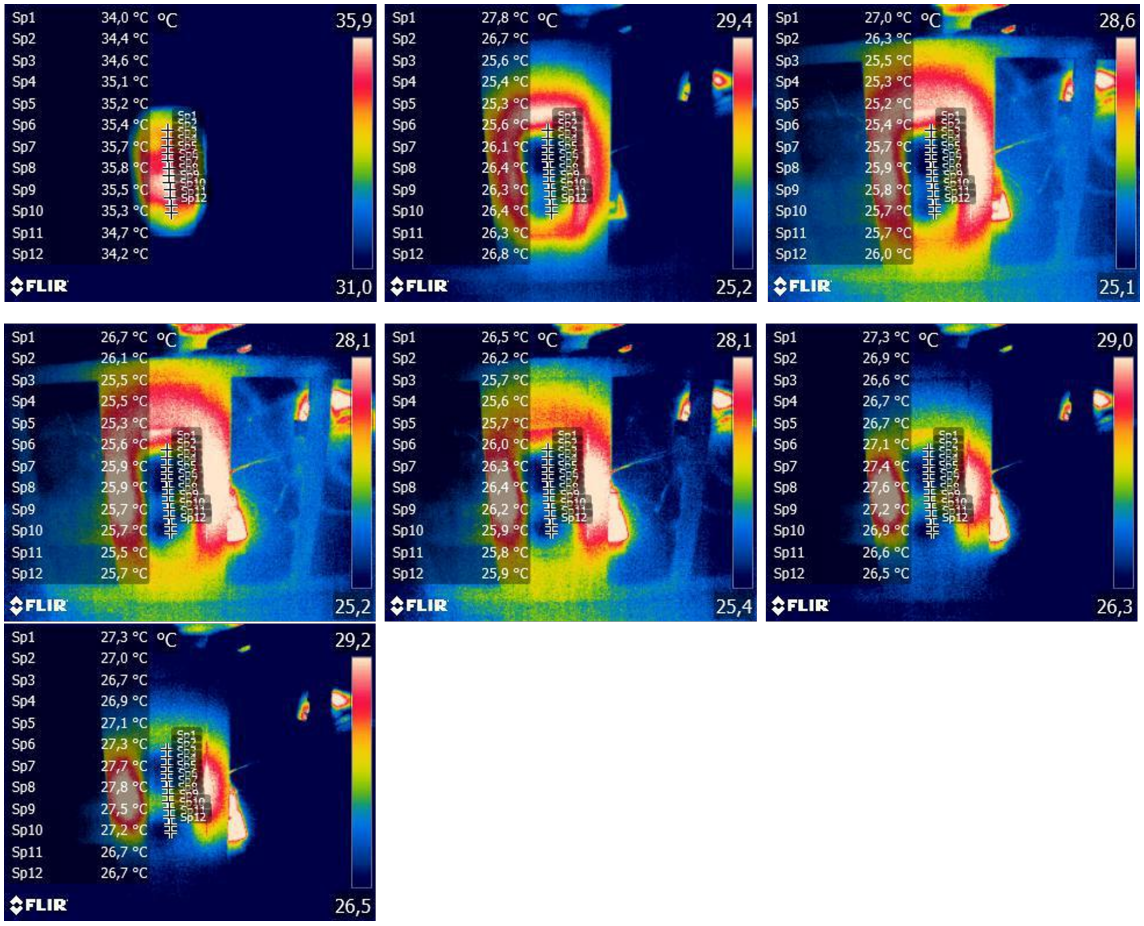

Figure G4: Thermal images of a test of cooling from room temperature. Fluid flow was from sp14 to point sp1 and was 35 $\mu L/min$

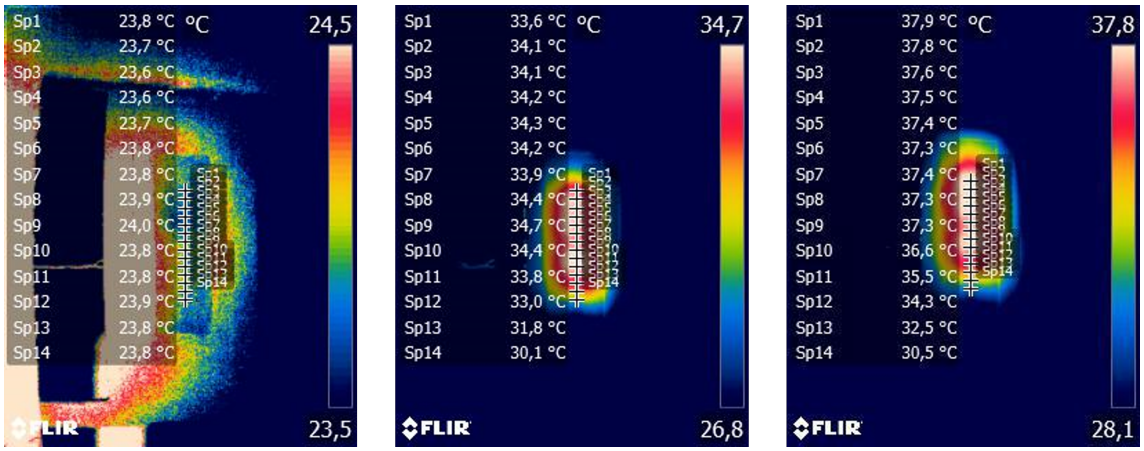

Figure G5: Thermal images of a test of heating from room temperature. Fluid flow was from sp14 to point sp1 and was 35 $\mu L/min$